# BRITTLE FRACTURE & BRITTLE to DUCTILE TRANSITION APPLICATIONS TO COMPONENTS

André PINEAU
Centre des Matériaux - Ecole des Mines de Paris. ParisTech
UMR CNRS 7633
andre.pineau@ensmp.fr

# BRITTLE FRACTURE & BRITTLE to DUCTILE TRANSITION APPLICATIONS TO COMPONENTS

André PINEAU
Centre des Matériaux - Ecole des Mines de Paris. ParisTech
UMR CNRS 7633
andre.pineau@ensmp.fr

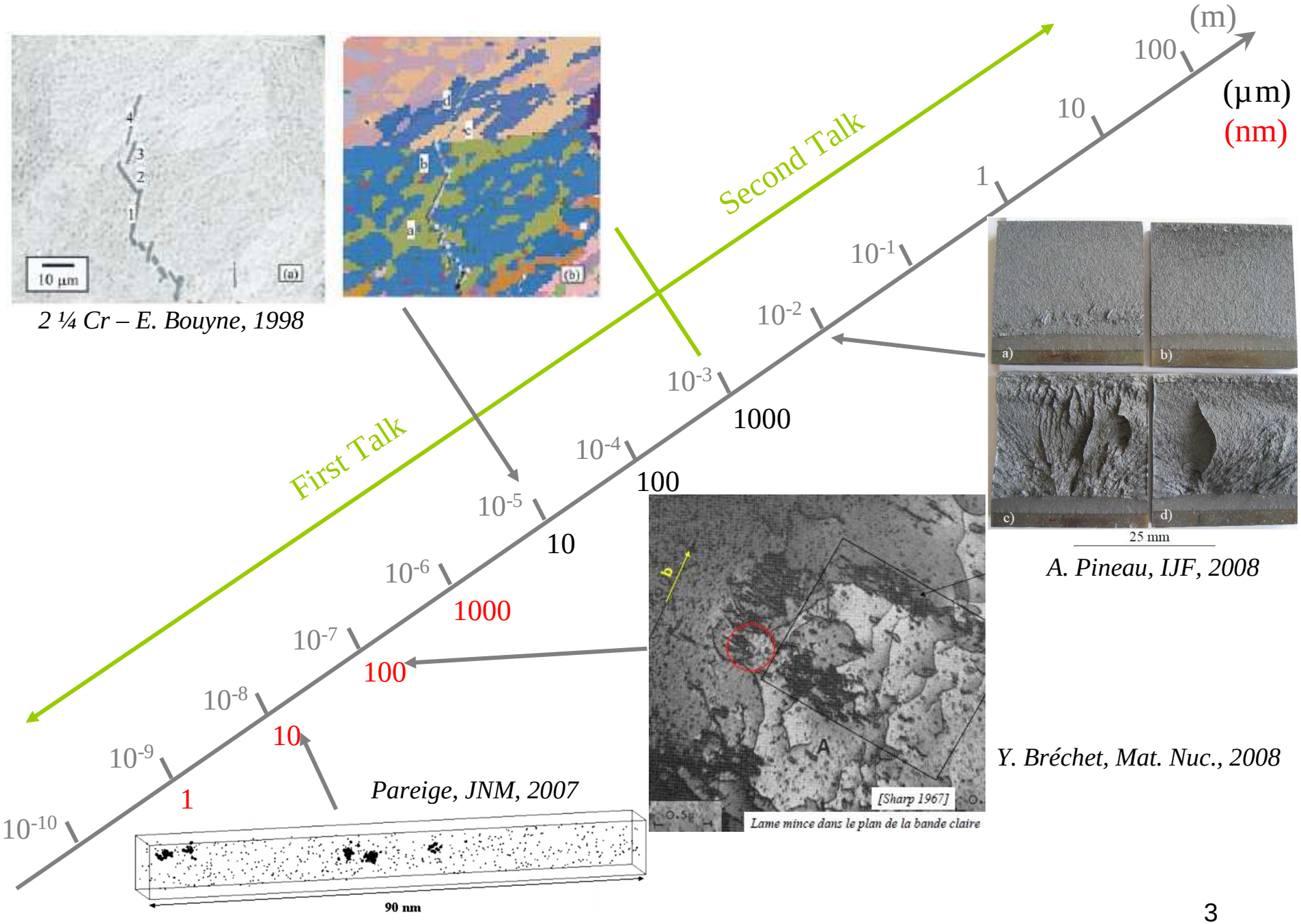


*2 ¼ Cr – E. Bouyne, 1998*

*A. Pineau, IJF, 2008*

*Y. Bréchet, Mat. Nuc., 2008*

*Pareige, JNM, 2007*

# BRITTLE FRACTURE & BRITTLE to DUCTILE TRANSITION APPLICATIONS TO COMPONENTS

André PINEAU
Centre des Matériaux - Ecole des Mines de Paris. ParisTech
UMR CNRS 7633
andre.pineau@ensmp.fr

# CONSTRAINT LOSS CORRECTION OF CTOD FRACTURE TOUGHNESS (1)

ISO 27306 : 2009

See ISO 27306:2009

# CONSTRAINT LOSS CORRECTION OF CTOD FRACTURE TOUGHNESS (2)

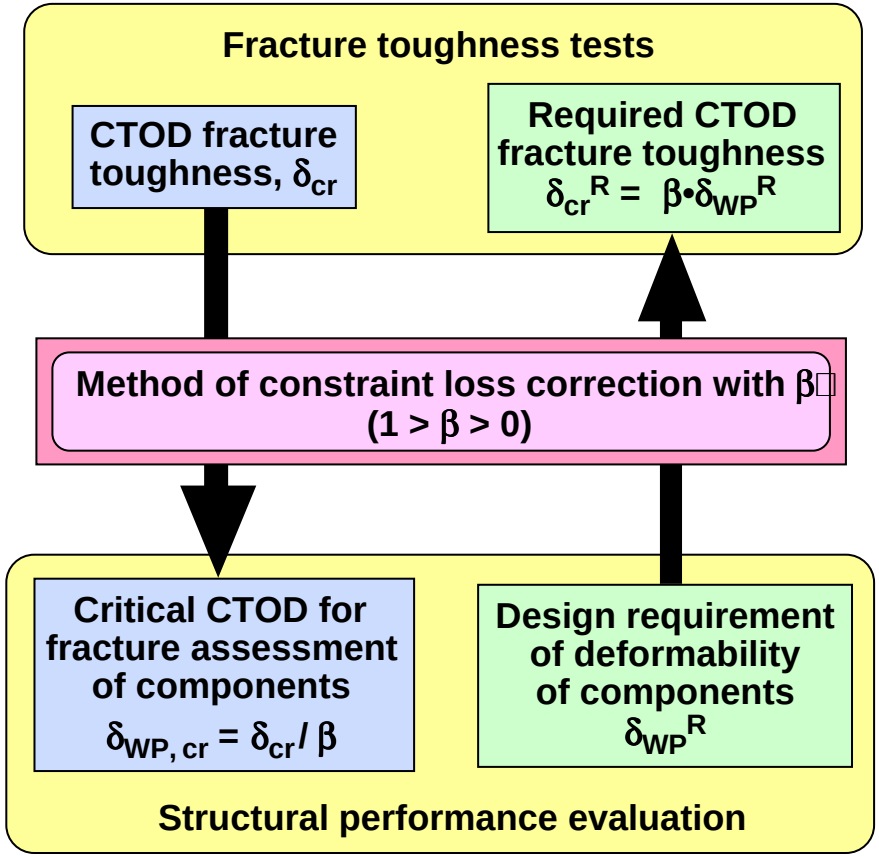


**Method of constraint loss corrections to link fracture toughness tests and structural performance evaluation**

**Principle**

- **Convert the CTOD fracture toughness obtained from standard fracture toughness specimens (3 PB or CT) with $0.45 < a_0 < 0.55$) characterized by high plastic constraint to an equivalent critical CTOD for structural components, usually characterized by less constraint**
- **Reverse procedure possible**
- **Critical CTOD for standard specimens determined in accordance with ISO 12135**
- **Fracture assessment of a cracked component using established methods, such as FAD (Failure Assessment Diagram)**

# CONSTRAINT LOSS CORRECTION OF CTOD FRACTURE TOUGHNESS (3)

Level I : Simplified assessment. No information available (mechanical properties, etc…) to calculate β

***Use β = 0.50 as an upper-bound approximation***

Level II : Normal assessment

- Mechanical properties are known
- Crack size is known
- Weibull shape parameter, m, unknown

***Use a lower-bound value for m***
***Nomographs derived as a function of m – value***

Level III : Material specific assessment - All information are known

***β values derived from nomographs but with a statistically determined m – value from a sufficient number of fracture toughness test results***

# CONSTRAINT LOSS CORRECTION OF CTOD FRACTURE TOUGHNESS (4)

Determination of average CTOD Fracture Toughness

$$\delta_{cr,ave-25} = \left\{ \sqrt{\delta_{min}} + \left[ \sqrt{\delta_{cr,ave-B}} - \sqrt{\delta_{min}} \right] \left( \frac{B}{25} \right)^{1/4} \right\}^2$$

$$\delta_{min} = \frac{500\left(1-\nu^2\right)}{\sigma_Y\, E} K_{min}^2$$

Determination of Weibull shape parameter m (level II)

$$m = 10 \text{ for } \delta_{cr,ave-25} \leq 0.05\,\text{mm}$$

$$m = 20 \text{ for } \delta_{cr,ave-25} > 0.05\,\text{mm}$$

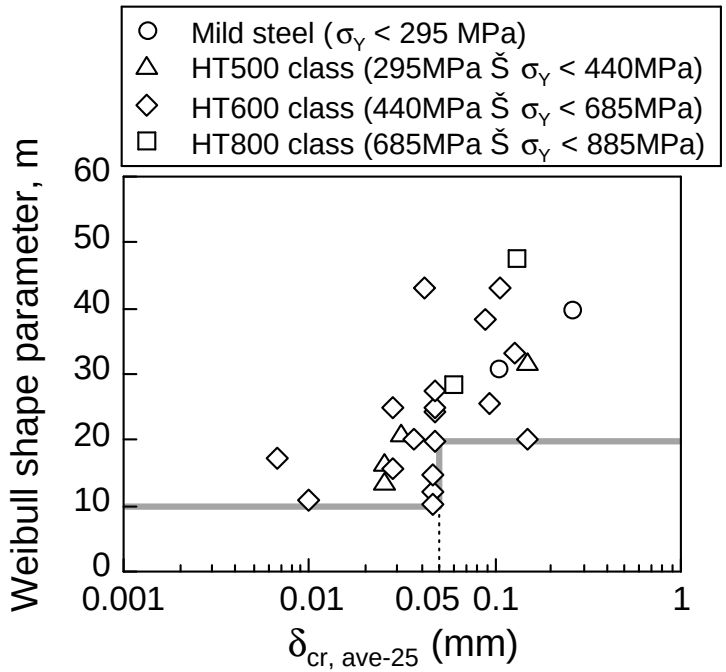


Relationship between Weibull parameter m and average CTOD

# CONSTRAINT LOSS CORRECTION OF CTOD FRACTURE TOUGHNESS (5)

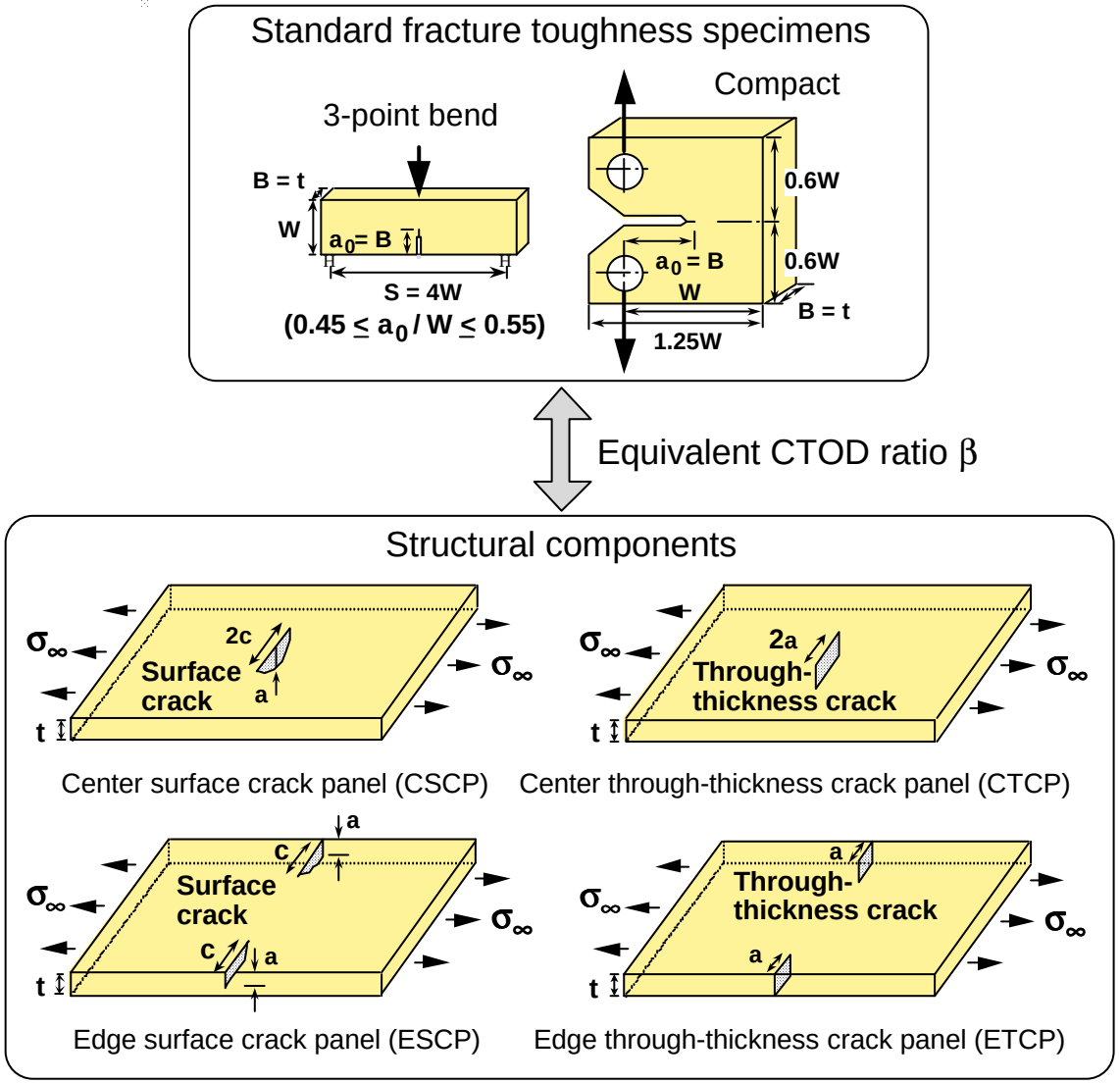


Standard Fracture Toughness specimens and wide plate components linked with the equivalent CTOD ratio β

# CONSTRAINT LOSS CORRECTION OF CTOD FRACTURE TOUGHNESS (6)

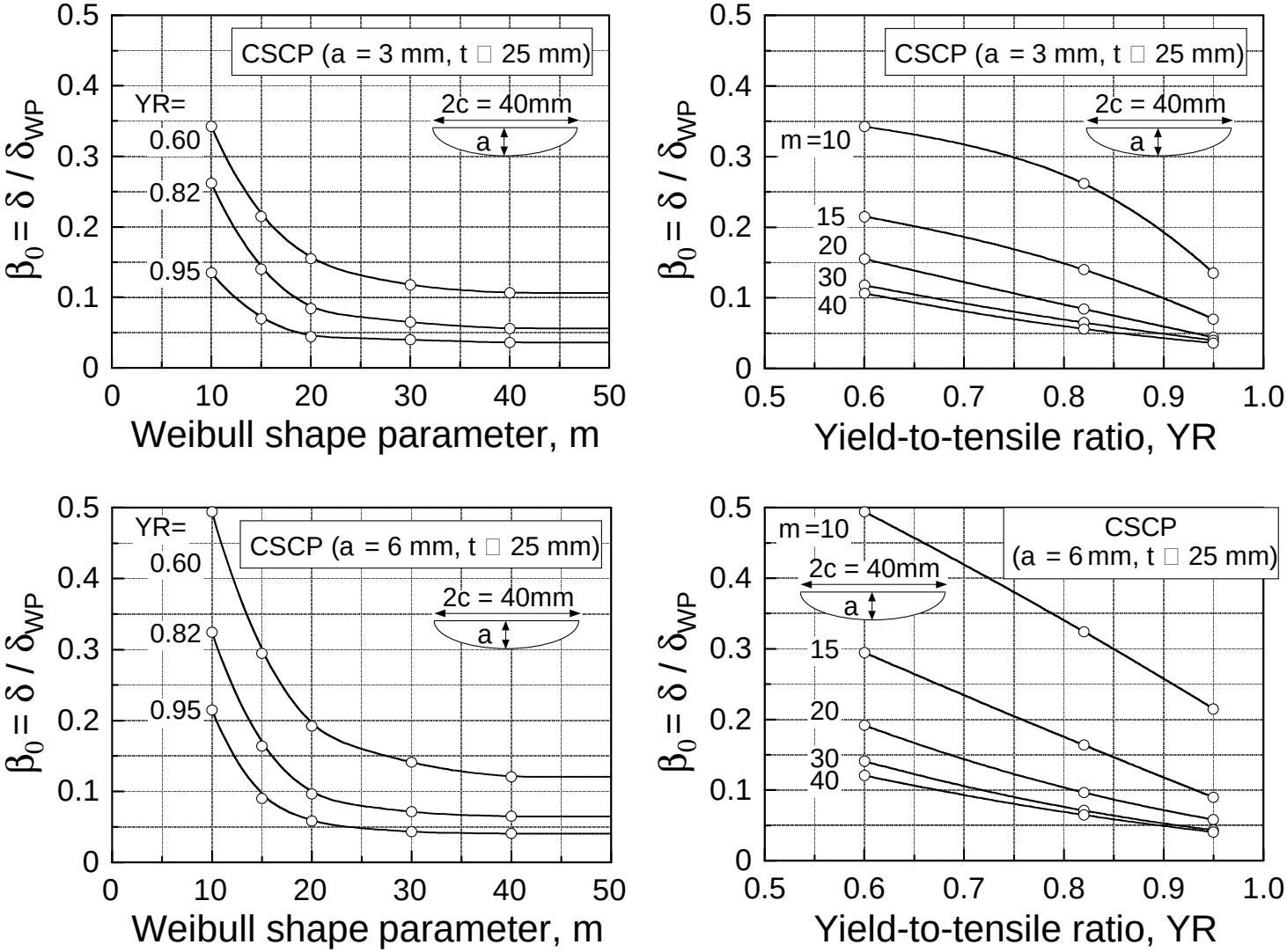


Nomographs of equivalent CTOD ratio, β for center surface crack panel

# CONSTRAINT LOSS CORRECTION OF CTOD FRACTURE TOUGHNESS (7)

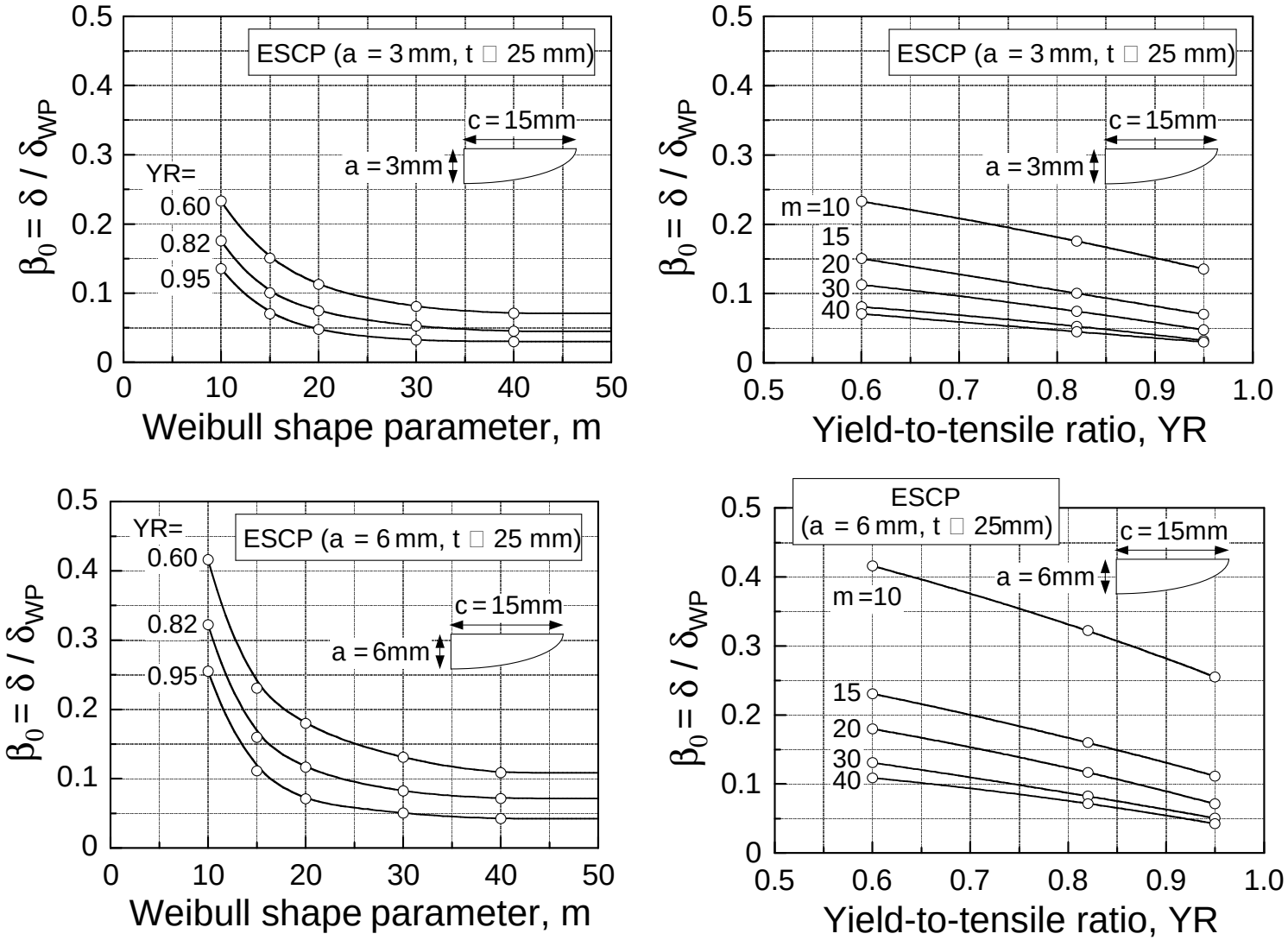


Equivalent CTOD ratio, β, for edge crack panel

# CONSTRAINT LOSS CORRECTION OF CTOD FRACTURE TOUGHNESS (8)

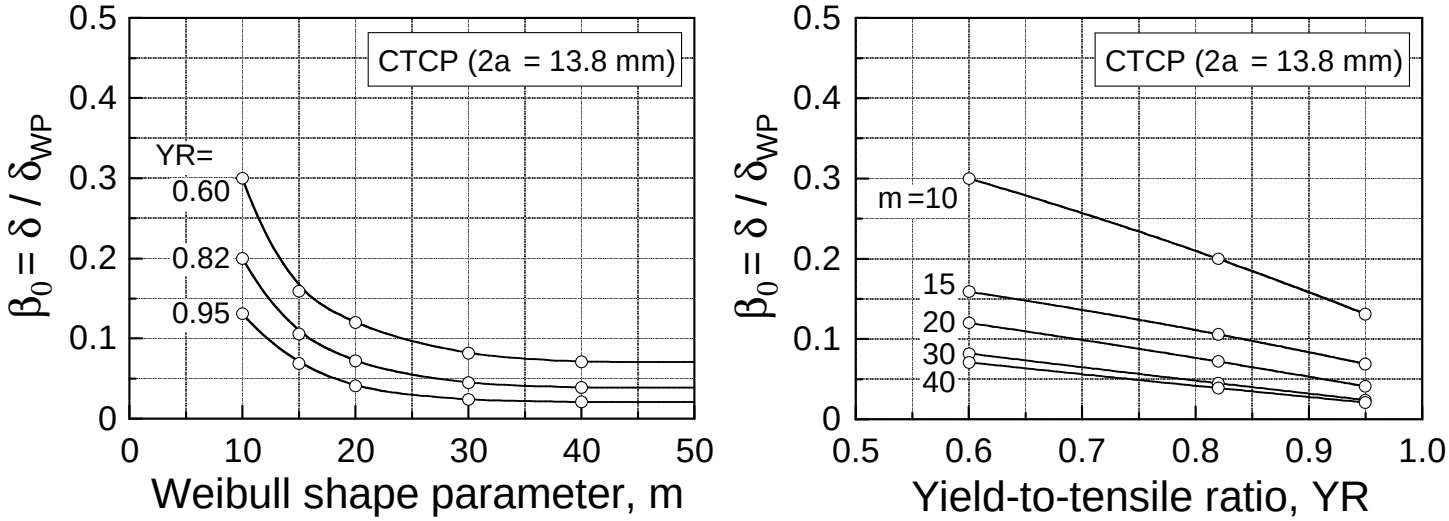


Equivalent CTOD ratio, β, for center through-thickness crack panel

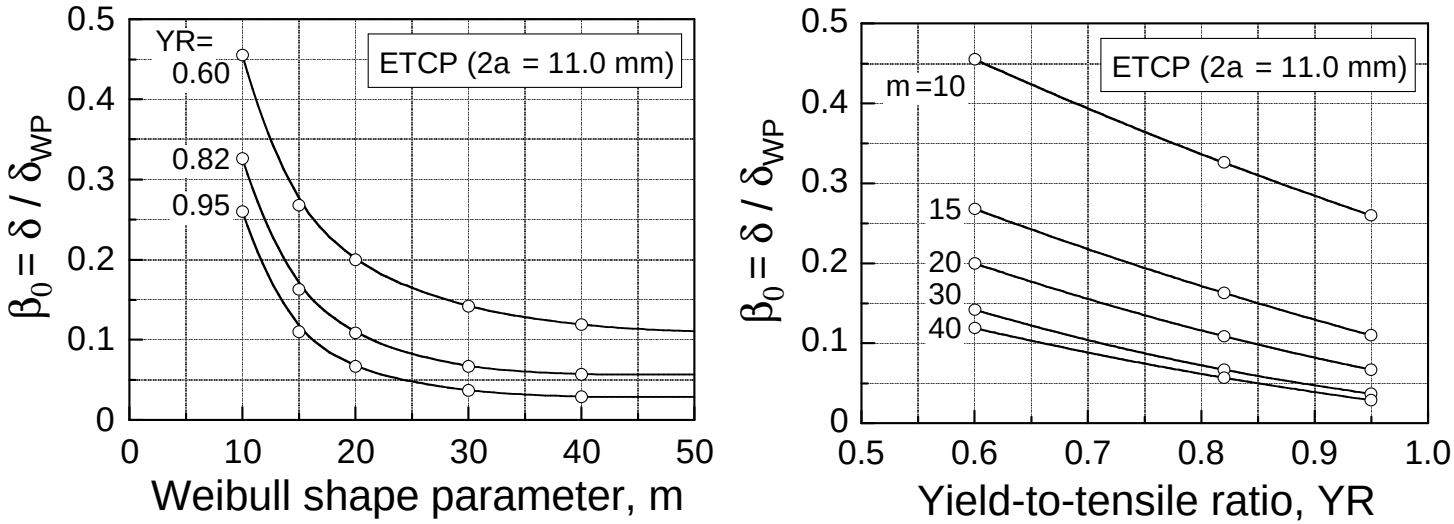


Equivalent CTOD ratio, β, for edge through-thickness crack panel

# CONSTRAINT LOSS CORRECTION OF CTOD FRACTURE TOUGHNESS (9)

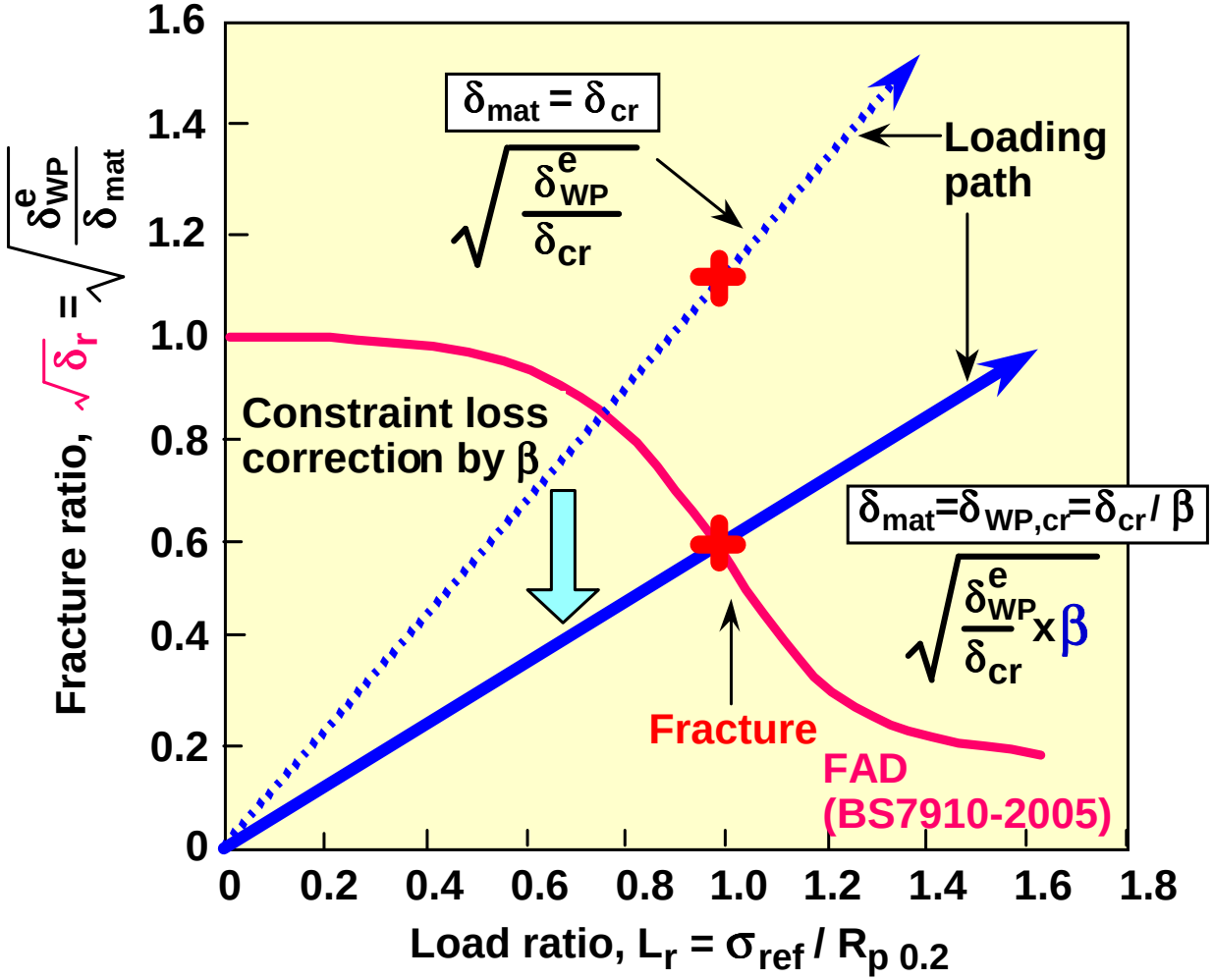


Application of the equivalent CTOD ratio β to the failure assessment diagram (FAD) in BS7910-2005

# CONSTRAINT LOSS CORRECTION OF CTOD FRACTURE TOUGHNESS (10)

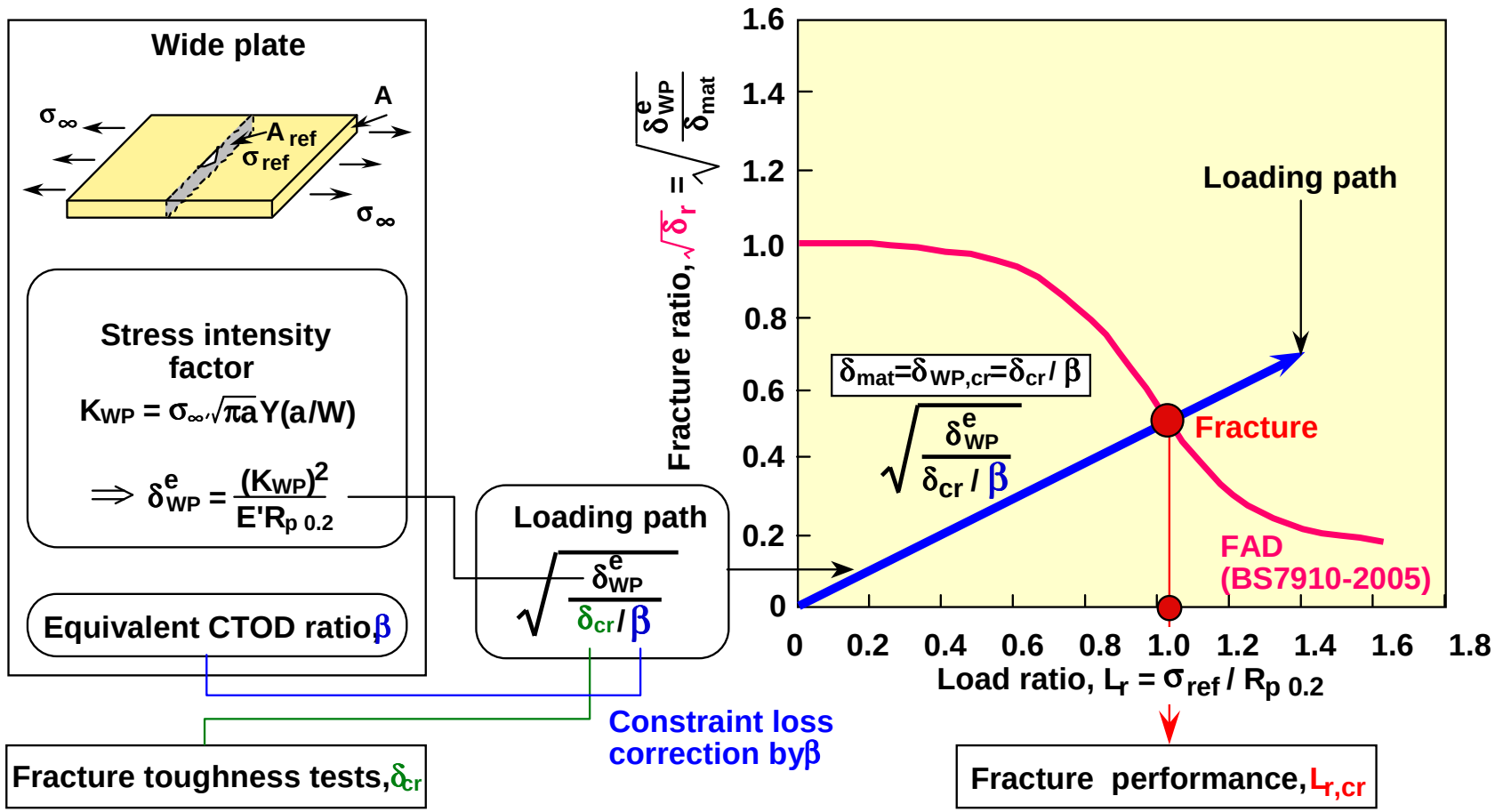


Procedure for failure assessment by FAD approach with equivalent CTOD ratio β

# BRITTLE FRACTURE & BRITTLE to DUCTILE TRANSITION APPLICATIONS TO COMPONENTS

André PINEAU
Centre des Matériaux - Ecole des Mines de Paris. ParisTech
UMR CNRS 7633
andre.pineau@ensmp.fr

# WARM-PRESTRESS EFFECT

*See also D.J. Smith, CSI 2003, pp. 289-345*

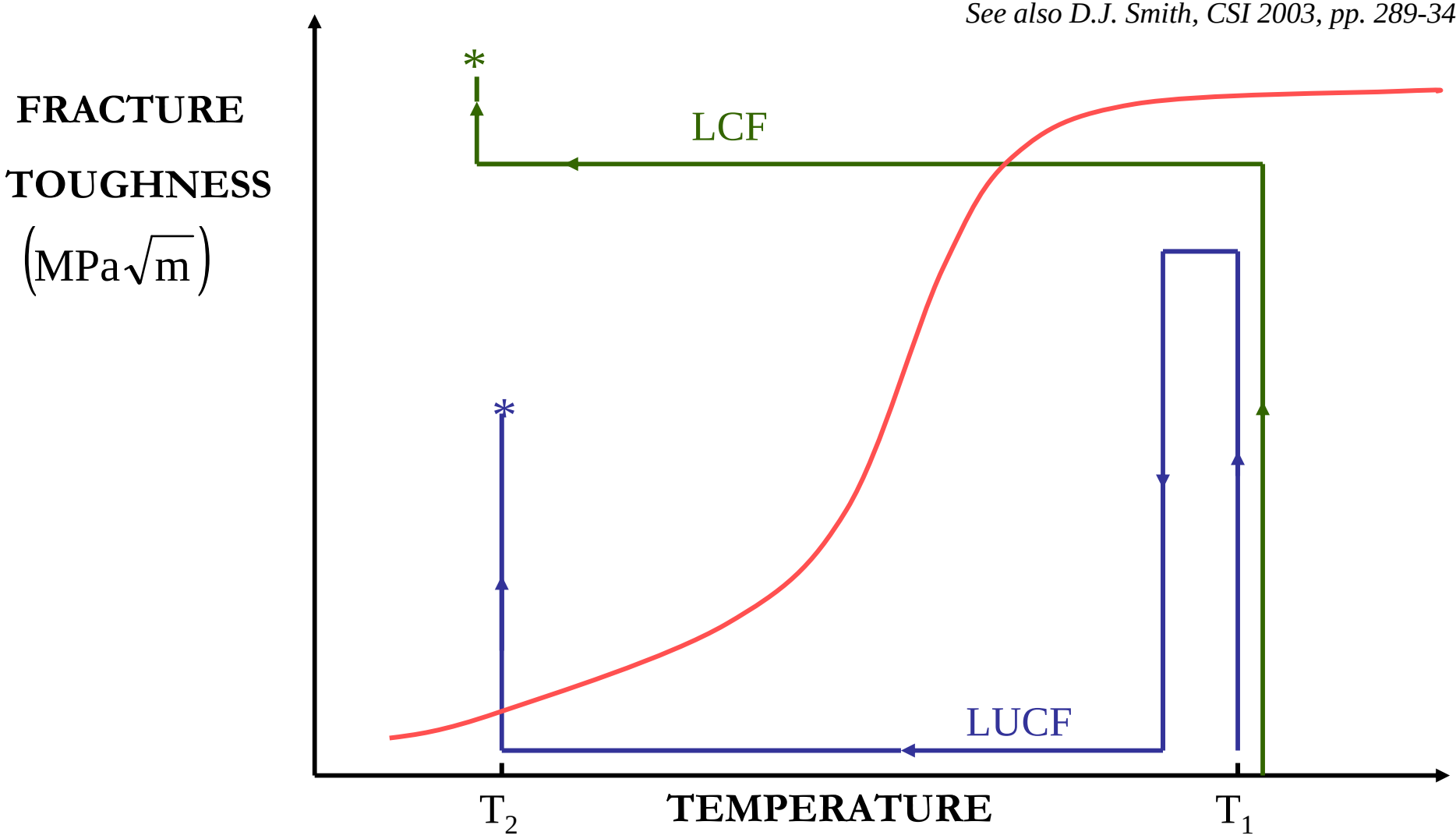

# WPS EFFECT (1)

*F.Mudry, PhD Thesis, (1982)*

*F.M. Beremin, ICF5, Cannes, (1981),825-832*

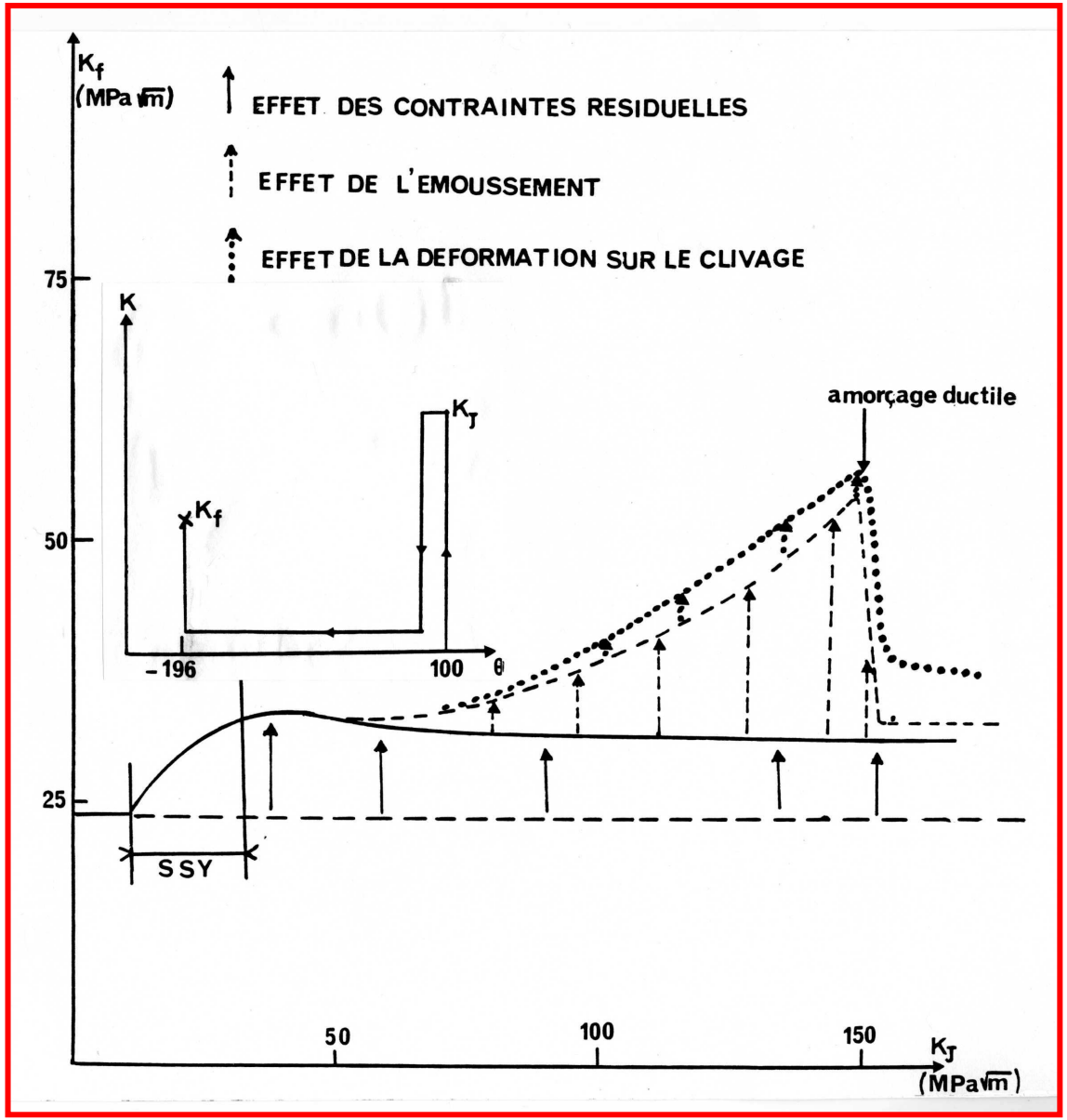


## THREE EFFECTS

- Residual Stresses ( LUCF )
- Crack Blunting (main factor)
- Prestrain effect on Cleavage Stress

# WPS EFFECT (2)

*S. Bordet et al., FFEMS, vol. 29, 2006, pp. 799-816*

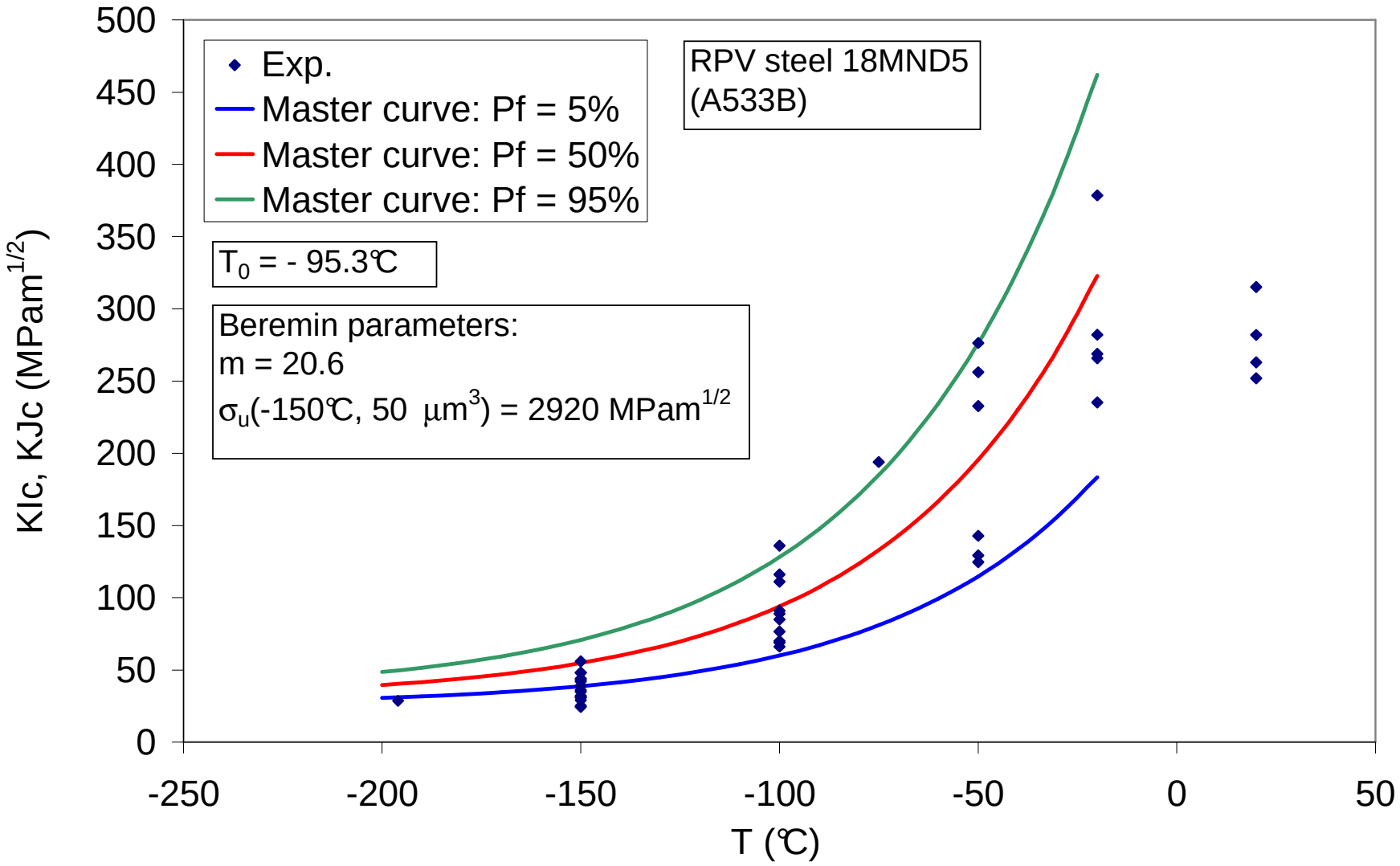

# WPS EFFECT (3)

*S. Bordet et al., FFEMS, vol. 29, 2006, pp. 799-816*

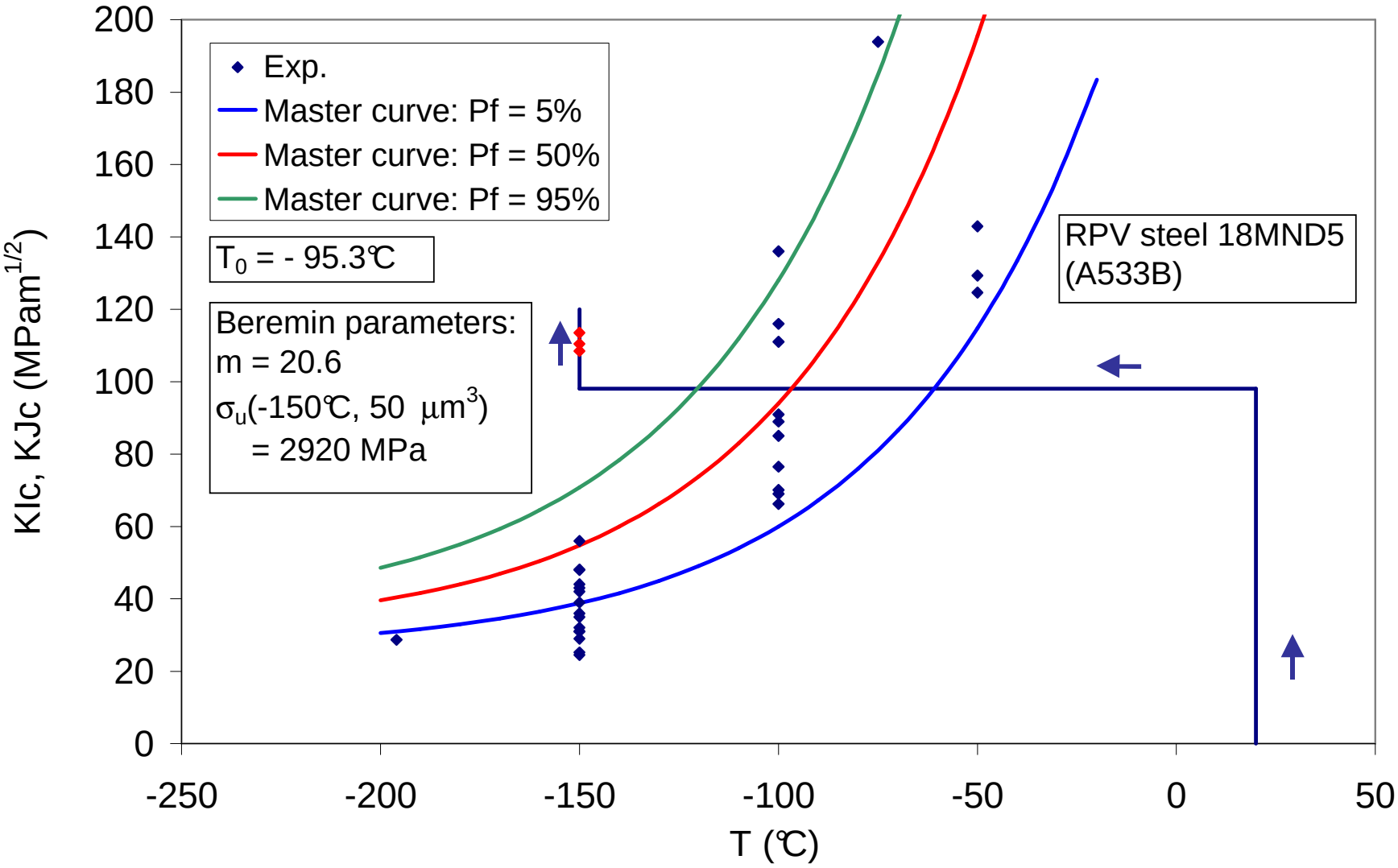

# WPS EFFECT (4)

*S. Bordet et al., FFEMS, vol. 29, 2006, pp. 799-816*

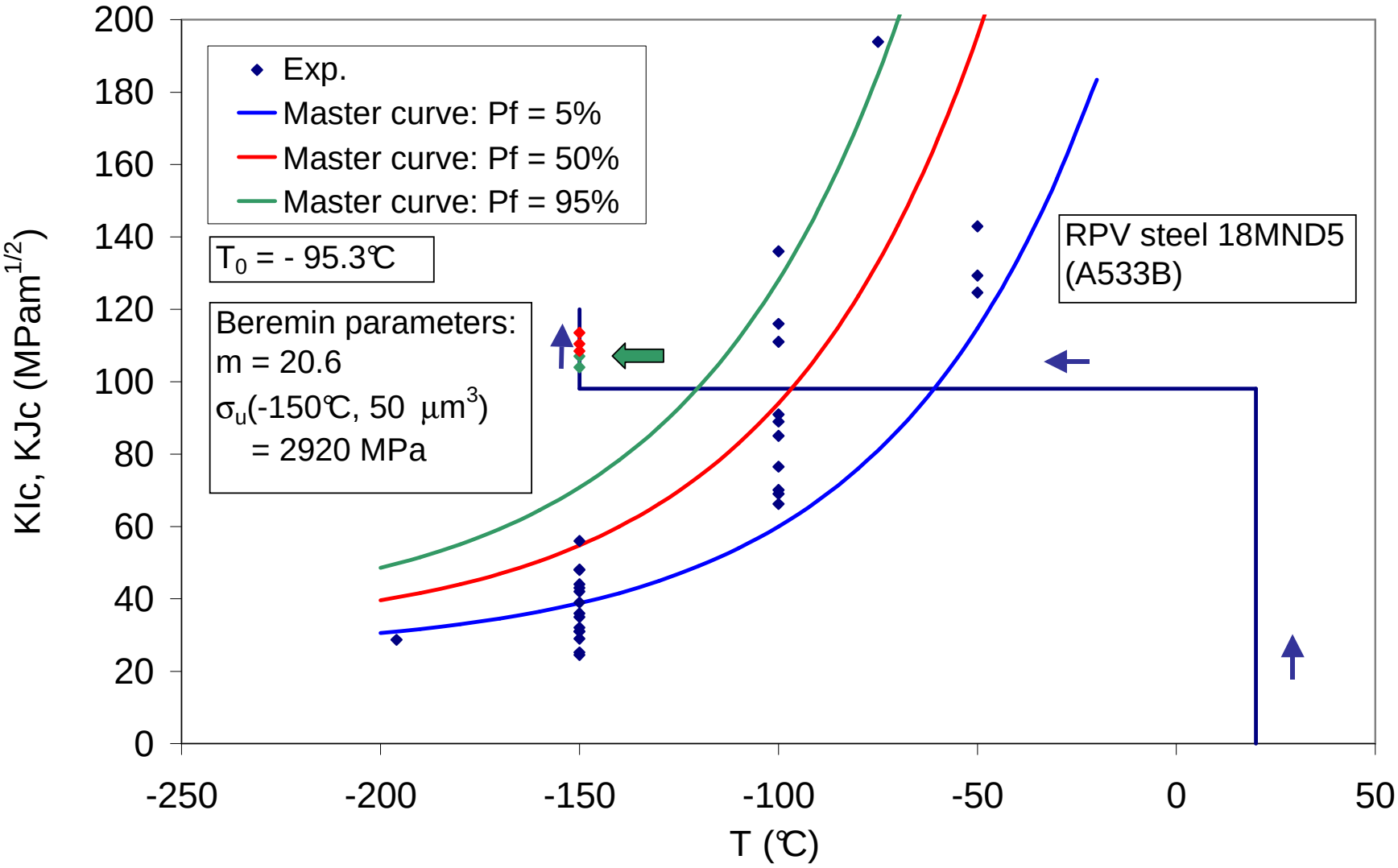

# WPS EFFECT (5)

*S. Bordet et al., FFEMS, vol. 29, 2006, pp. 799-816*

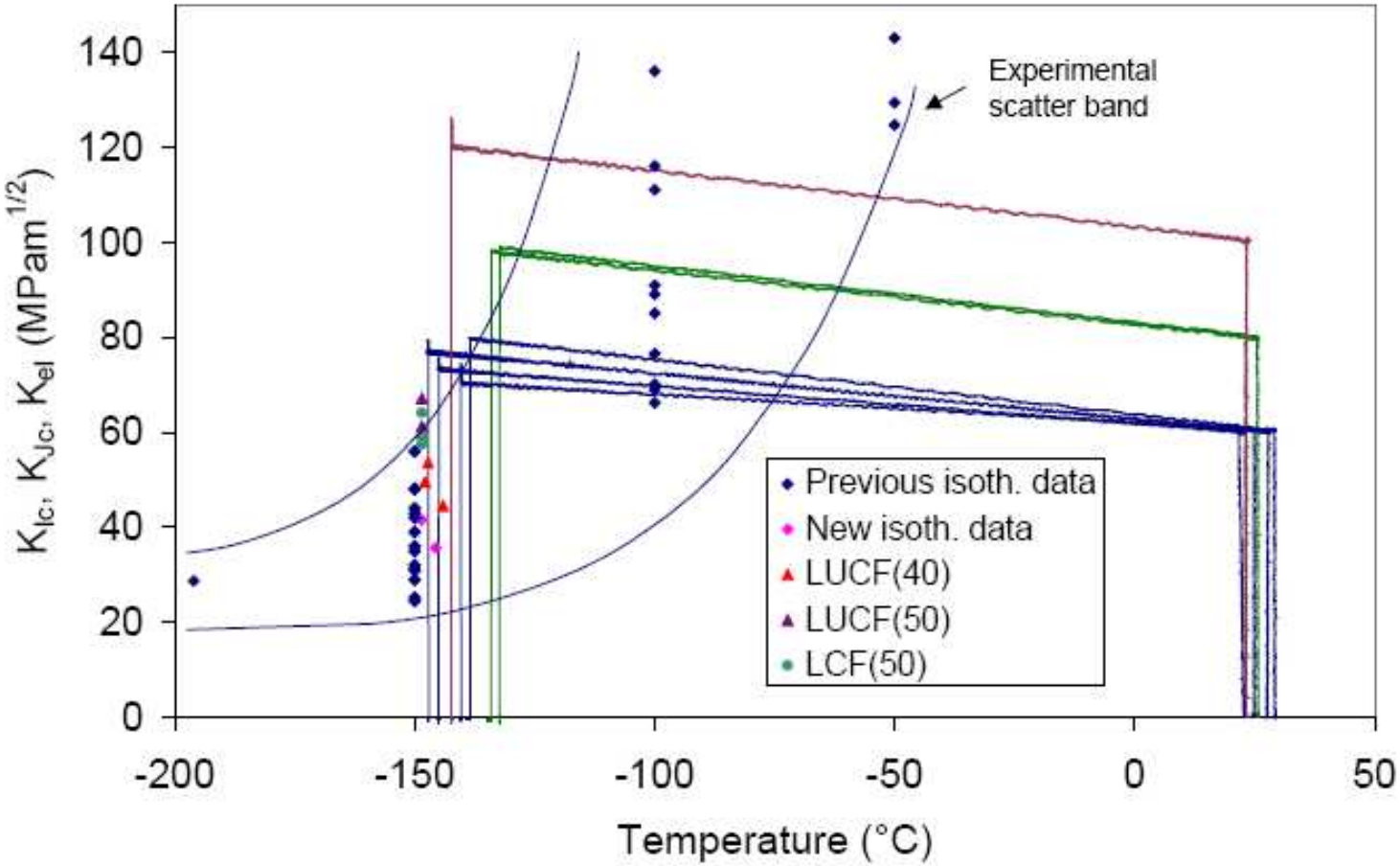

# PRESSURIZED THERMAL SHOCK (1)

*D. Moinereau et al., IJPVP, vol.78, 2001, pp. 69-83*

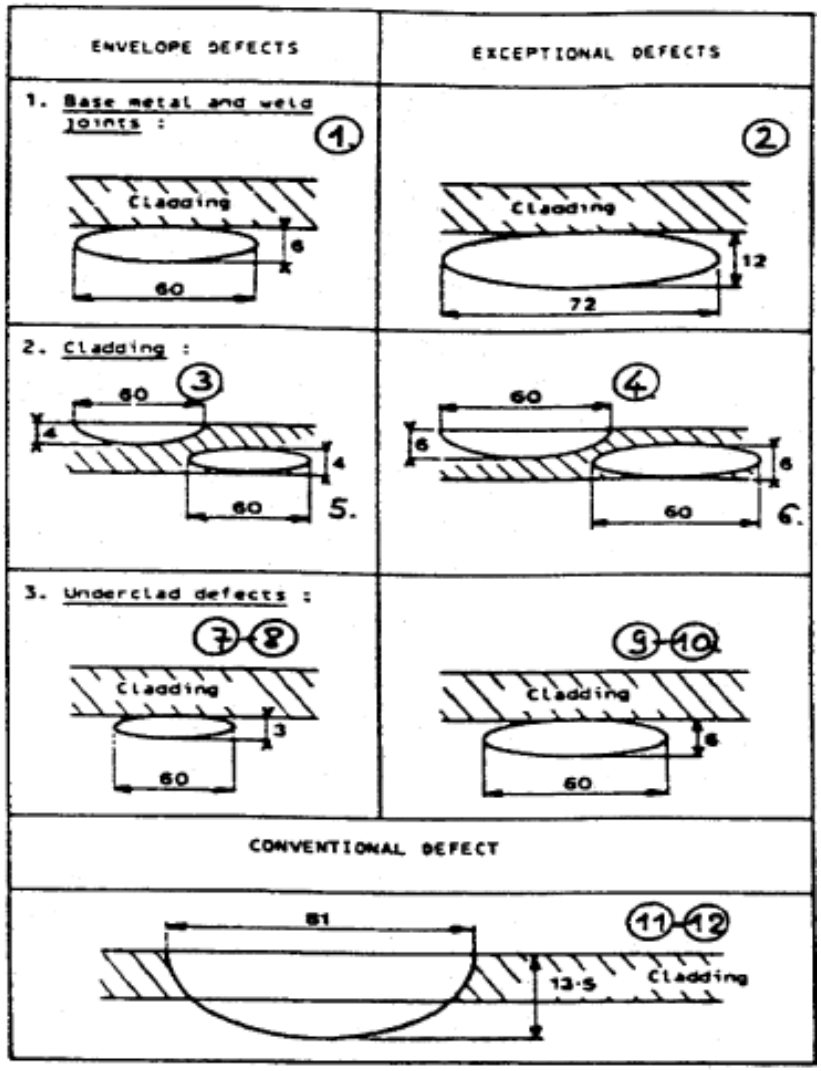


Reference Defects for Vessel Beltline
(dimensions in mm)

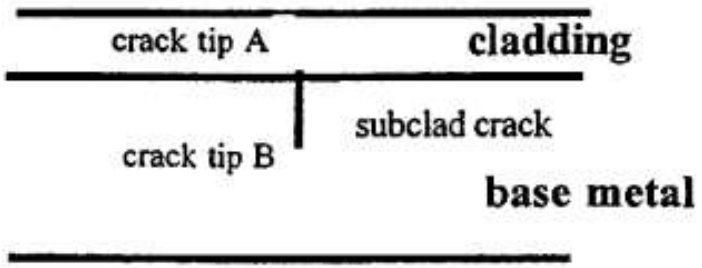


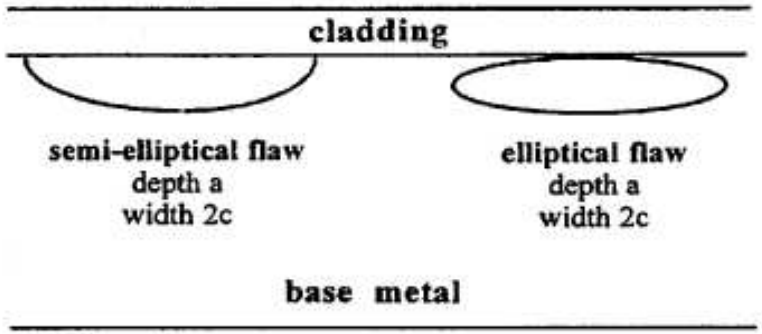

# PRESSURIZED THERMAL SHOCK (2)

*D. Moinereau et al., IJPVP, vol.78, 2001, pp. 69-83*

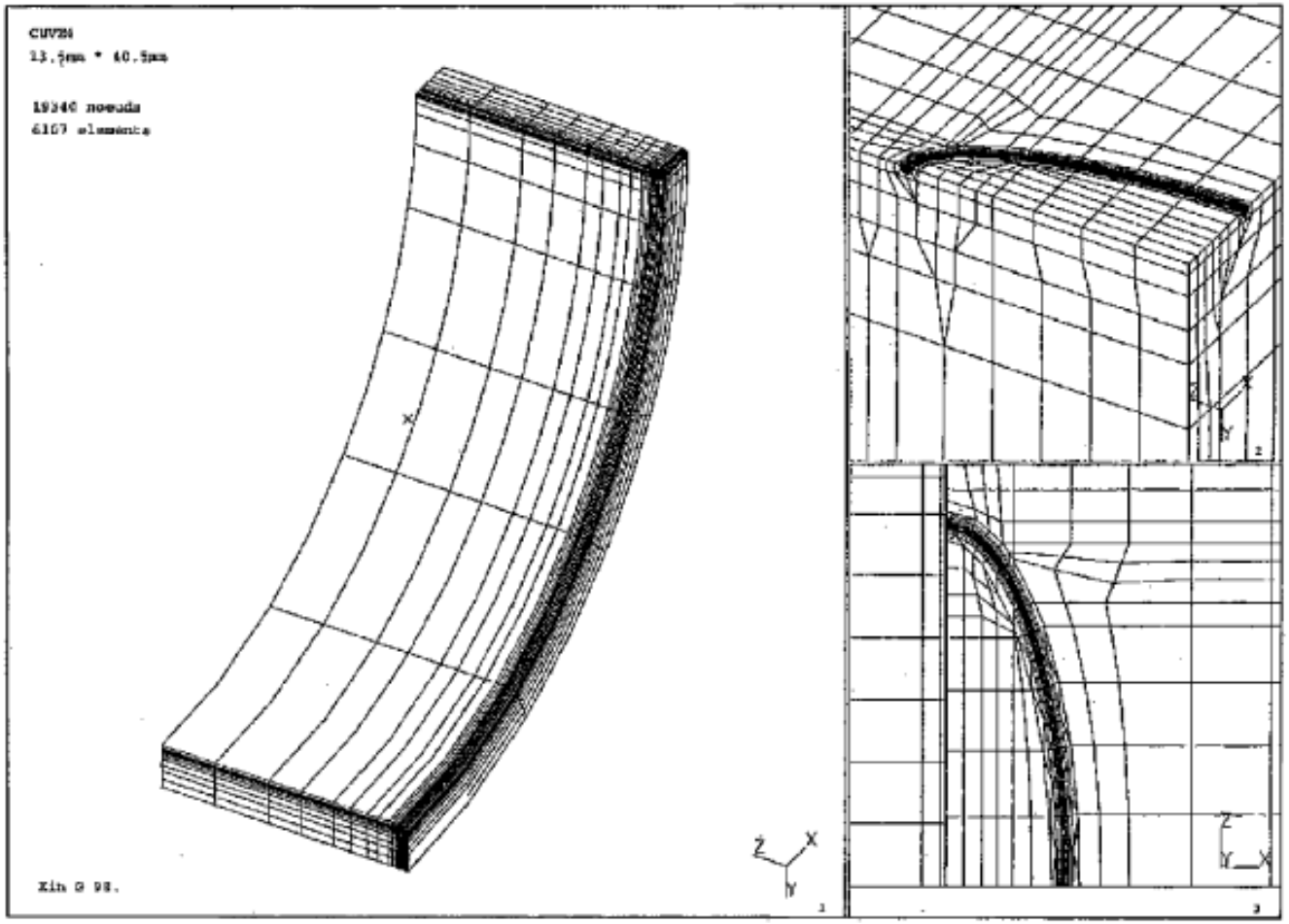

3D-Mesh of a cladded Vessel containing a 13.5 mm Deep through clad Surface Crack

# PRESSURIZED THERMAL SHOCK (3)

*D. Moinereau et al., IJPVP, vol.78, 2001, pp. 69-83*

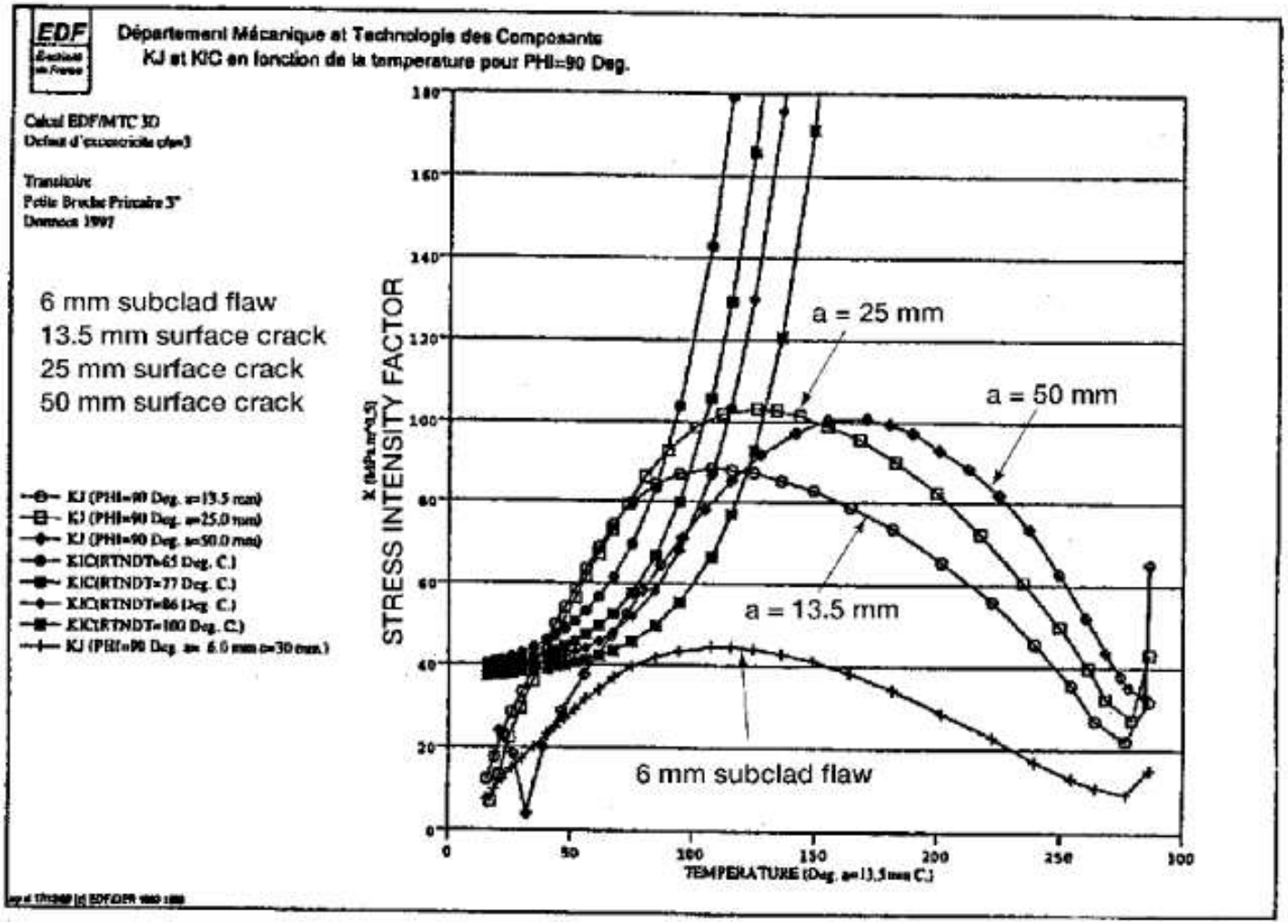


Comparison between through clad Surface & shallow Subclad Flaws

1975-80


49° 30'
50° 00'
50° 30'
Manama
Al Rifa' al Gharbi
Sitrah
Awali
Bahrain
Ar Rumaythah
Madinat ash Shamal
Persian Gulf
Al Khuwayr
Ra's 'Ushayriq
Al Ghashamiyah
26° 00'
Al Ka'ban
Al Ghuwairiyah
Gulf of Bahrain
Al Busayyir
Al Khawr
Umm Swai Jah
Hawar (disputed between Qatar and Bahrain)
Al Jumailiyah
Ar Rufayq
25° 30'
Bi'r Zekrit
Dukhan
Umm Salal Mohammed
Ash Shahaniyah
Al Gharrafah
Doha
Qatar
Ar Rayyan
Umm Bab
Al Wakrah
Al Wukayr
Kuwait
Iran
Al Kir'anah
Umm Said
25°00'
Al Kharrarah
Area mapped
Qatar
Saudi Arabia
U.A.E.
As Salwá
N
Saudi Arabia
U. A. E.
0
20 km
0
15 mi
©1997 MAGELLAN Geographix℠
(805) 685-3100 www.maps.com

1975-80

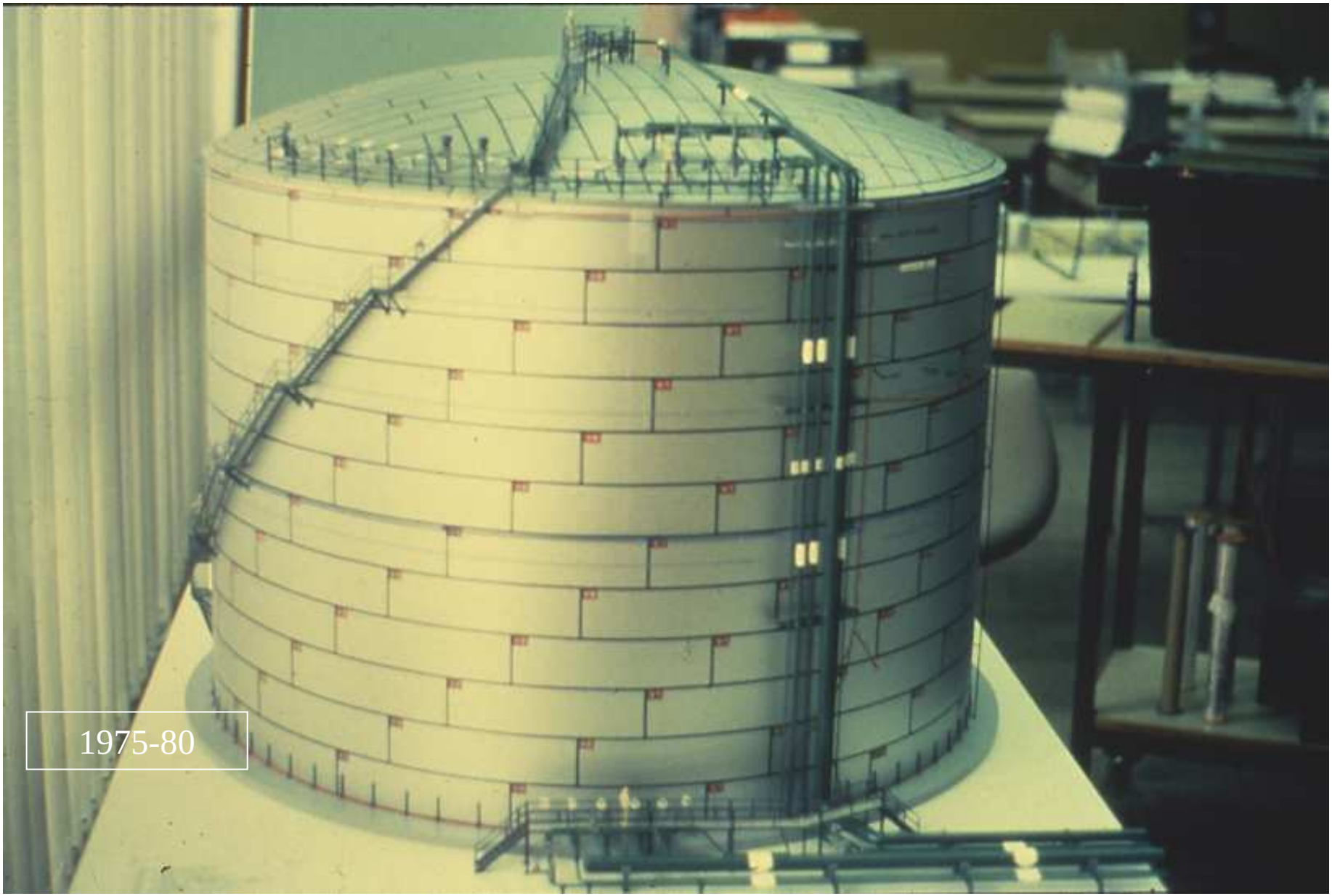
1975-80


1975-80


1975-80


1975-80


1975-80


1975-80

# BRITTLE FRACTURE & BRITTLE to DUCTILE TRANSITION APPLICATIONS TO COMPONENTS

André PINEAU
Centre des Matériaux - Ecole des Mines de Paris. ParisTech
UMR CNRS 7633
andre.pineau@ensmp.fr

# HETEROGENEOUS MATERIALS (1)

*C. Naudin, PhD Thesis, 1999*

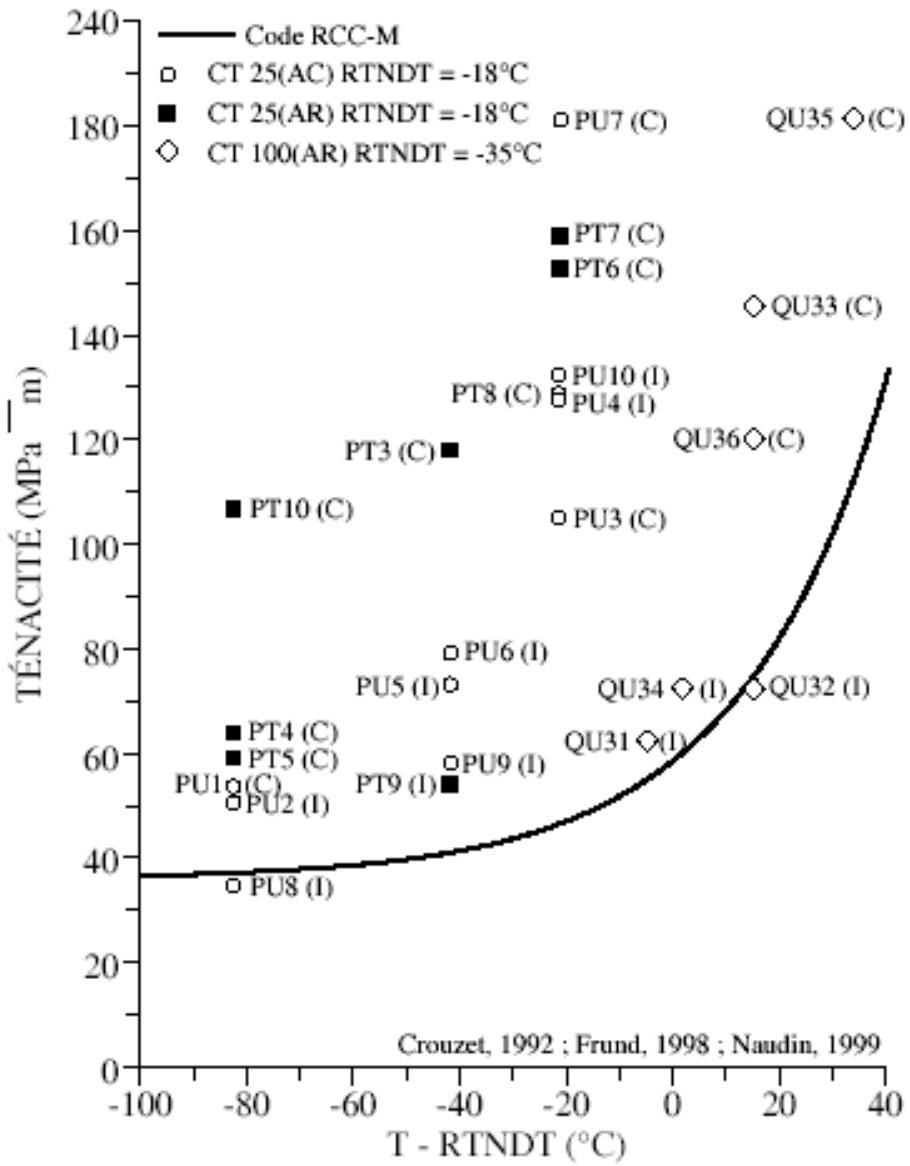


EDF

# INTERGRANULAR FRACTURE - 16MND5 STEEL

*C. Naudin, PhD Thesis, 1999*

CT Specimen. Number PU5
Intergranular Initiation Site
Temperature = - 60°C

$K_{IC} = 74\,MPa\sqrt{m}$

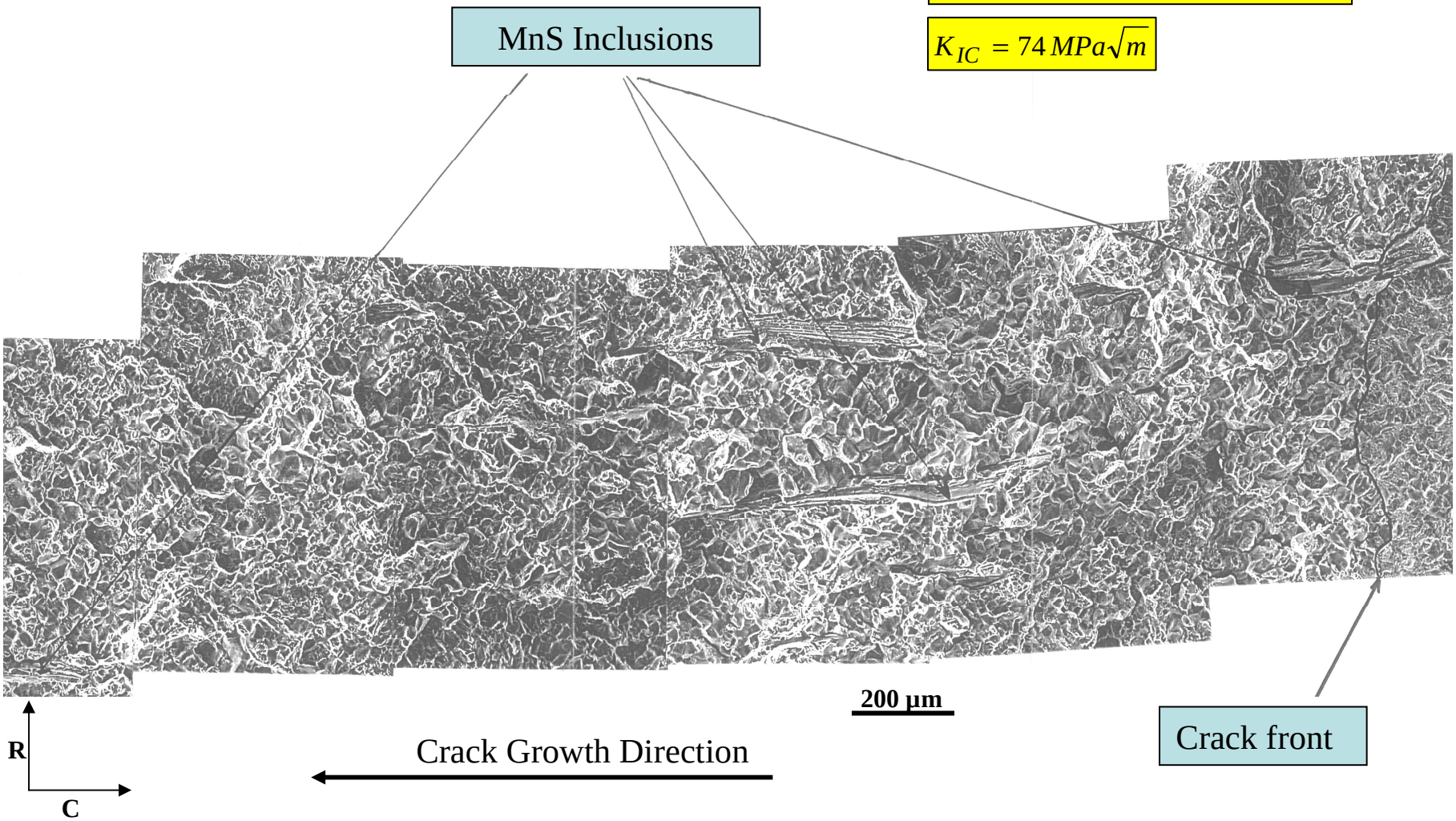

# GHOST LINES (1)

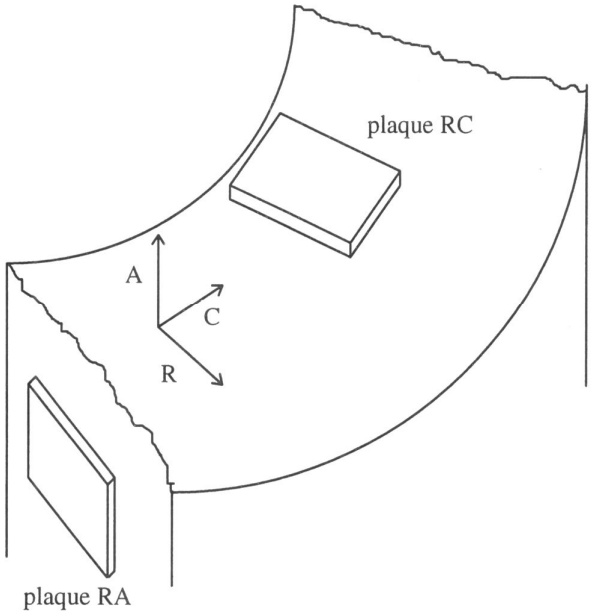


A = sens axial
C = sens circonférentiel
R = sens radial

↓ peau interne ↓

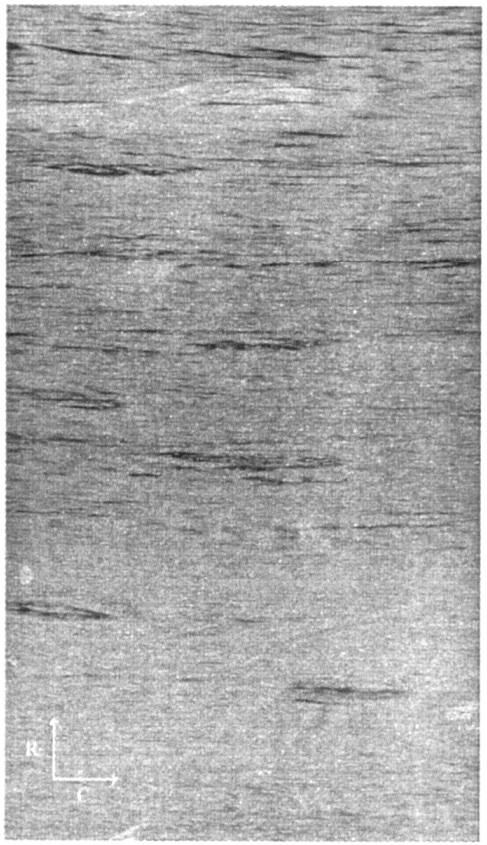

↑ mi-épaisseur ↑

Plan RC

100 mm

↓ peau interne ↓

↑ mi-épaisseur ↑

Plan RA

# GHOST LINES (2)

*C. Naudin, PhD Thesis, 1999*

Composition chimique (% poids)

| % en poids | C | Mn | Ni | Cr | Mo | Si | Cu | P |
|---|---|---|---|---|---|---|---|---|
| Métal de base | 0,16 | 1,35 | 0,70 | 0,19 | 0,50 | 0,25 | 0,02 | 0,008 |
| Teneur moy. dans 1 V.S. | 0,25 | 1,88 | 0,86 | 0,22 | 1,22 | 0,28 | 0,09 | 0,025 |
| Teneur max. dans 1 V.S. | 0,4 | 2,3 | 1 | 0,4 | 2 | 0,4 | 0,14 | 0,045 |
| Enrichis-sement % | 15 à 30 | 20 à 70 | 10 à 50 | 30 à 80 | 40 à 300 | 15 à 75 | 15 à 75 | 25 à 500 |

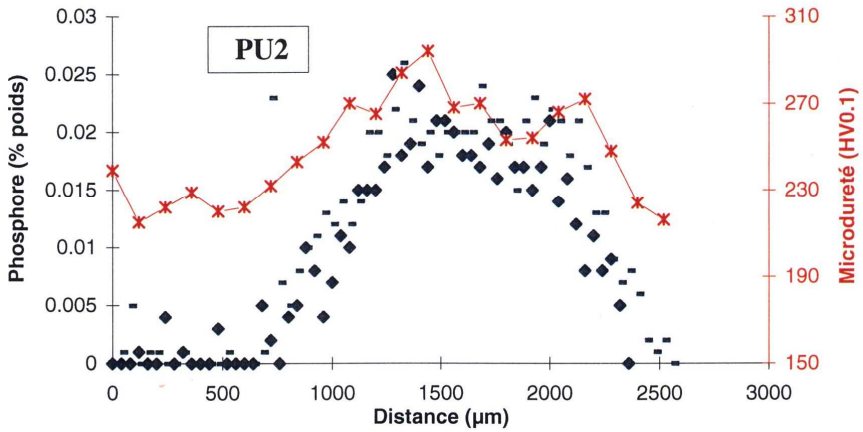


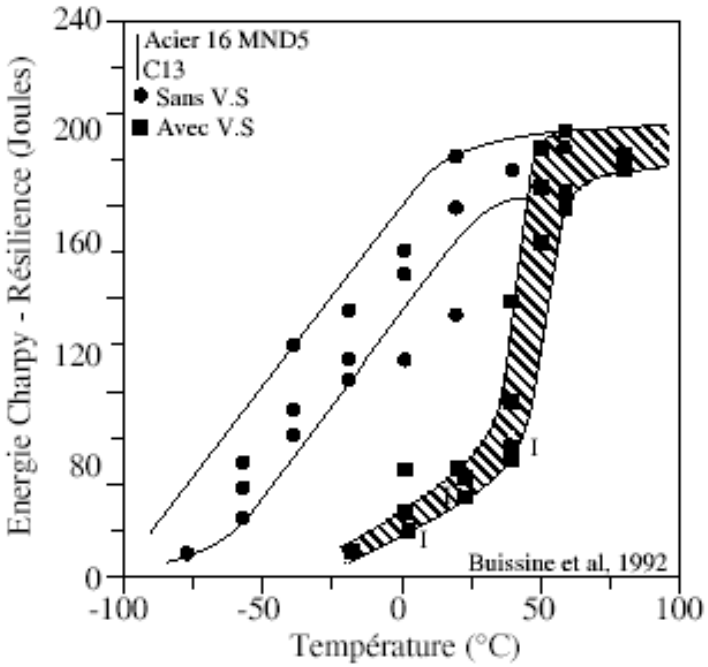

# ARTIFICIAL GHOST LINES (1)

*C. Naudin, PhD Thesis, 1999*

Composition chimique (% poids)

| Matériau | C | Mn | Ni | Mo | P | Cr | S | Cu | Si | Sn |
|---|---|---|---|---|---|---|---|---|---|---|
| Métal de base | 0,15 | 1,28 | 0,74 | 0,5 | 0,008 | 0,18 | 0,009 | 0,06 | 0,15 | 0,005 |
| Acier MS | 0,25 | 1,88 | 0,86 | 1,22 | 0,025 | 0,22 | 0,009 | 0,09 | 0,28 | 0,019 |

Traitement thermique de détensionnement simulé

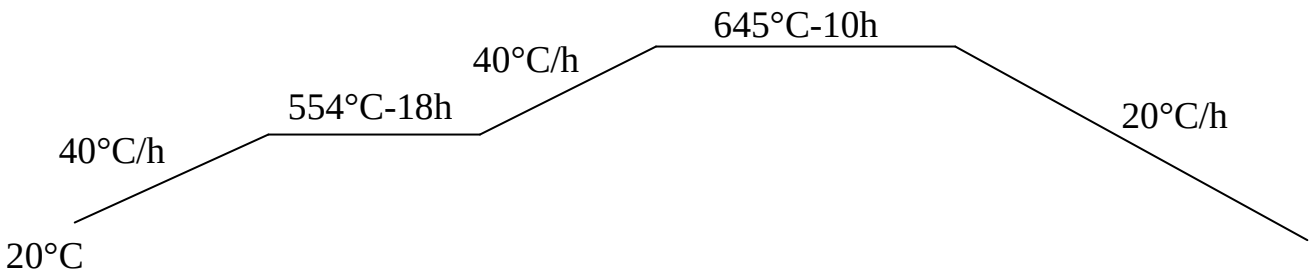


Caractéristiques mécaniques (20 et 300°C)

| Matériau | T(°C) | Re (MPa) | Rm (MPa) | A (%) | S (%) |
|---|---|---|---|---|---|
| Métal | 20 | 576 | 693 | 22 | 70 |
| de base | 300 | 499 | 640 | 25 | 68 |
| | 20 | 645 | 773 | 20 | 57 |
| Acier MS | 300 | 614 | 759 | 16 | 53 |

# ARTIFICIAL GHOST LINES (2)

*C. Naudin, PhD Thesis, 999*

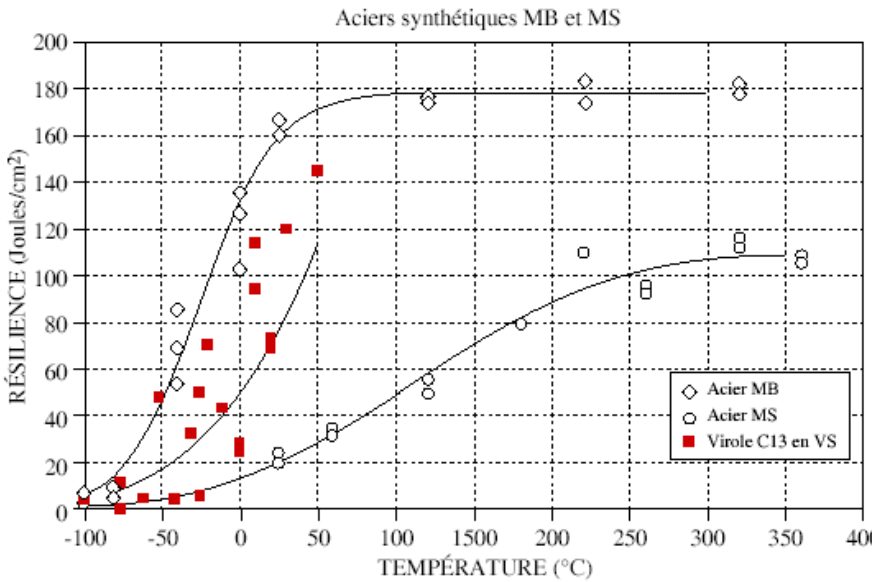


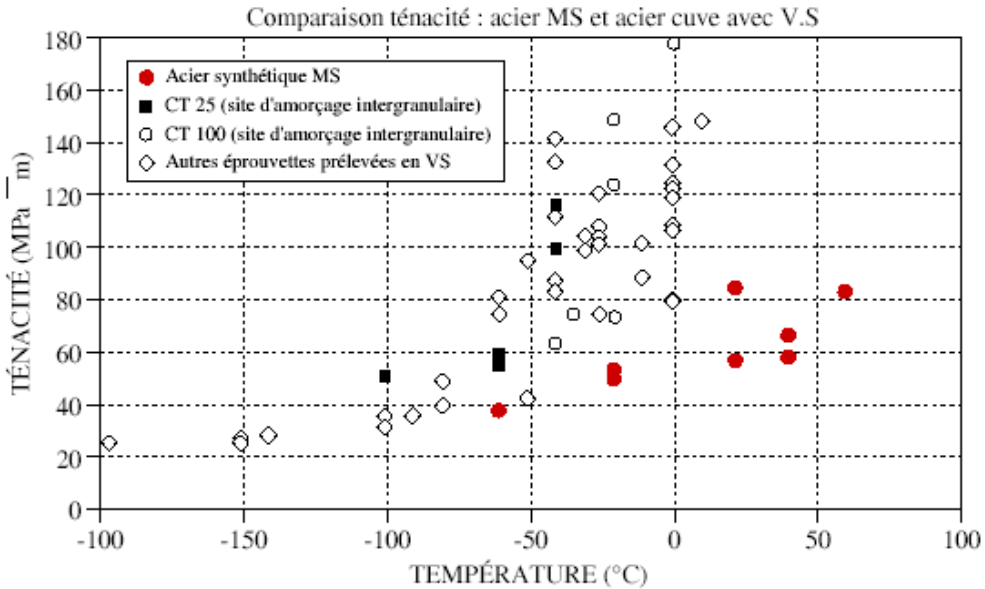


+ Application de divers traitements thermiques de fragilisation dont refroidissement étagé

# ARTIFICIAL GHOST LINES (3)

*C. Naudin, PhD Thesis, 1999*

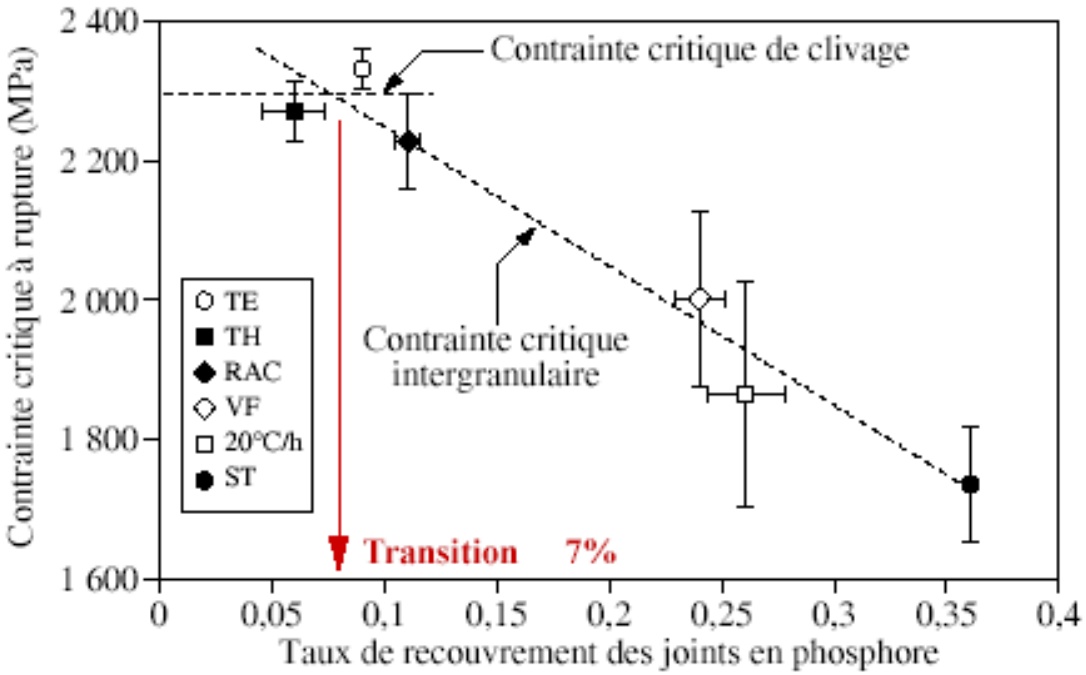


- TE : Trempe eau (4 000°C/min)
- TH : Trempe huile (720°C/min
- RAC : Refroidissement air calme (43°C/min)
- VF : Refroidissement au four (5°C/min)
- 20°C/h
- ST : Refroidissement étagé

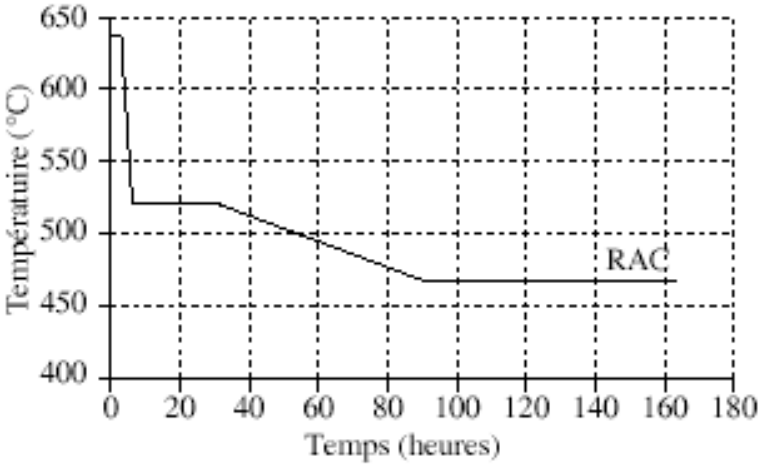

# EQUILIBRIUM SEGREGATION (1)

D. Mc Lean, 1957

- Impureté : Phosphore. Pas d'interaction avec d'autres éléments
- Données expérimentales obtenues par refroidissement étagé (C. Naudin, 1999)
  Matériau reconstitué représentatif des veines sombres (P = 0,025 % Poids) (0,045 % At.)

$$C_b(C_g, T) = C_g \exp\left(\frac{E_b}{kT}\right) \Big/ \left[1 + C_g \exp\left(\frac{E_b}{kT}\right)\right] \qquad (1)$$

$$E_b = 63000 - 21{,}0\,T \ (\text{Joule / mole}) \qquad (E_b = 0{,}52\,eV \ \text{à } 320°C)$$

$$C_x(C_g, T, t) = C_g + (C_b - C_g)\left[1 - \exp\left(\frac{4D_i t}{\alpha^2 d_1^2}\right) erfc\left(\frac{2\sqrt{D_i t}}{\alpha\, d_1}\right)\right] \qquad (2)$$

$$\alpha = \frac{C_b}{C_g}$$

$$D_i = D_{io} \exp\left(-\frac{Q_i}{kT}\right) \qquad (cm^2\, s^{-1})$$

$$D_{io} = 0{,}25; \qquad Q_i = 200\,KJ\,/\,\text{mole} = 2{,}08\,eV$$

$$d_1 = \text{épaisseur du joint} = 8\ 10^{-8}\,cm$$

# EQUILIBRIUM SEGREGATION (2)

**Cg=0.01% At**

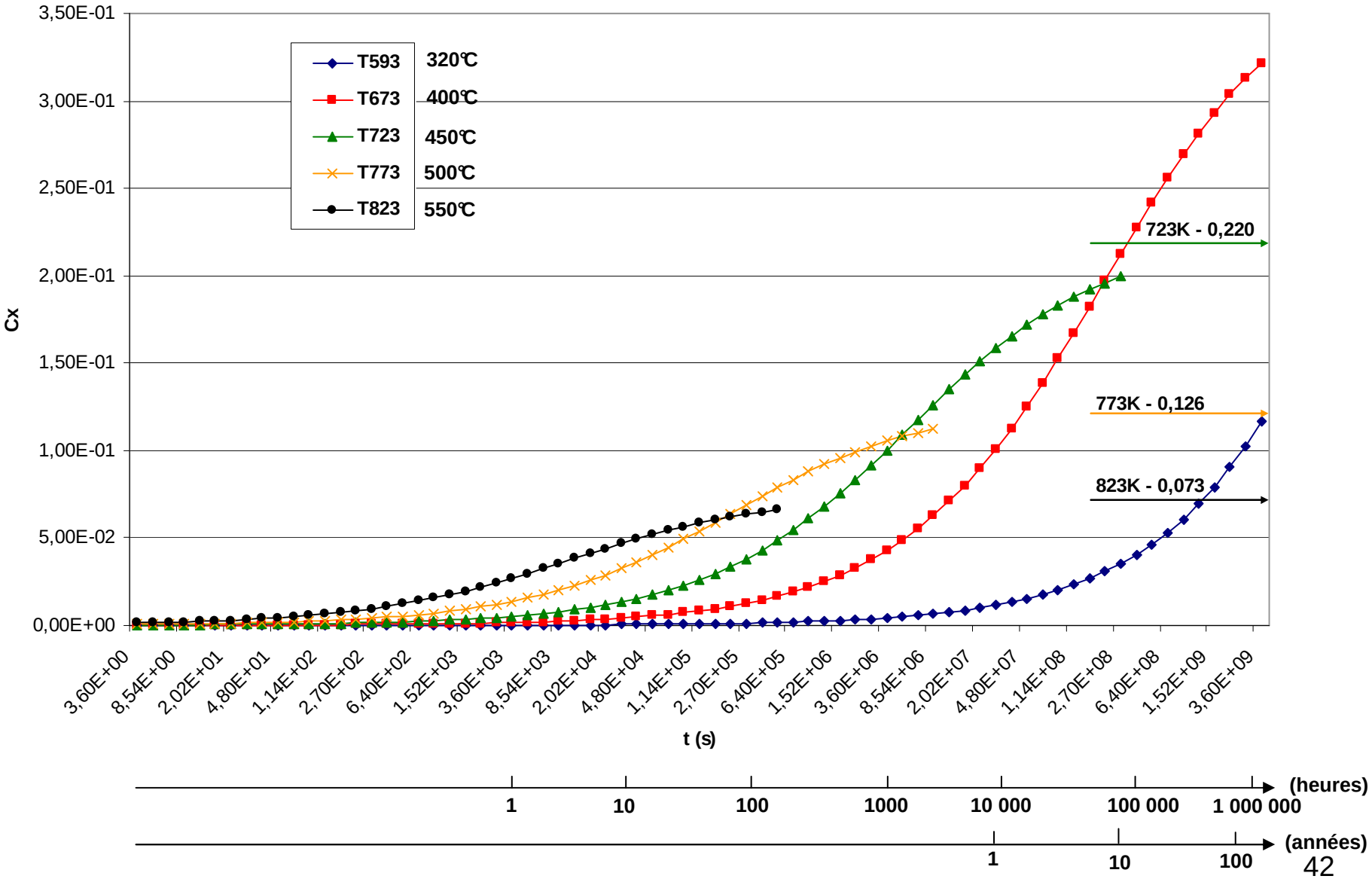

# EQUILIBRIUM SEGREGATION (3)

Cg=0.035% At

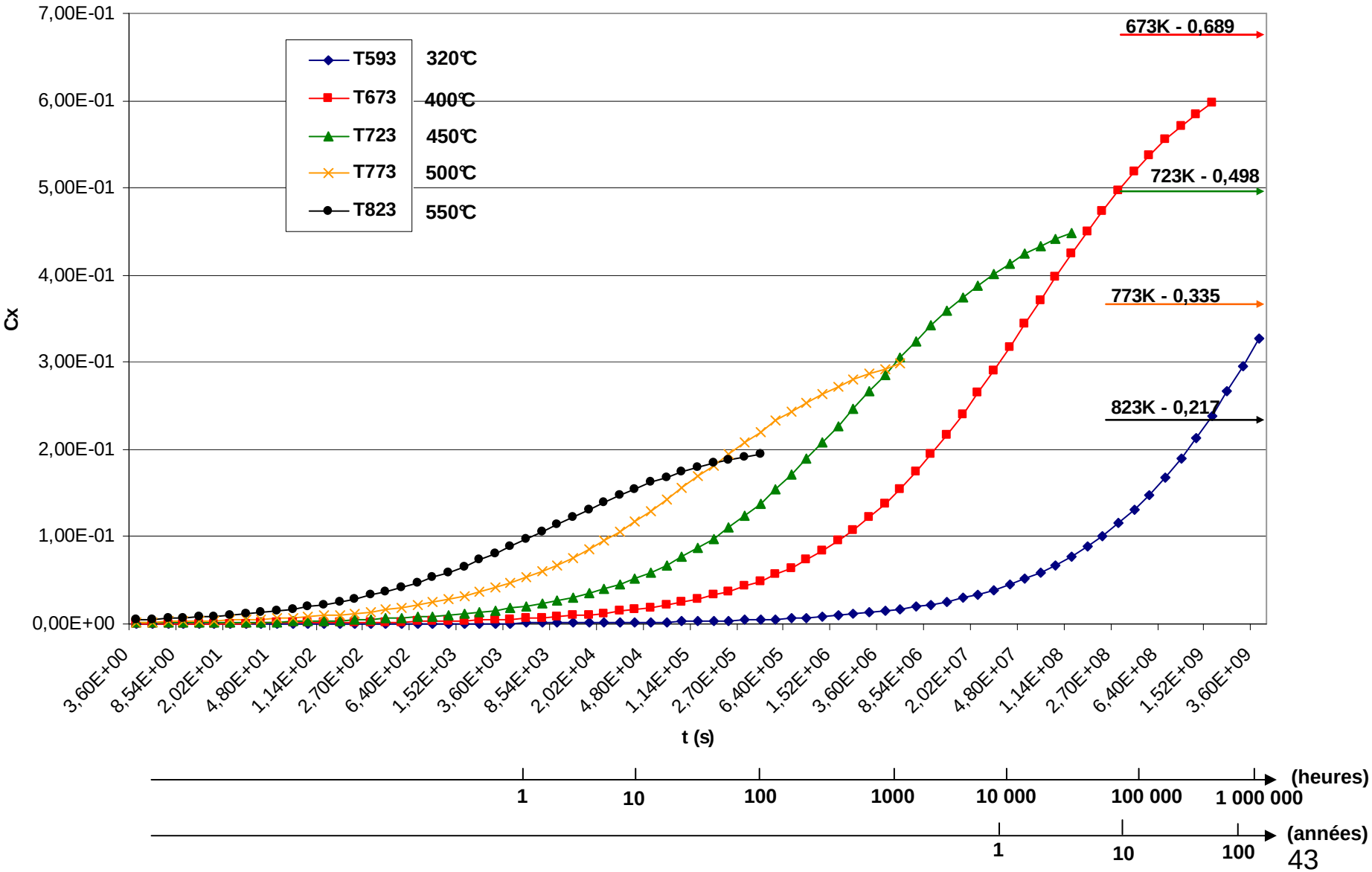

# EQUILIBRIUM SEGREGATION (4)

Cg=0.07% At

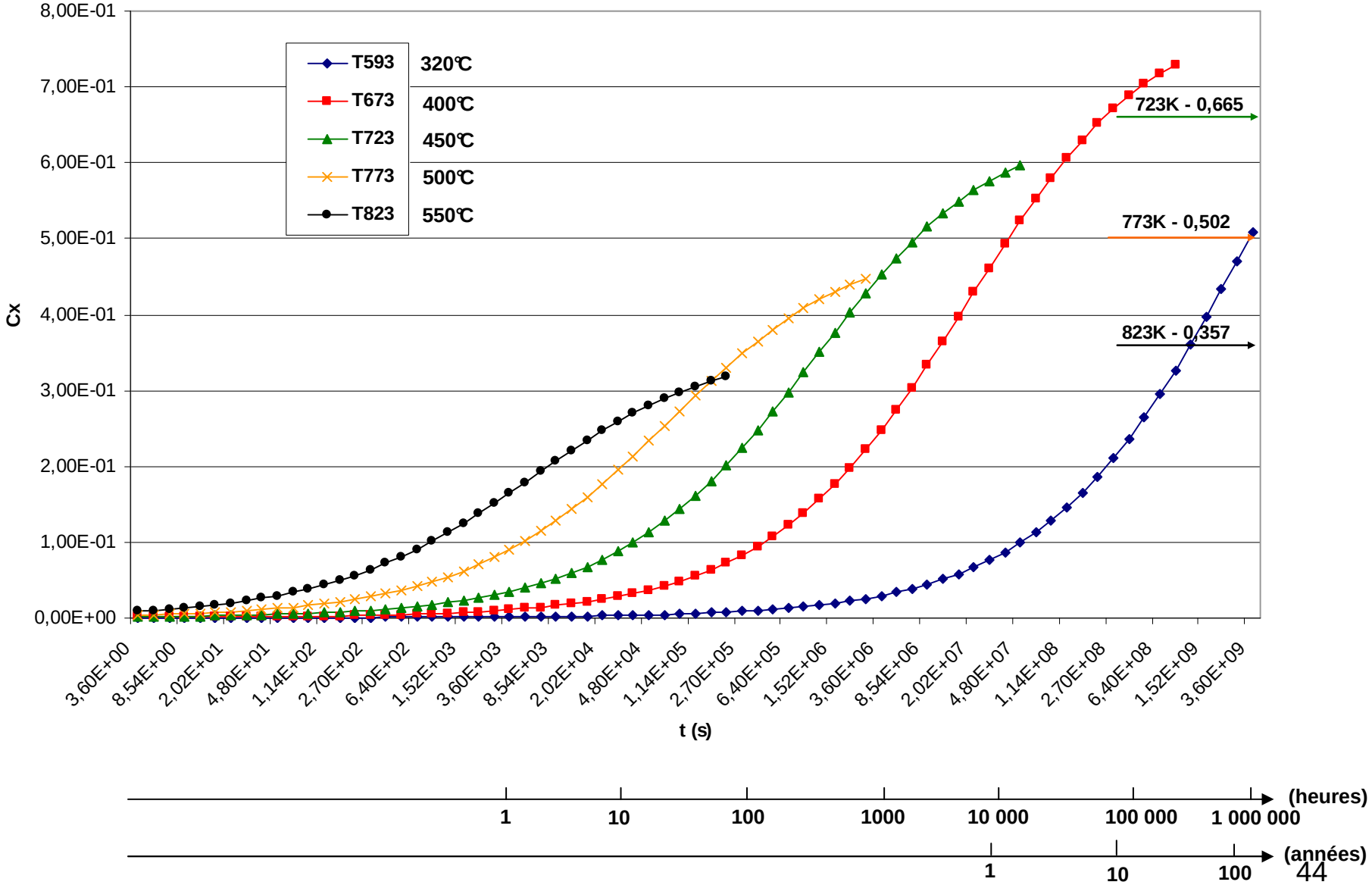

# MODELLING OF MIXED INTERGRANULAR and CLEAVAGE FRACTURE IN SEGREGATED STEELS

CT Specimen W = 20 mm

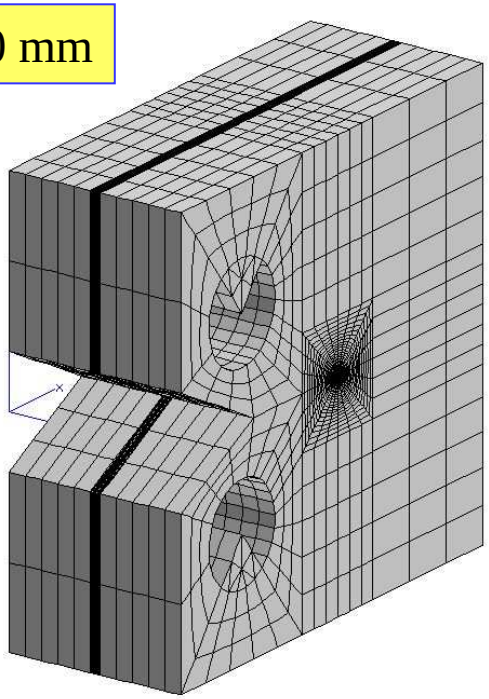

Double Isotropic Hardening For Both Materials

| A T=-100°C | E (GPa) | $R_{0.2}$ (MPa) | B1 | Q1 | B2 | Q2 |
|---|---|---|---|---|---|---|
| MB | 200 | 539.6 | 12.16 | 324.3 | 0.422 | 296 |
| MI | 240 | 750 | 12.16 | 434 | 0.422 | 450 |

Constitutive Equations

| T = -100°C | $\sigma_u$ (MPa) | m | $V_0$ en $\mu m^3$ |
|---|---|---|---|
| MI | 3700 | 15 | 50 |
| MB | 2710 | 22 | 50 |

Fracture Properties

# Stress – Strain Curves ( n = 0.15 )

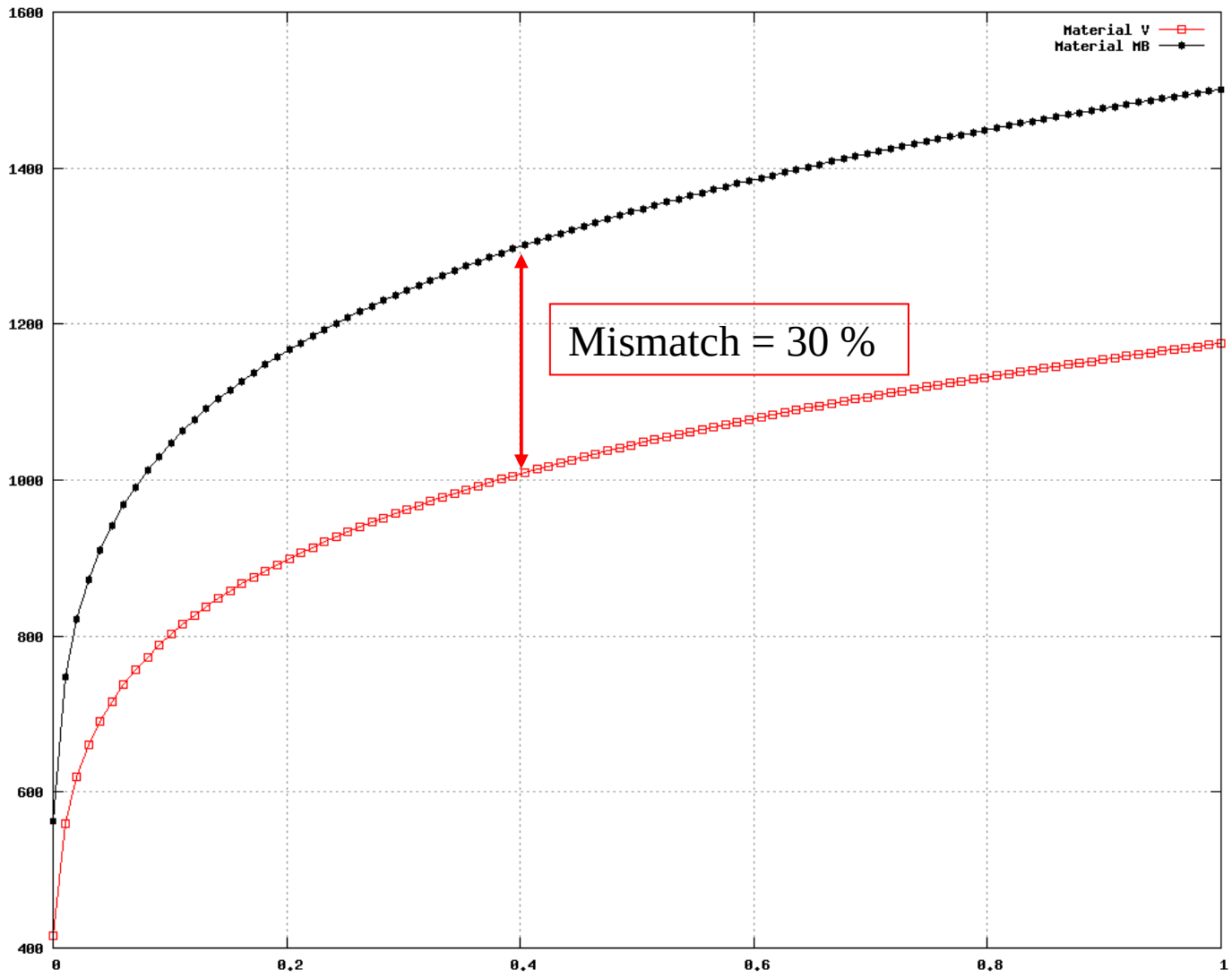

CRACK TIP

K = 45 MPa.m^0.5

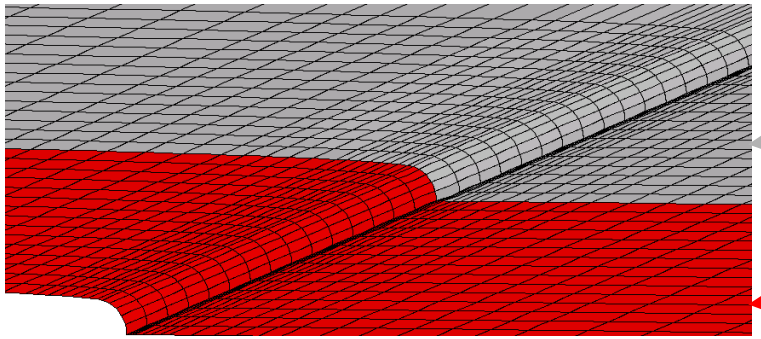

MATRIX – Soft & Tough material

SEGREGATED Material
Strong & Brittle

K = 60 MPa.m^0.5

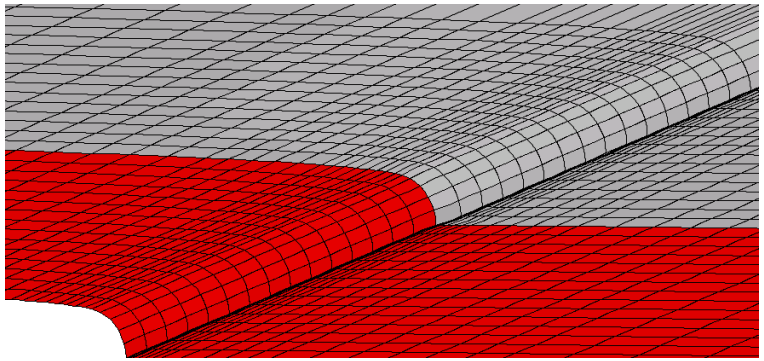

K = 75 MPa.m^0.5

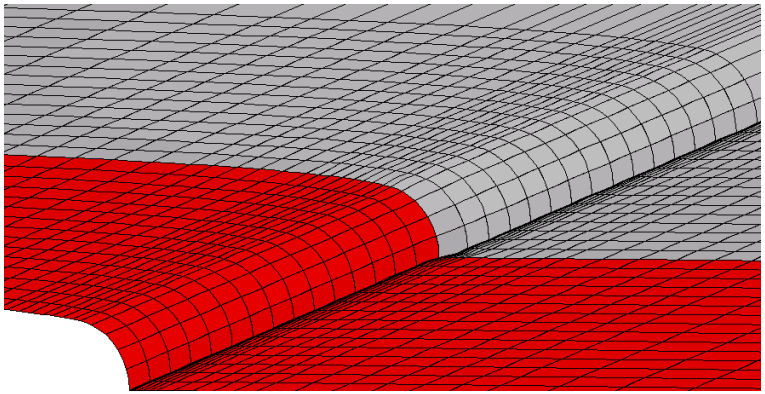

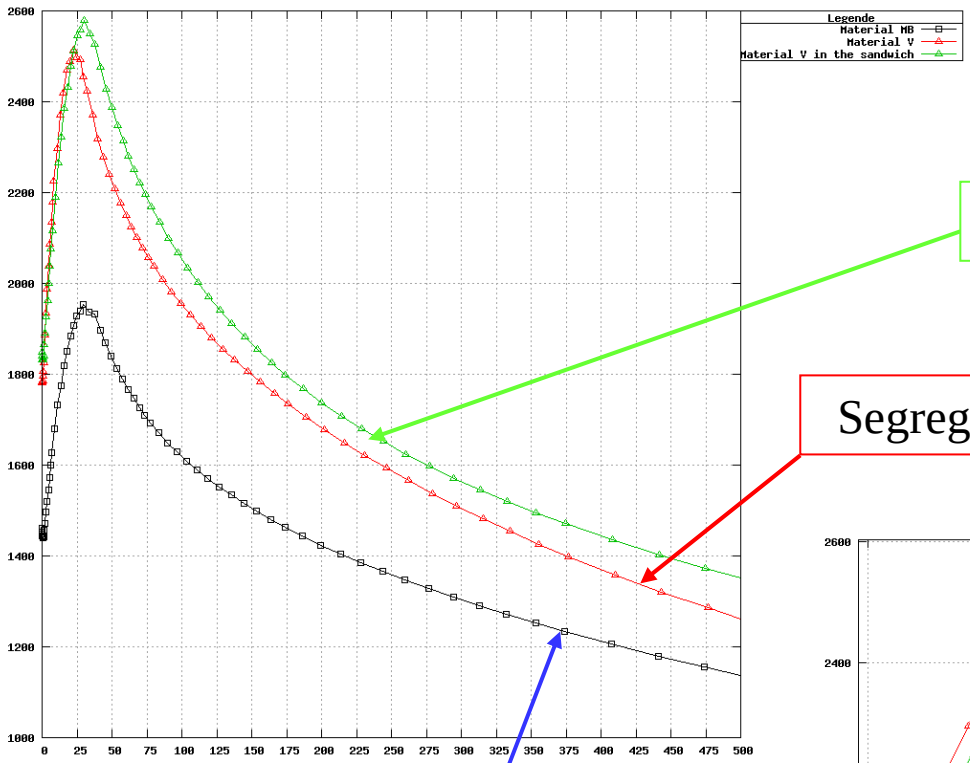


Segregated Material within the Matrix

Segregated Material Alone

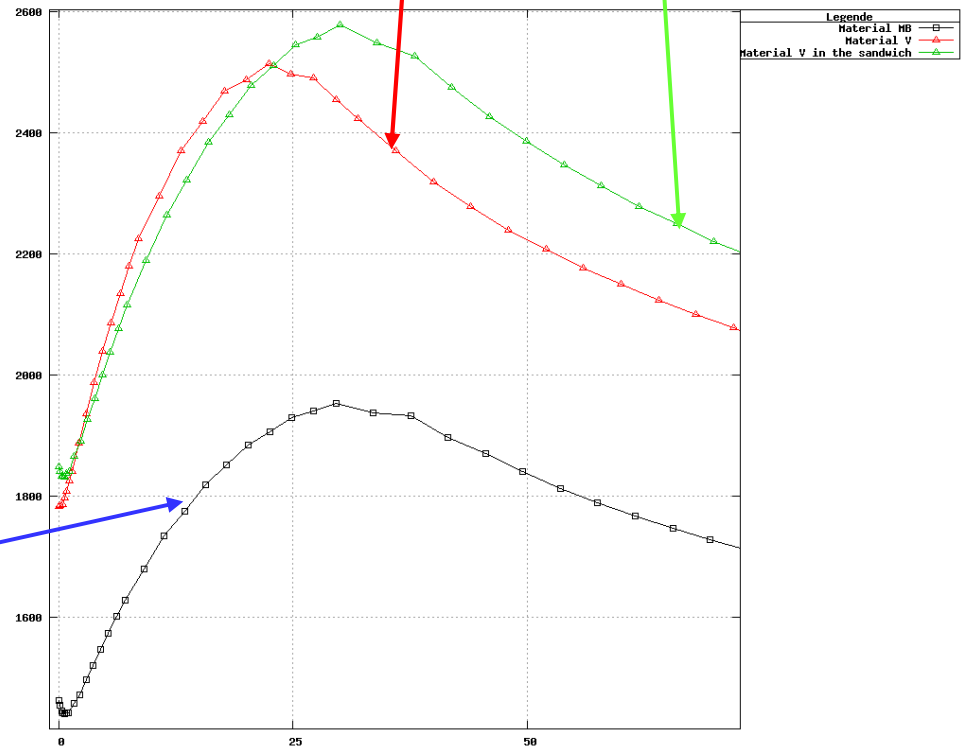


Base Material Alone

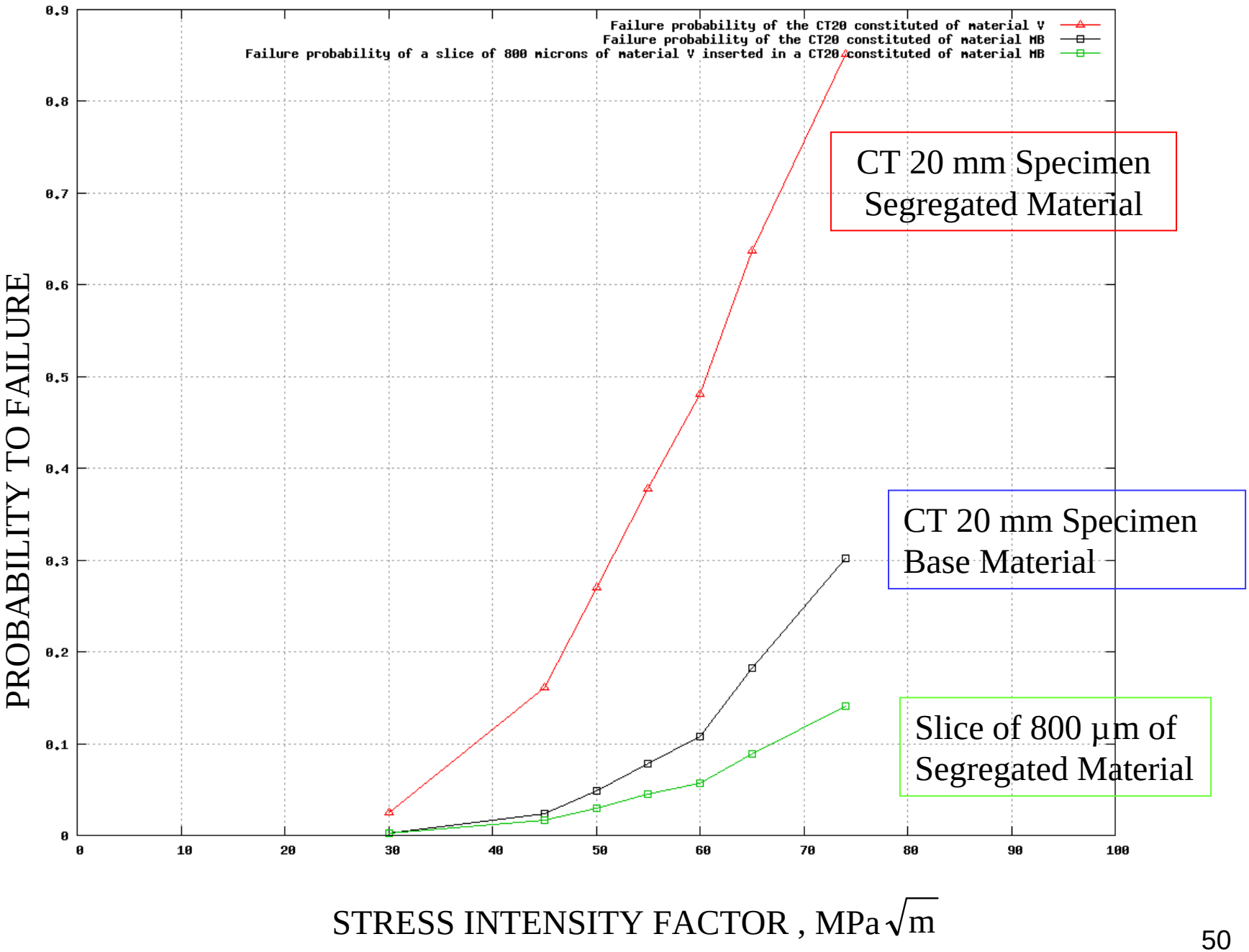
Failure probability of the CT20 constituted of material V
Failure probability of the CT20 constituted of material MB
Failure probability of a slice of 800 microns of material V inserted in a CT20 constituted of material MB
CT 20 mm Specimen
Segregated Material
CT 20 mm Specimen
Base Material
Slice of 800 µm of
Segregated Material
PROBABILITY TO FAILURE
STRESS INTENSITY FACTOR , MPa √m
0
0.1
0.2
0.3
0.4
0.5
0.6
0.7
0.8
0.9
0
10
20
30
40
50
60
70
80
90
100

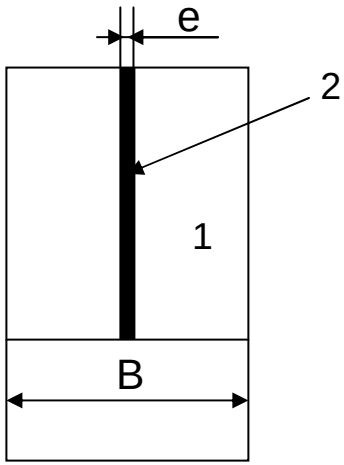


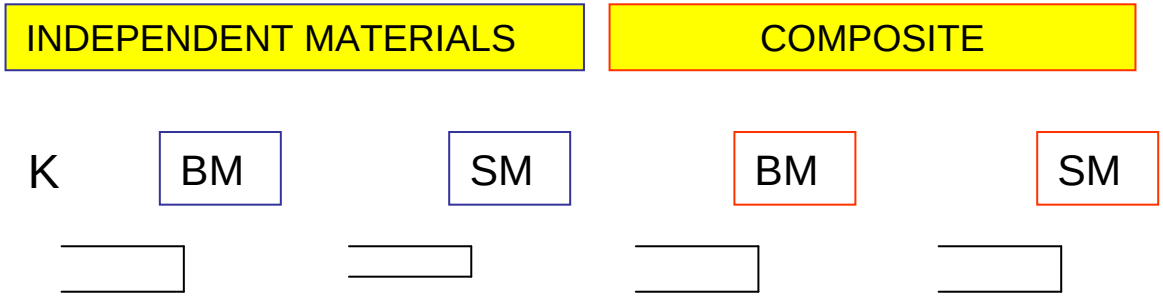


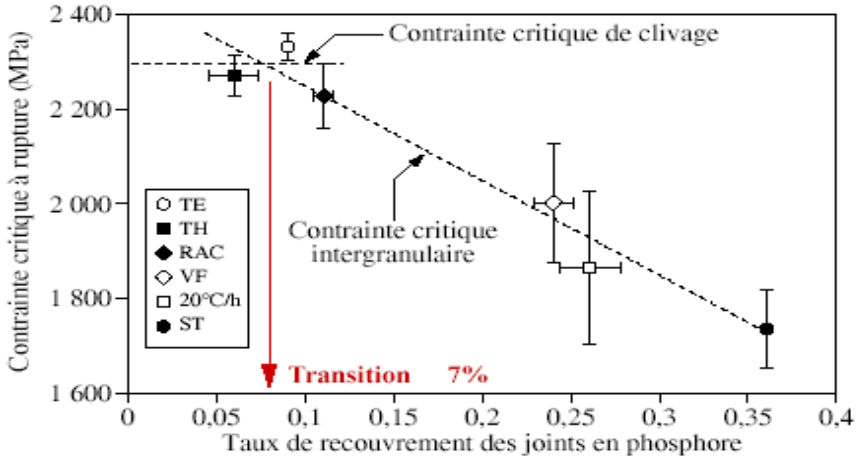


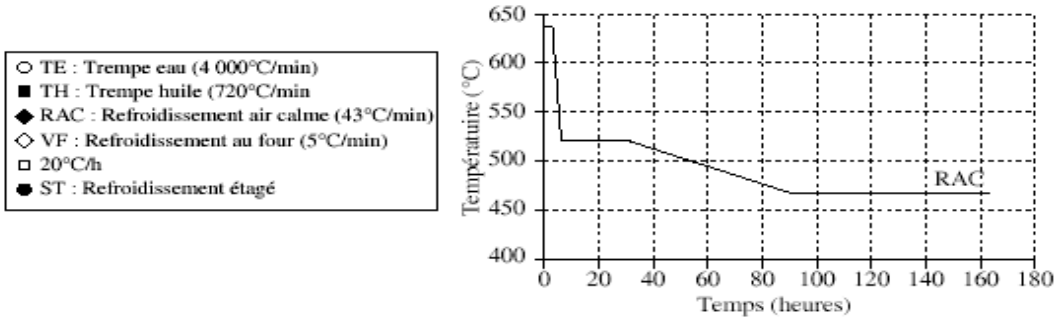


$$CTOD = \frac{K^2}{E\,\sigma_Y}$$

$$K_{I,1} = K_{I,2}\left(\frac{\sigma_{Y,1}}{\sigma_{Y,2}}\right)^{1/2}$$

$$P_{R1} = P_{R2}$$

$$\frac{e}{B} = \frac{\sigma_{Y1}^{m_1}}{\sigma_{Y2}^{m_2}}\,\frac{V_{0,2}}{V_{0,1}}\,\frac{\sigma_{u,2}^{m_2}}{\sigma_{u,1}^{m_1}}\,\frac{C_{m_1}}{C_{m_2}}$$

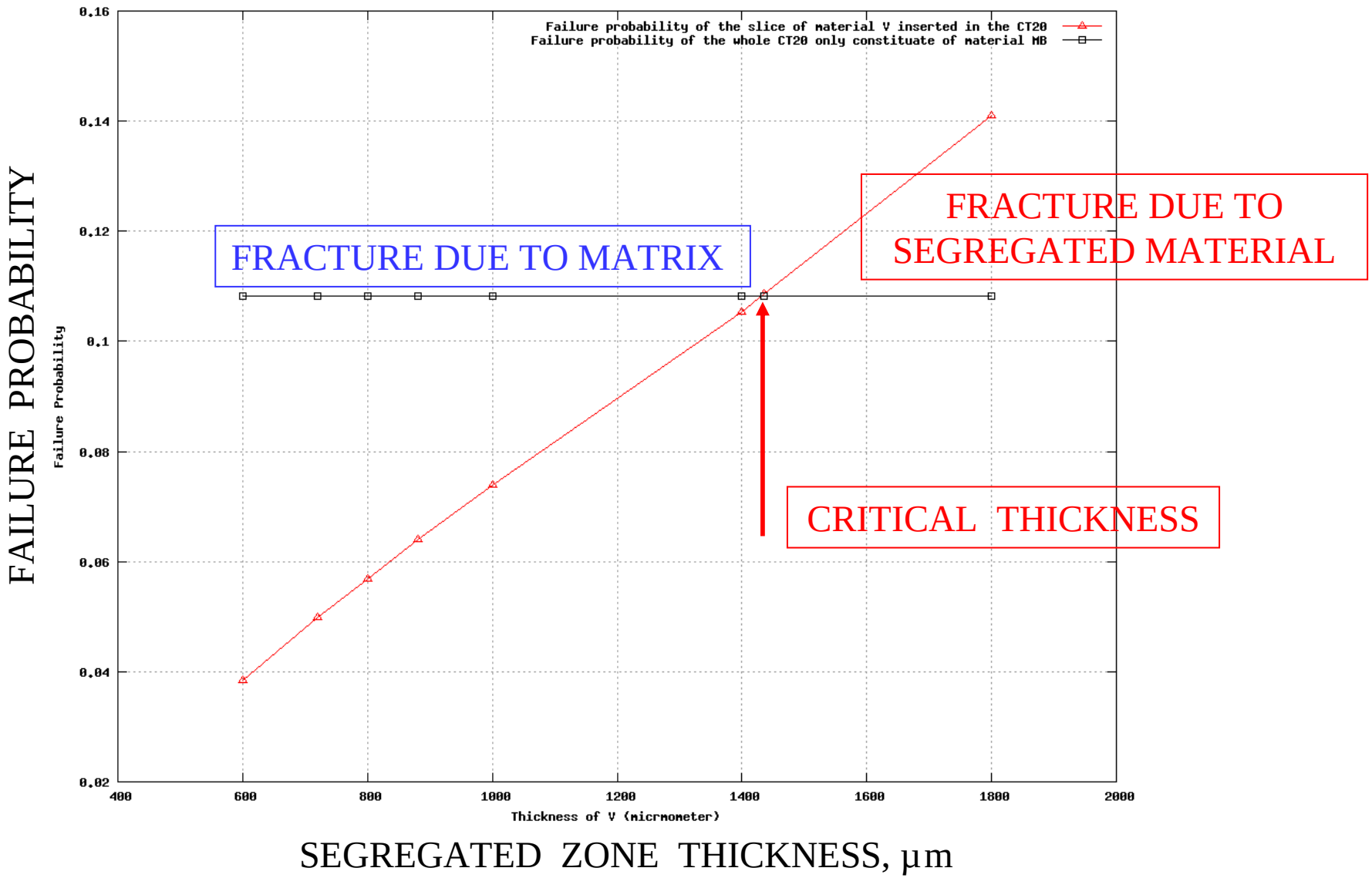
FAILURE PROBABILITY
Failure Probability
Failure probability of the slice of material V inserted in the CT20
Failure probability of the whole CT20 only constituate of material MB
FRACTURE DUE TO MATRIX
FRACTURE DUE TO SEGREGATED MATERIAL
CRITICAL THICKNESS
0.16
0.14
0.12
0.1
0.08
0.06
0.04
0.02
400
600
800
1000
1200
1400
1600
1800
2000
Thickness of V (micrmometer)
SEGREGATED ZONE THICKNESS, µm

# INITIATION OF INTERGRANULAR CRACKS IN AN AL ALLOY

# Experimental investigations of intergranular Brittle Fracture in AA5083

Edouard Pouillier
edouard.pouillier@mat.ensmp.fr
E. Busso, A-F. Gourgues

*Mines ParisTech, CNRS UMR 7633*
*Centre des Materiaux*
*BP 87, 91003 Evry cedex, France*

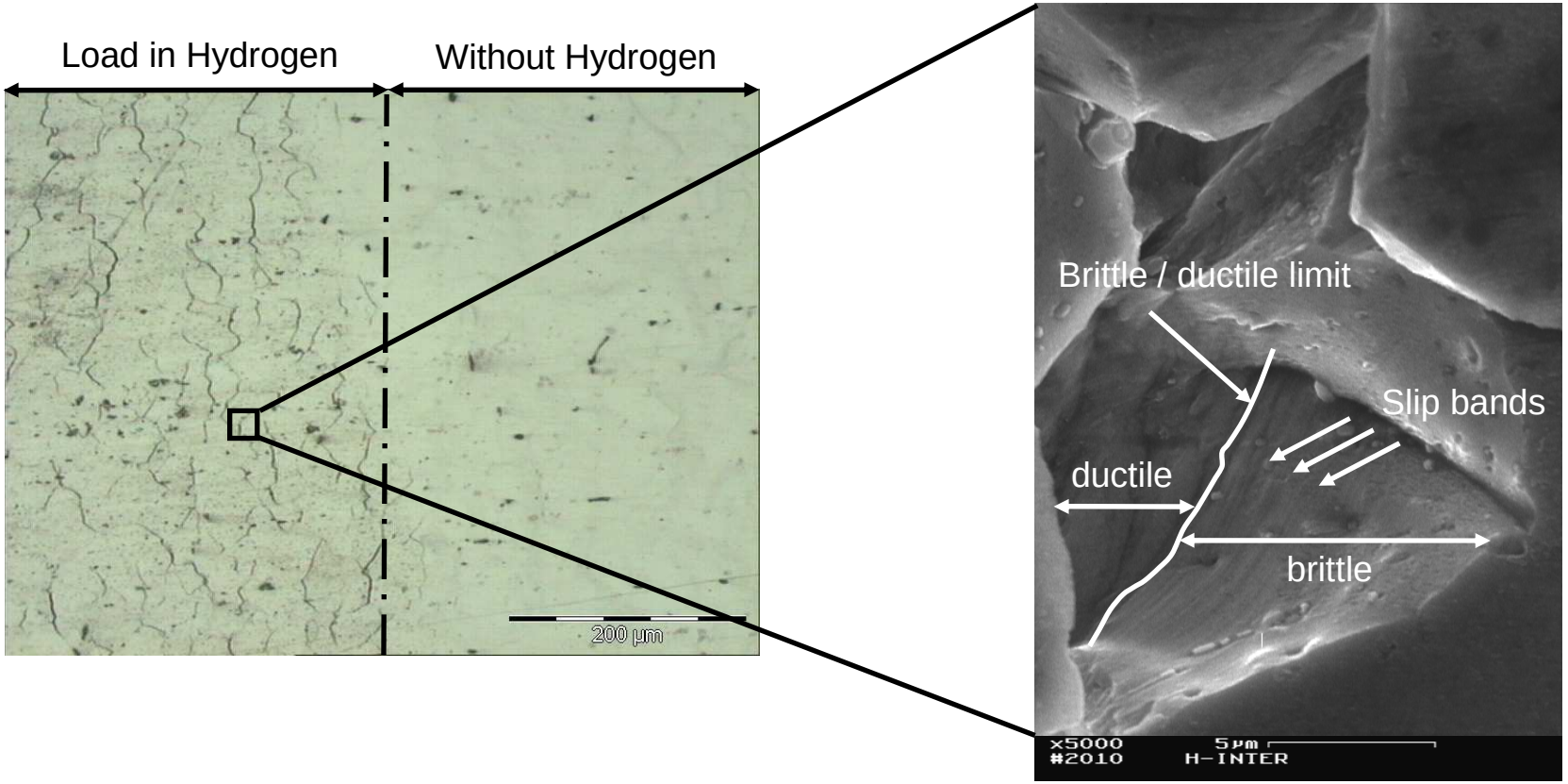


*Example of intergranular cracks after 5% of macroscopic strain*

Intergranular hydrogen embrittlement ⇨ major impact on mechanical strength

---

Aim of the study: establish the link between intergranular cracks and plasticity.

- Applications : Ship building, Rail cars, Vehicle bodies, Tip truck bodies, Mine skips and cages, Pressure vessels.

- Mechanical properties

| | |
|---|---|
| Proof Stress 0.2 (MPa) | 125 |
| Tensile Strength (MPa) | 250 |
| Shear Strength (MPa) | 175 |
| Elongation A5 | 23 |
| Hardness Vickers | 75 |

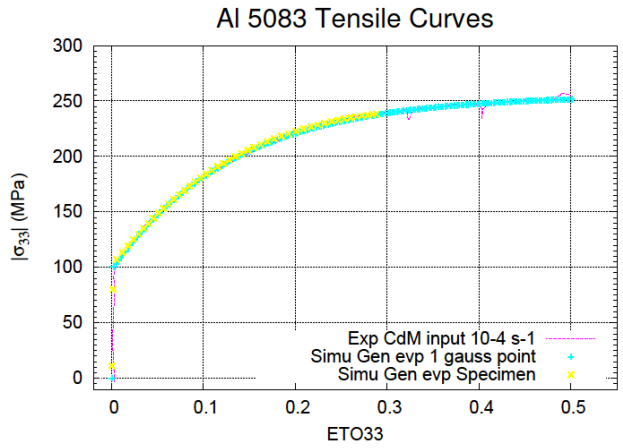


- Manufacturing process

Extruded rod end bar
Rotative hammering 30% of deformation

Curing:
Recrystallization 1h 450 ℃
Aging 7d 150 ℃

⇩

$Al_3Mg_2$ precipitation at grain boundaries

- Chemical composition

| Element | Si | Fe | Cu | Mn | Mg | Zn | Ti | Cr | Al |
|---|---|---|---|---|---|---|---|---|---|
| Present | 0.4 | 0.4 | 0.1 | 0.7 | 4.5 | 0.25 | 0.15 | 0.25 | Balance |

- Hydrogen charging in Al 5083

Inside a boric acid solution (pH 4) and negative electric current on the specimen surface :
Aluminium matrix and $Al_3Mg_2$ became a galvanic couple
Aluminium matrix and $Al_3Mg_2$ are cathodically polarized

⇨ Embrittlement due to trapped hydrogen at grain boundaries

Coupling between experimental measurements : Electron backscatter diffraction (EBSD) and Digital image correlation (DIC) during tensile test inside scanning electron microscope

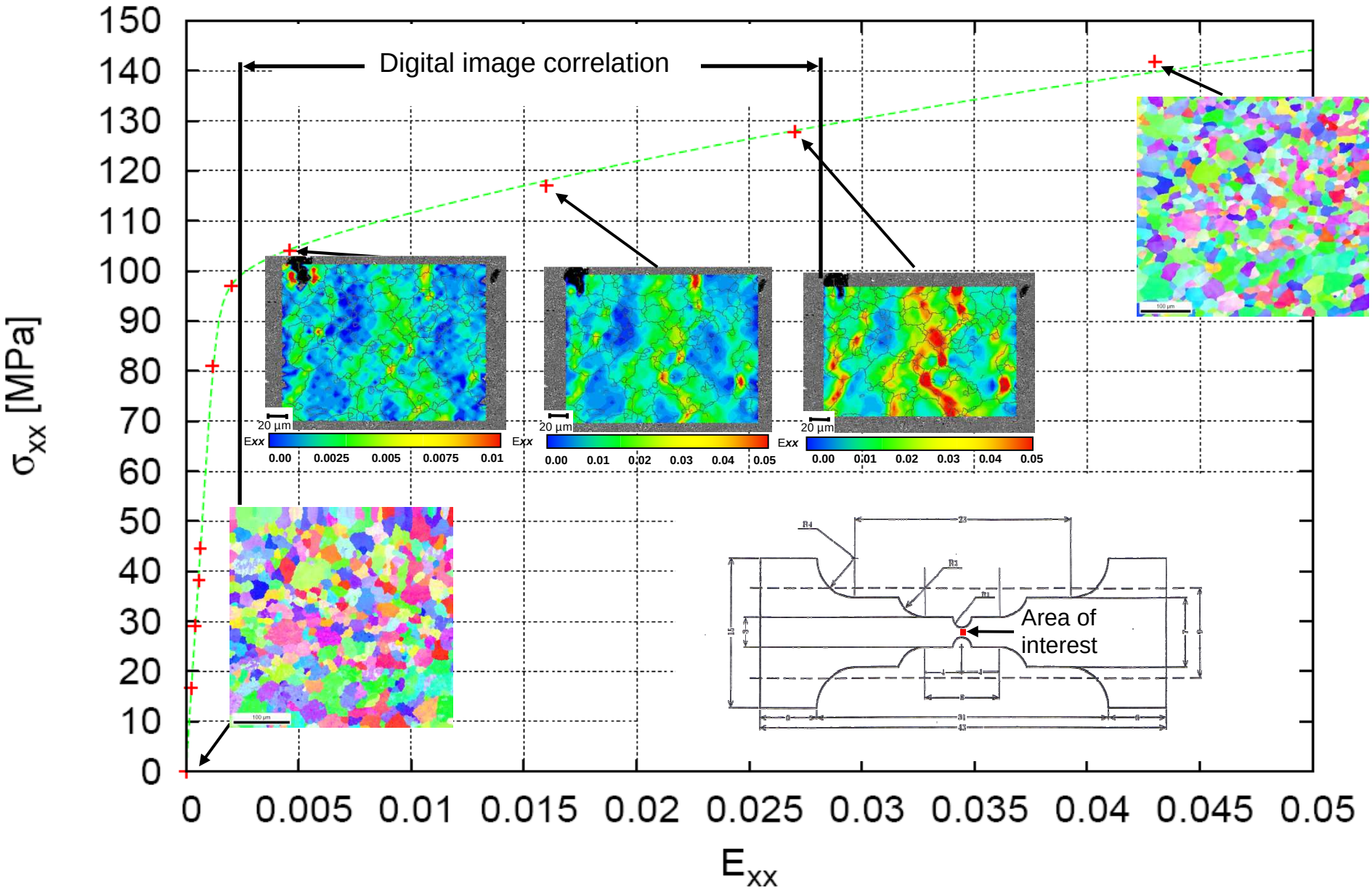

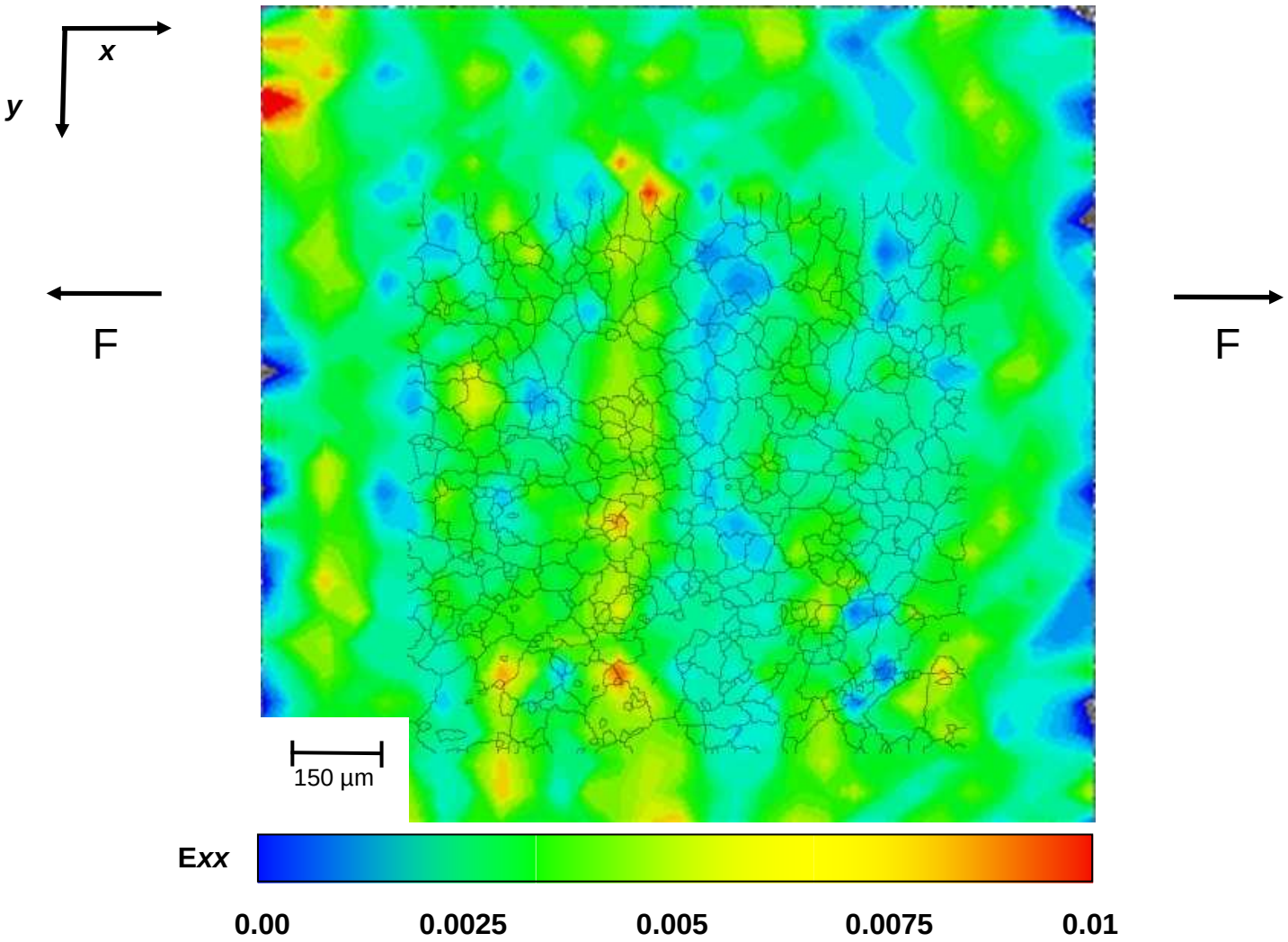


Experimental strain field Exx with grain boundaries, from tensile test performed to 0.45% of macroscopic strain.



⇨ Close relation between cracks and large deformed strip

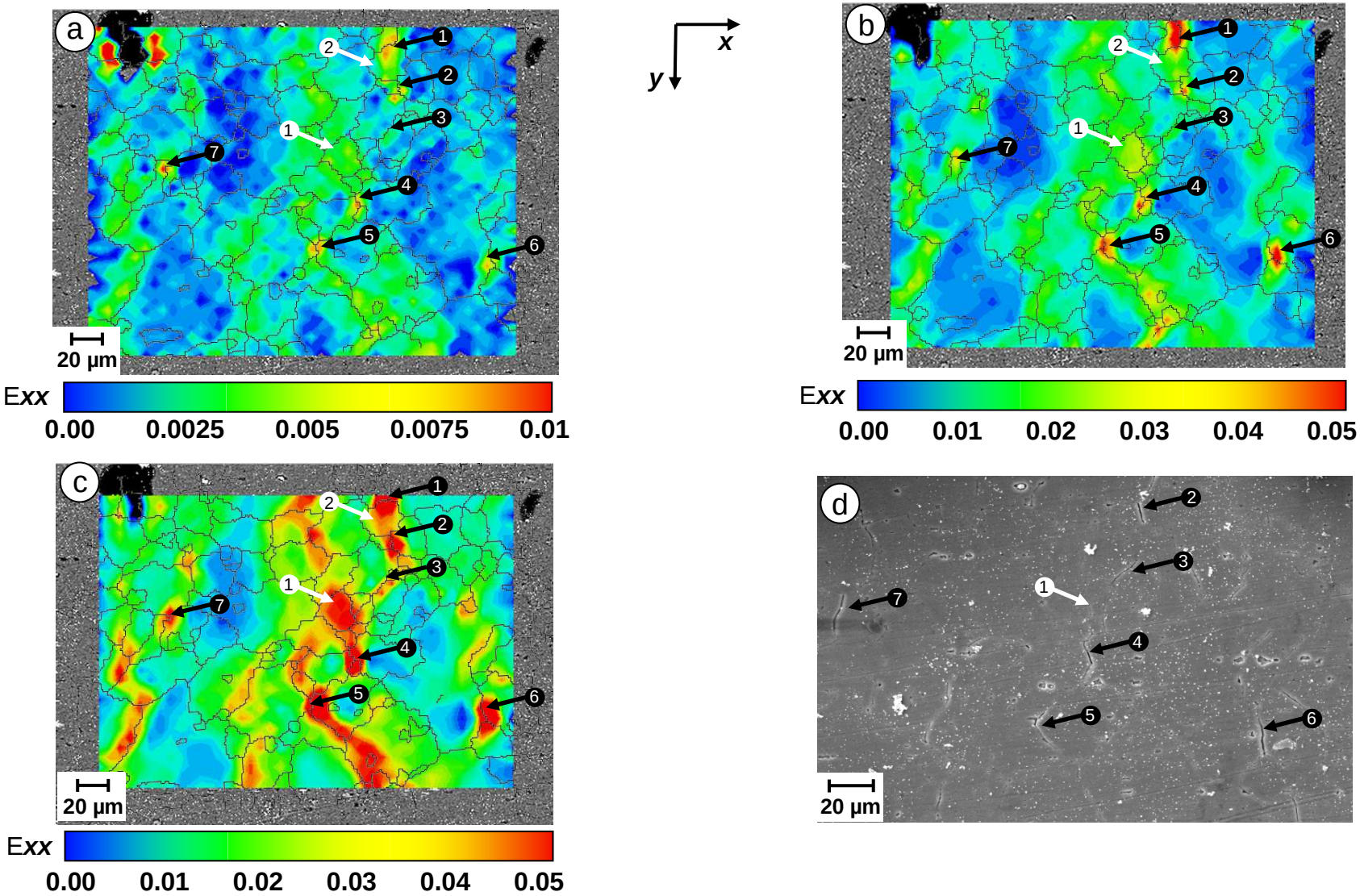


Experimental strain field Exx from tensile test performed to (a) 0.45%, (b) 1.6% (c) 2.7% (d) SEM image to 4.5%, of macroscopic strain.

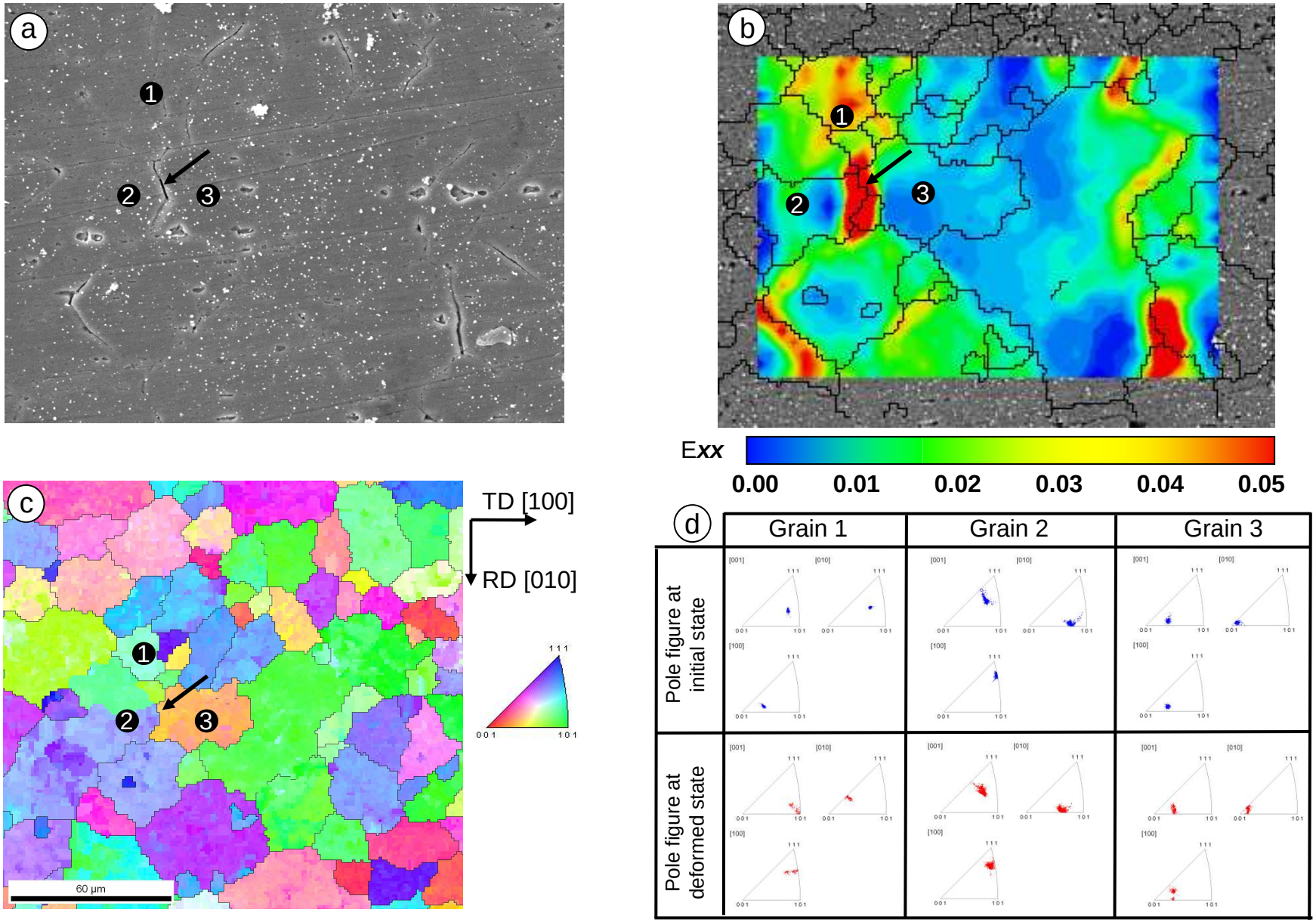


(a) SEM image to 4.5%, of macroscopic strain. (b) Experimental strain field Exx from tensile test performed to 1.6%, (c) Inverse pole figure,(d) pole figure before and after 4.5%, of macroscopic strain.

# BRITTLE FRACTURE & BRITTLE to DUCTILE TRANSITION APPLICATIONS TO COMPONENTS

André PINEAU
Centre des Matériaux - Ecole des Mines de Paris. ParisTech
UMR CNRS 7633
andre.pineau@ensmp.fr

*A.S. Kim et al., Int. J. Solids and Structures,vol.36,1999,pp. 1845-1864*

GLOBAL AND LOCAL APPROACHES TO BRITTLE FRACTURE NORMAL TO INTERFACES

# CRACKS at INTERFACES (1)

*A.S. Kim et al., Int. J. Solids Struct., vol. 36, 1999, pp. 1845-1864*

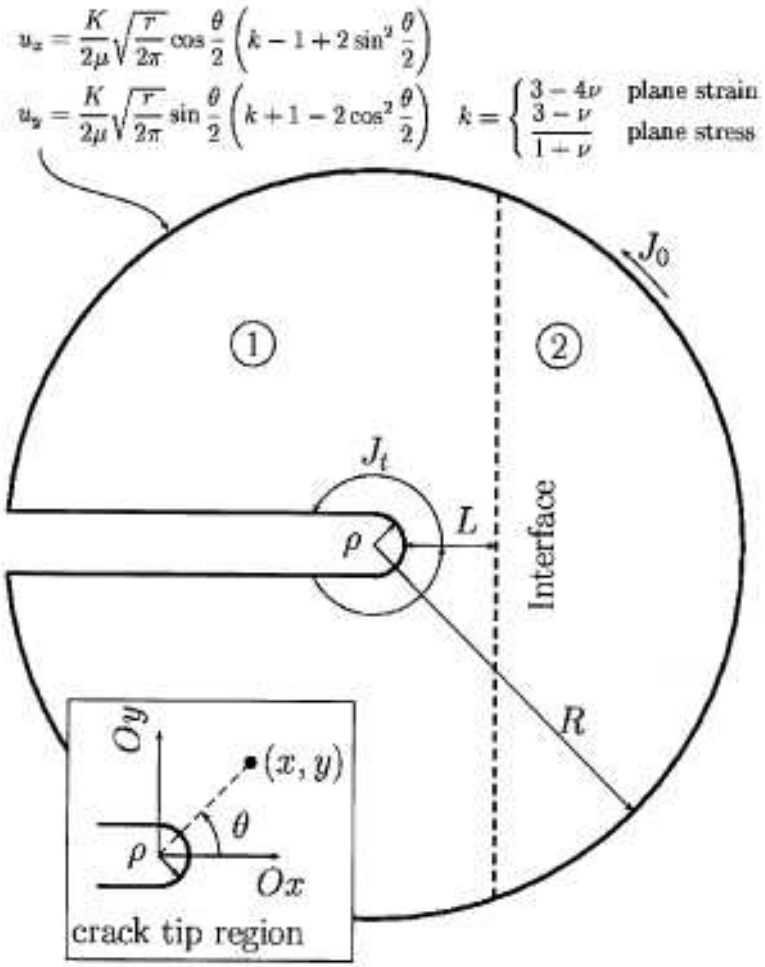


Sketch showing Geometry & Conventions for a Crack approaching an Interface

$$\varepsilon = \frac{\sigma_i}{E}\left(\frac{\sigma}{\sigma_{Yi}}\right)^{n_i}$$

$$i = 1,2$$

$$K = \sigma_{Y1} / \sigma_{Y2}$$

$$E_1 = E_2 \; ; \; \nu_1 = \nu_2$$

# CRACKS at INTERFACES (2)

*A.S.Kim et al.,Int. J.Solids and Structures , vol. 36,1999, pp.1845-1864*

PLANE STRAIN

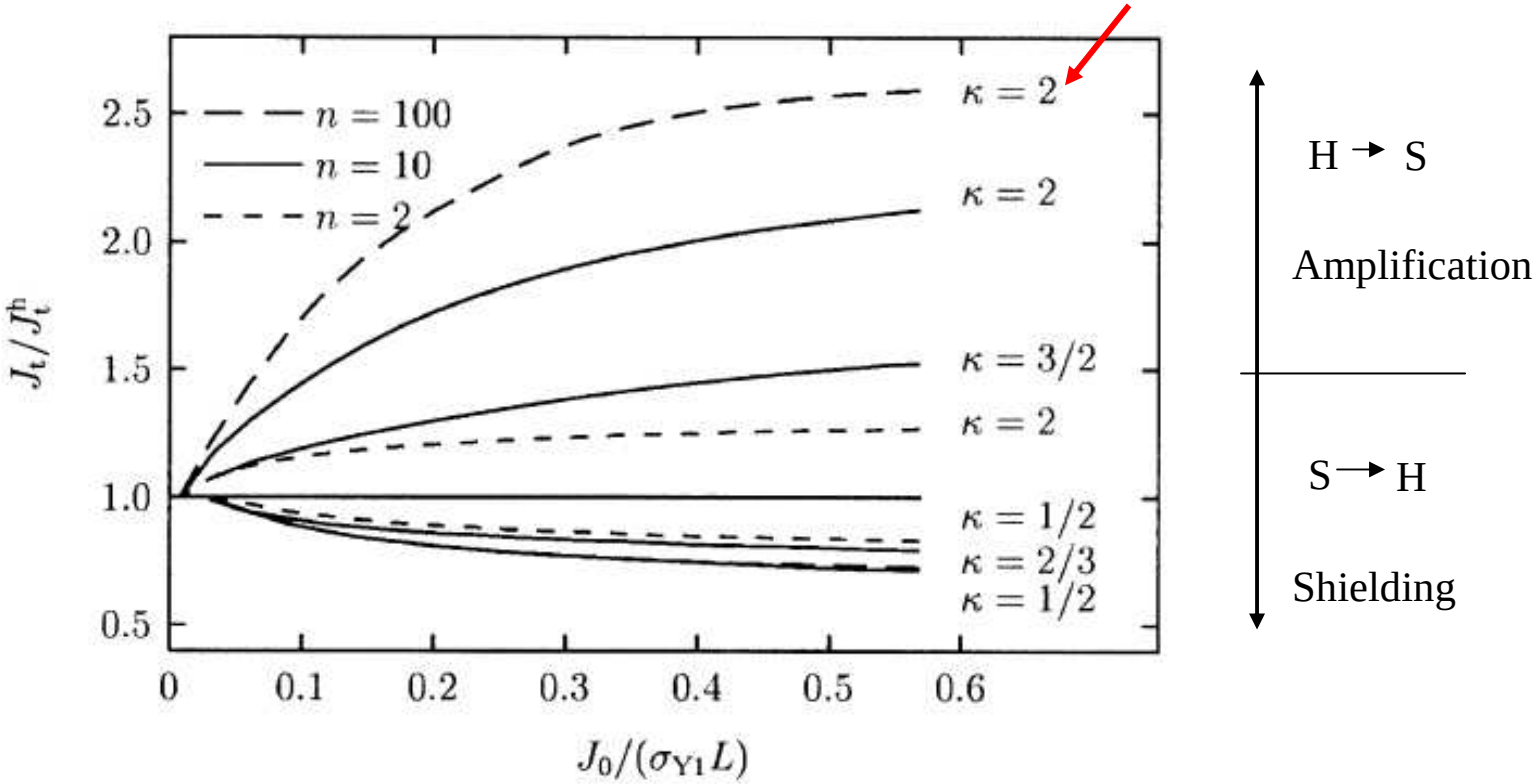


. Variation in normalized $J_t$ as a function of normalized load for various $\kappa$ and $n$ (pl

# CRACKS at INTERFACES (3)

*A.S.Kim et al.,Int. J.Solids and Structures , vol. 36,1999, pp.1845-1864*

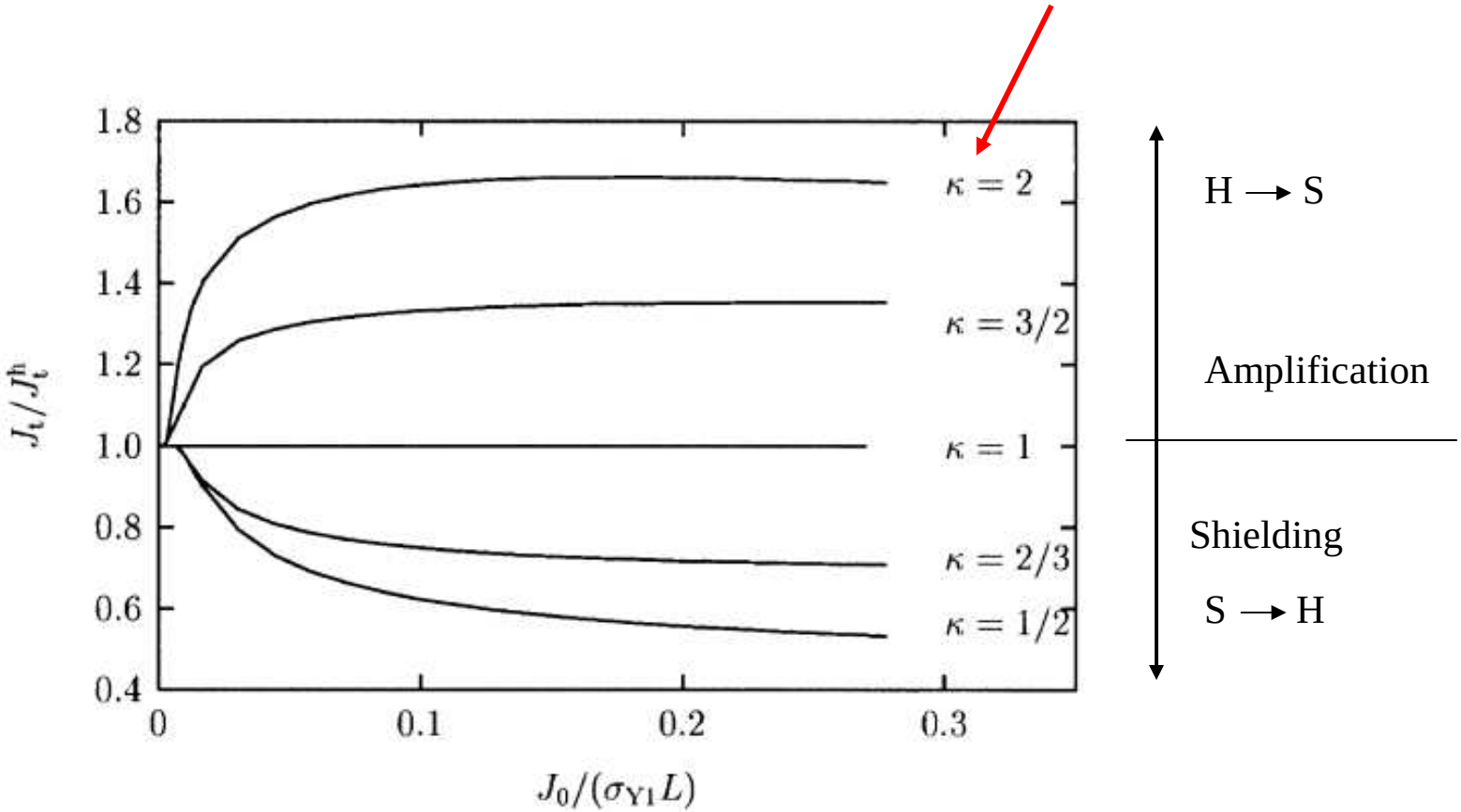


Variation in normalized $J_t$ as a function of a normalized load for various $\kappa$ with $n =$

# CRACKS at INTERFACES (4)

*A.S. Kim et al., Int. J. Solids Struct., vol. 36, 1999, pp. 1845-1864*

n = 10

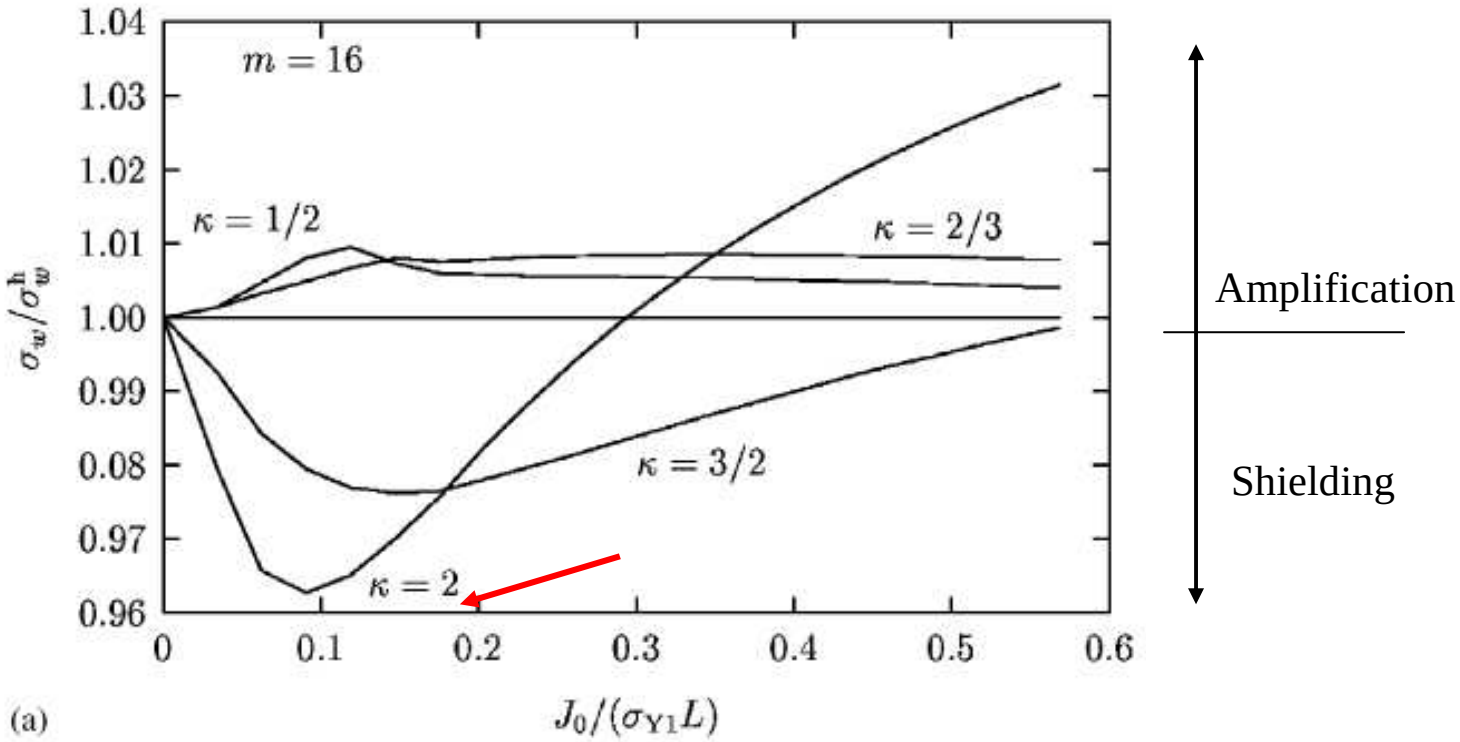

# CRACKS at INTERFACES (5)

*A.S. Kim et al., Int. J. Solids Struct., vol. 36, 1999, pp. 1845-1864*

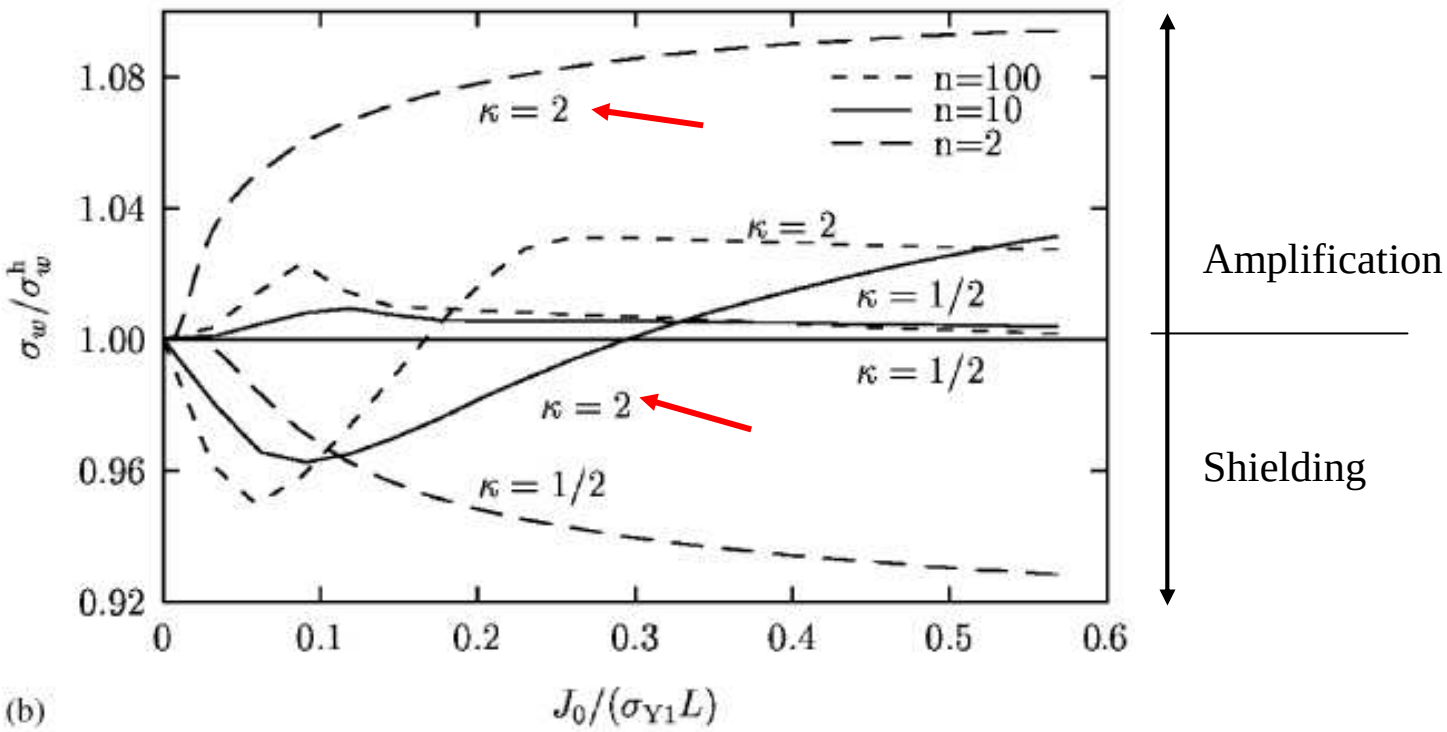


For materials with n = 10 the local model indicates a small shielding effect at low loads contrarily to global approach

# CRACKS ALONG INTERFACES

# TOUGHNESS OF LASER WELDED JOINTS IN THE DUCTILE-BRITTLE TRANSITION

*B. Bezensek , J.W. Hancock , EFM, Vol. 74, 2007, pp; 2395-2419*

## APPLICATION OF LAF TO THE PREDICTION OF CRACK PATH

Chemical composition of Lloyd's Grade L36N steel (in wt%)

| C | Mn | Si | S | P | Ni | Cr | Mo | Nb | Cu | Al |
|---|---|---|---|---|---|---|---|---|---|---|
| 0.10 | 1.36 | 0.48 | 0.002 | 0.007 | 0.35 | 0.058 | 0.016 | 0.024 | 0.13 | 0.032 |

Tensile properties of Lloyd's grade L36N steel at three temperatures

| | 20 °C | −50 °C | −100 °C |
|---|---|---|---|
| 0.2% Yield stress (MPa) | 392 | 411 | 482 |
| Tensile strength (MPa) | 518 | 544 | 648 |
| % Elongation | 42 | 38 | 33 |
| Strain hardening exponent[a] | 10 | 10 | 10 |

[a] Derived from constancy of volume during plastic flow.

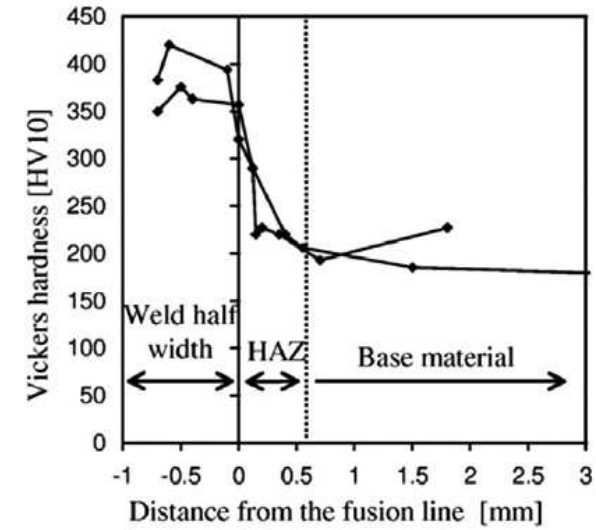


Measurements of Vickers hardness across the width of a laser welded joint.

STRONG MISMATCH EFFECT

Mechanical Tests : 4P Bend Tests (a/W = 0.50 & 0.10)
W = 22 mm , B = 11mm , L = 120 mm
Mode I + Mixed Mode ( I + II)

*B. Bezensek , J.W. Hancock , EFM, Vol. 74, 2007, pp; 2395-2419*

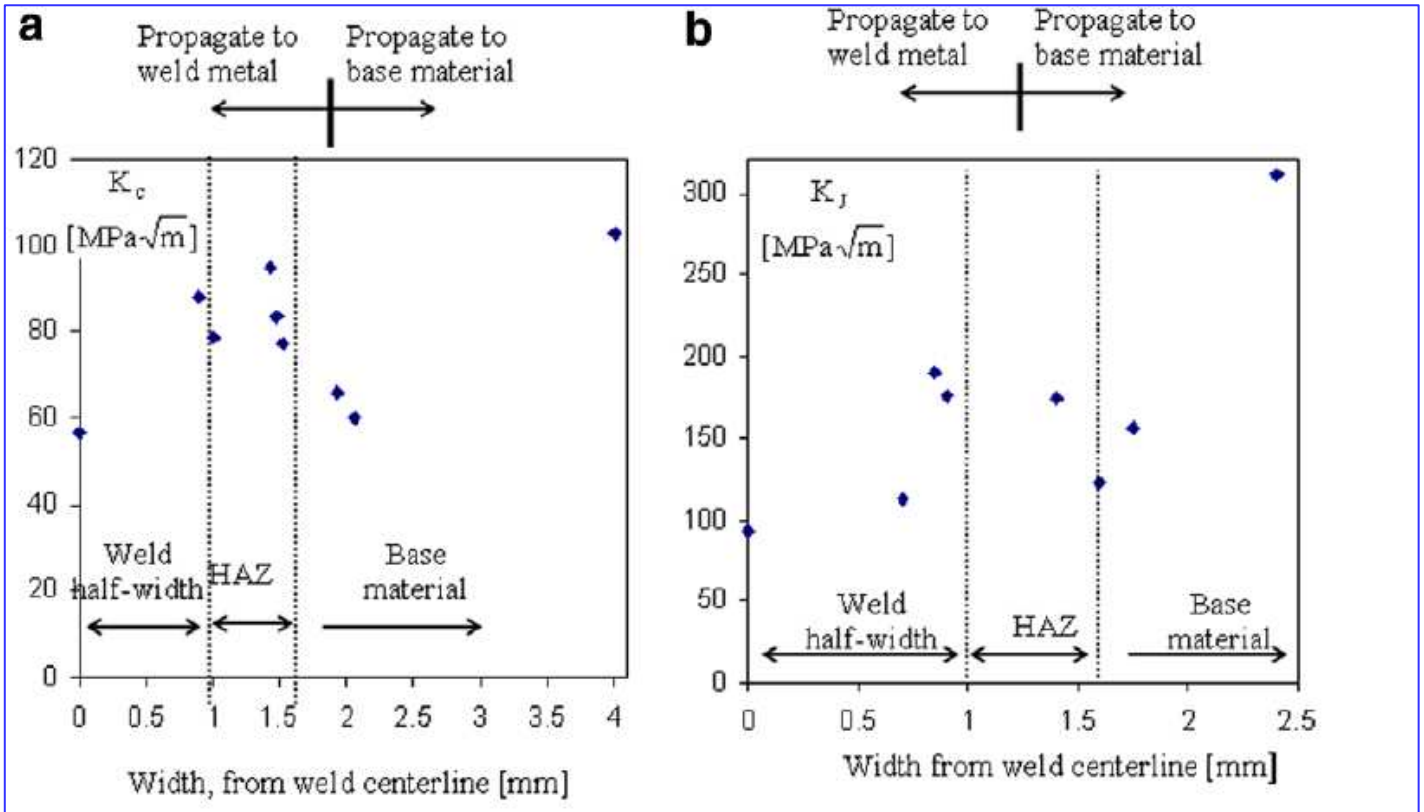


Apparent fracture toughness at −130 °C in (a) and −60 °C in (b) for mode I deep cracks ($a/W = 0.5$).

→ MEASURED FRACTURE TOUGHNESS HIGHEST FOR CRACKS IN THE HAZ & LOWEST FOR THE WELD METAL OR EDGE OF THE HAZ

CRACK PATH

T = -130°C , a/w = 0.50

*B. Bezensek , J.W. Hancock , EFM, Vol. 74, 2007, pp; 2395-2419*

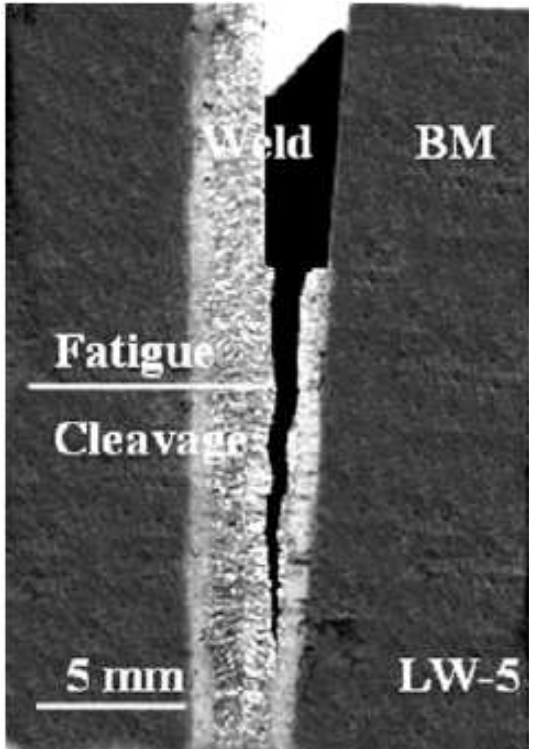


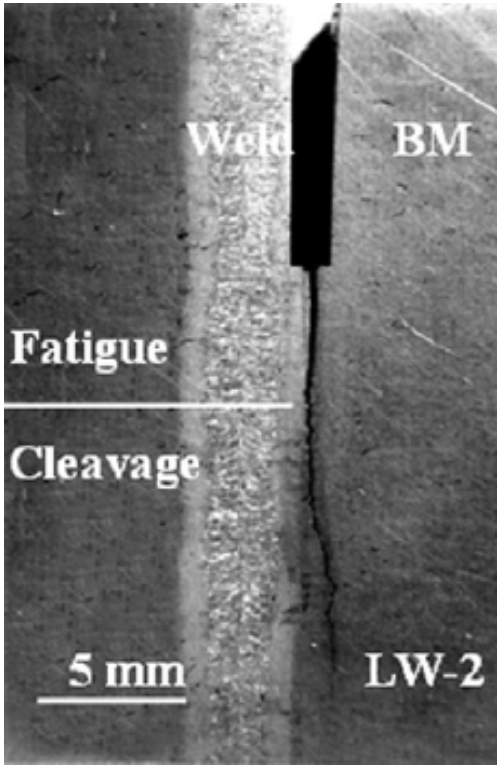


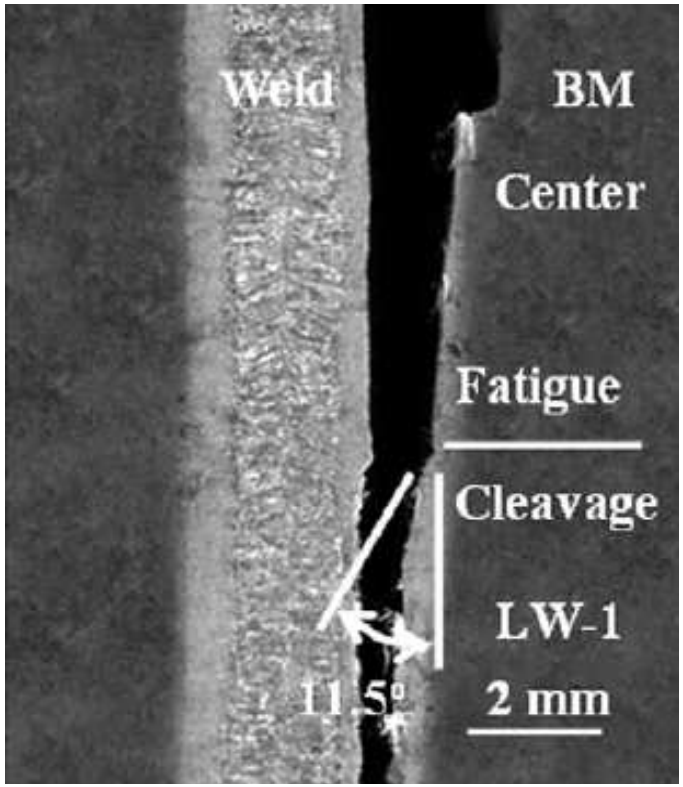


On Fusion Line
DWC = 1 mm
CPA = 9 degrees

Base Metal near HAZ
DWC = 1.82 mm
CPA = 5 (towards BM)

HAZ
DWC = 1.425 mm
CPA = 11.5 , 9.3 degrees

DWC = Distance from Weld Centerline ; CPA = Crack Propagation Angle

# MODELLING WITH WEIBULL STRESS

*B. Bezensek , J.W. Hancock , EFM, Vol. 74, 2007, pp; 2395-2419*

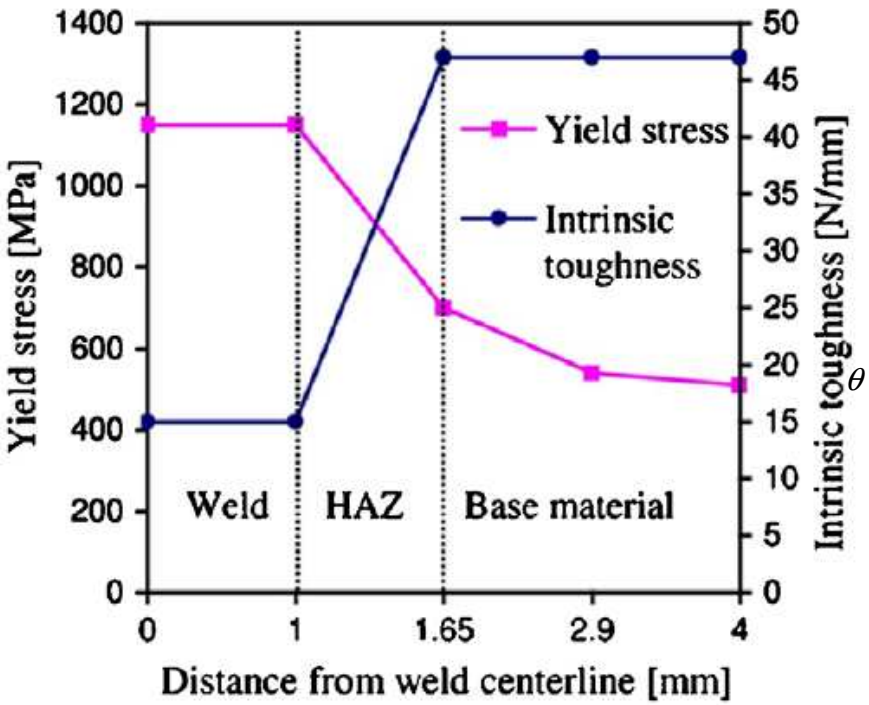


The yield stress and intrinsic toughness across the laser welded joint at −130 °C.

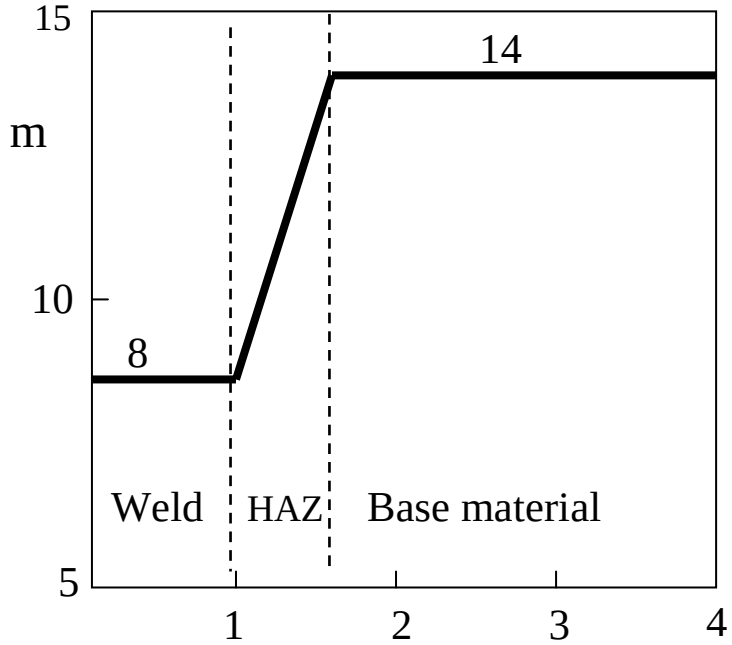


Crack Tip Divided into Angular Sectors ( *see Becker et al. , EFM, Vol. 69,2002, pp.1521-1555* )
Calculation prob. density function , p (θ)

*B. Bezensek , J.W. Hancock , EFM, Vol. 74, 2007, pp; 2395-2419*

## Mean crack propagation angle using the local approach model

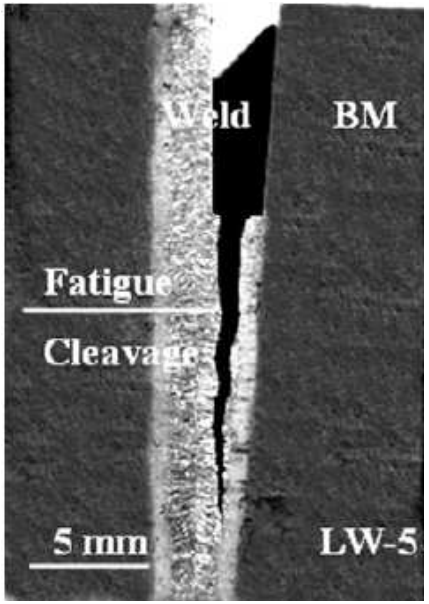


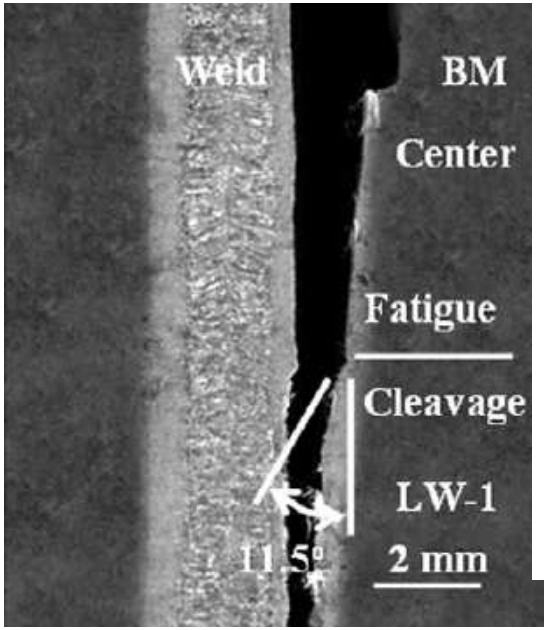


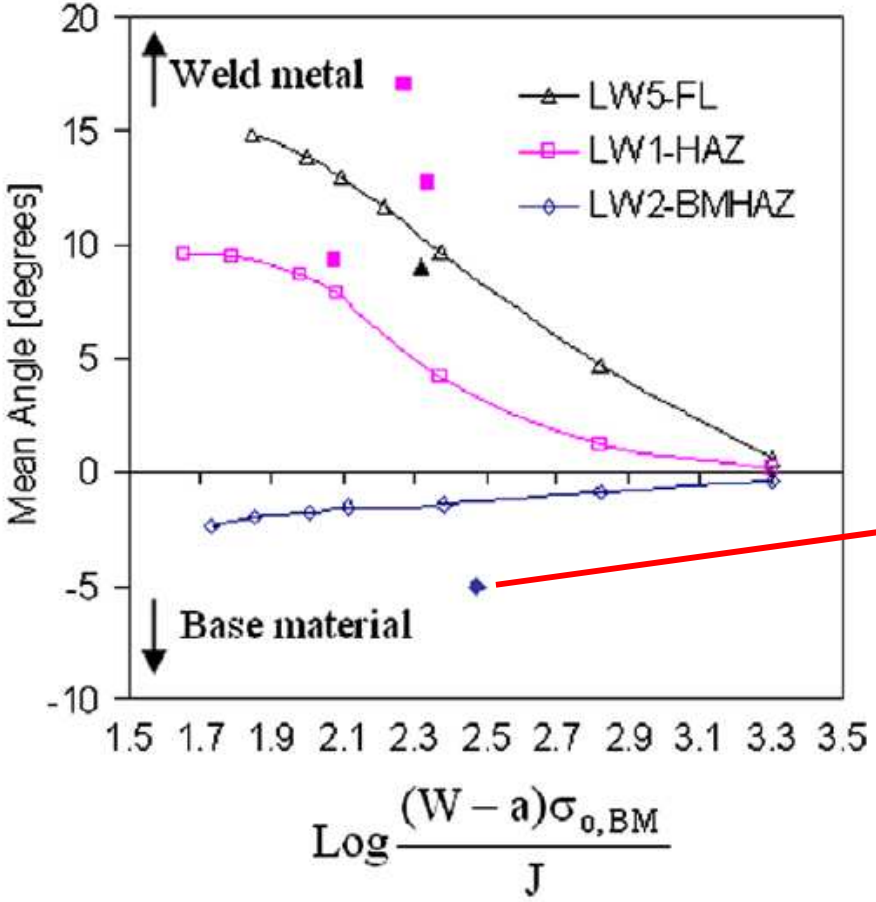


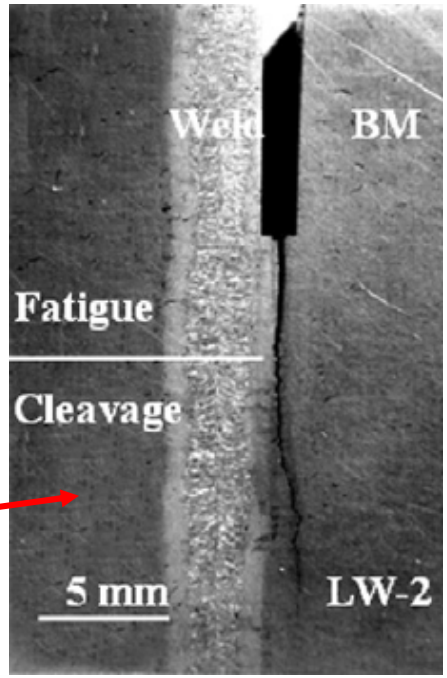

*B. Bezensek , J.W. Hancock , EFM, Vol. 74, 2007, pp; 2395-2419*

DEEP CRACKS a/W = 0.50 T = -130°C

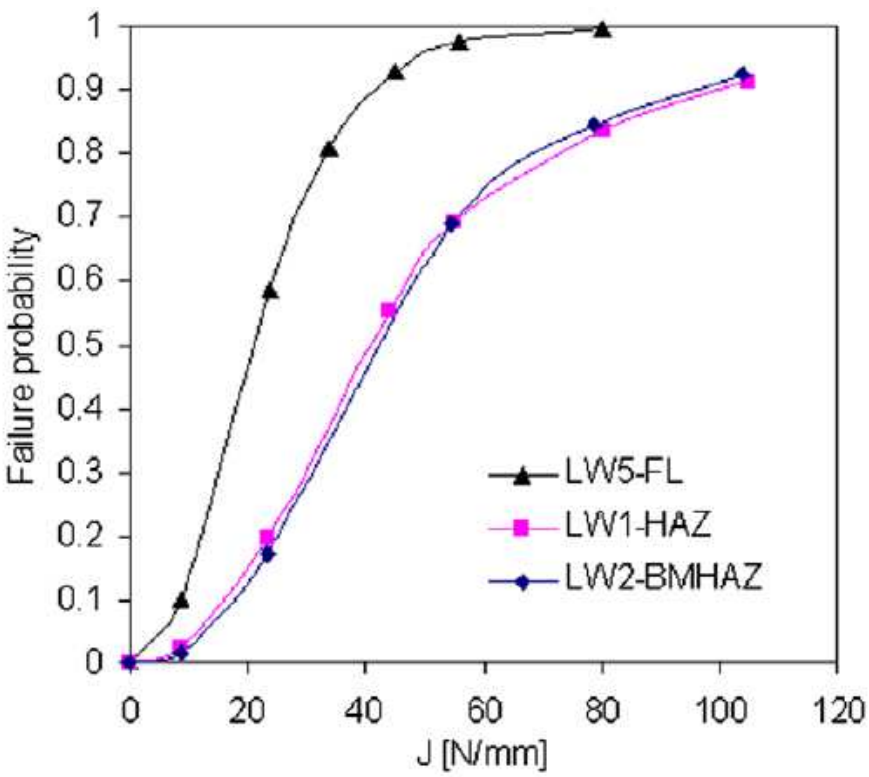


SHORT CRACKS a/W = 0.10 T = - 90°C

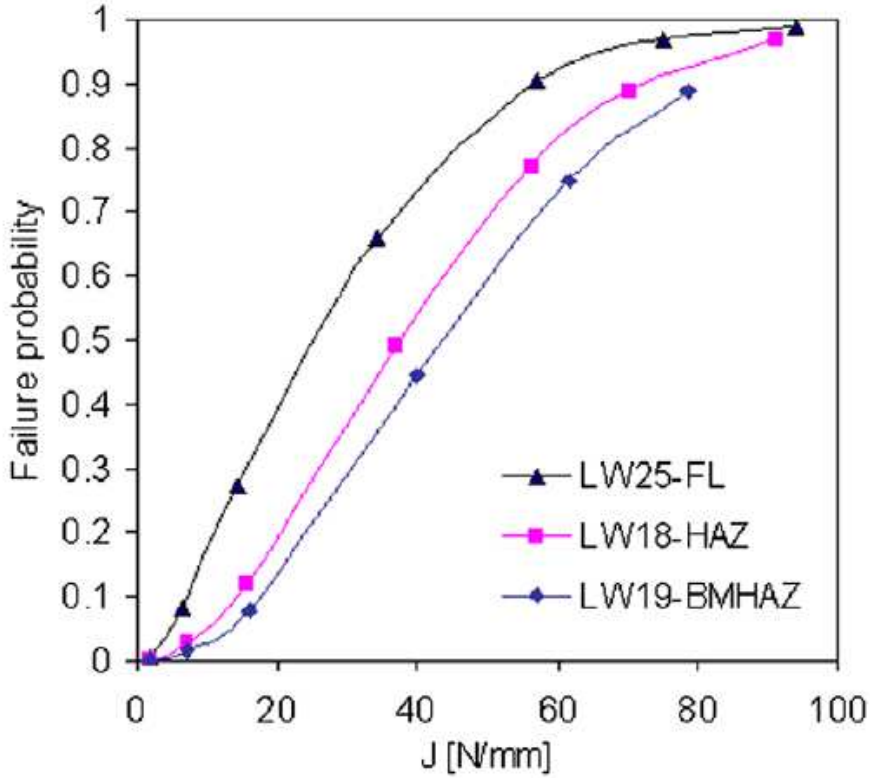

# BRITTLE FRACTURE & BRITTLE to DUCTILE TRANSITION APPLICATIONS TO COMPONENTS

André PINEAU
Centre des Matériaux - Ecole des Mines de Paris. ParisTech
UMR CNRS 7633
andre.pineau@ensmp.fr

# WELDS (1)

*C.G. Matos, R.H. Dodds, Eng. Struct., vol. 22, 2000, pp. 1103-1120*
*N. Cardinal et al., Euromech-Mecamat, J. Phys. IV, vol. 6, 1996, pp. C6-C6-194*

## Residual Stresses

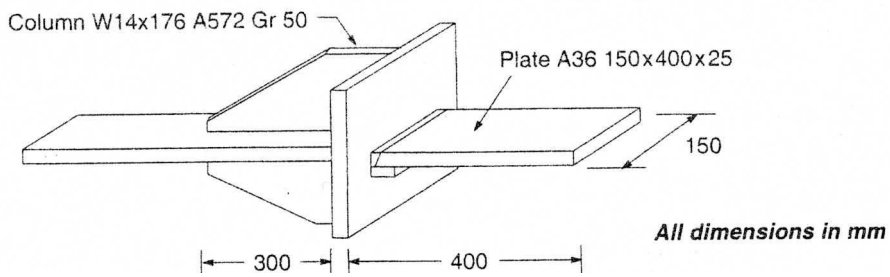


Plate Specimen with Dimensions

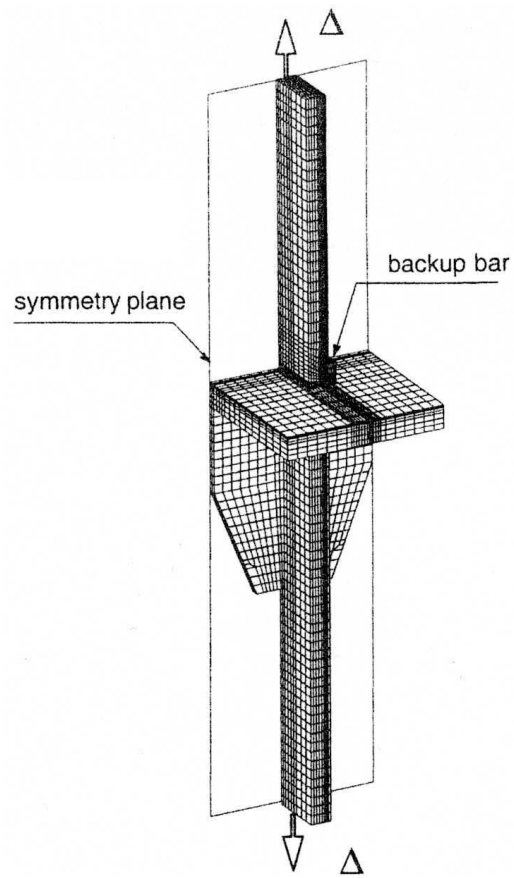


3D FE Model

Distribution of Stress Transverse to the Weld

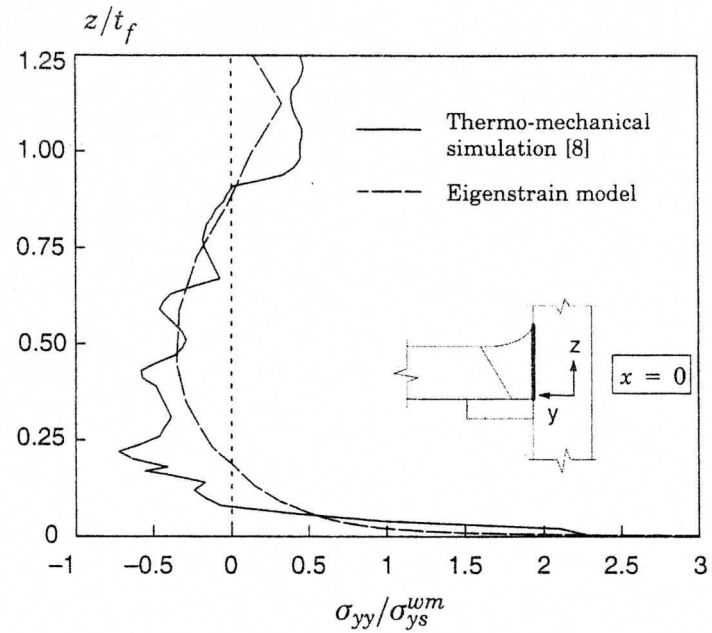

# WELDS (2)

*M. Ohata et al., J. Phys., vol. 6, 1996, pp. C6-C6-269*

## Mismatch Effect (1)

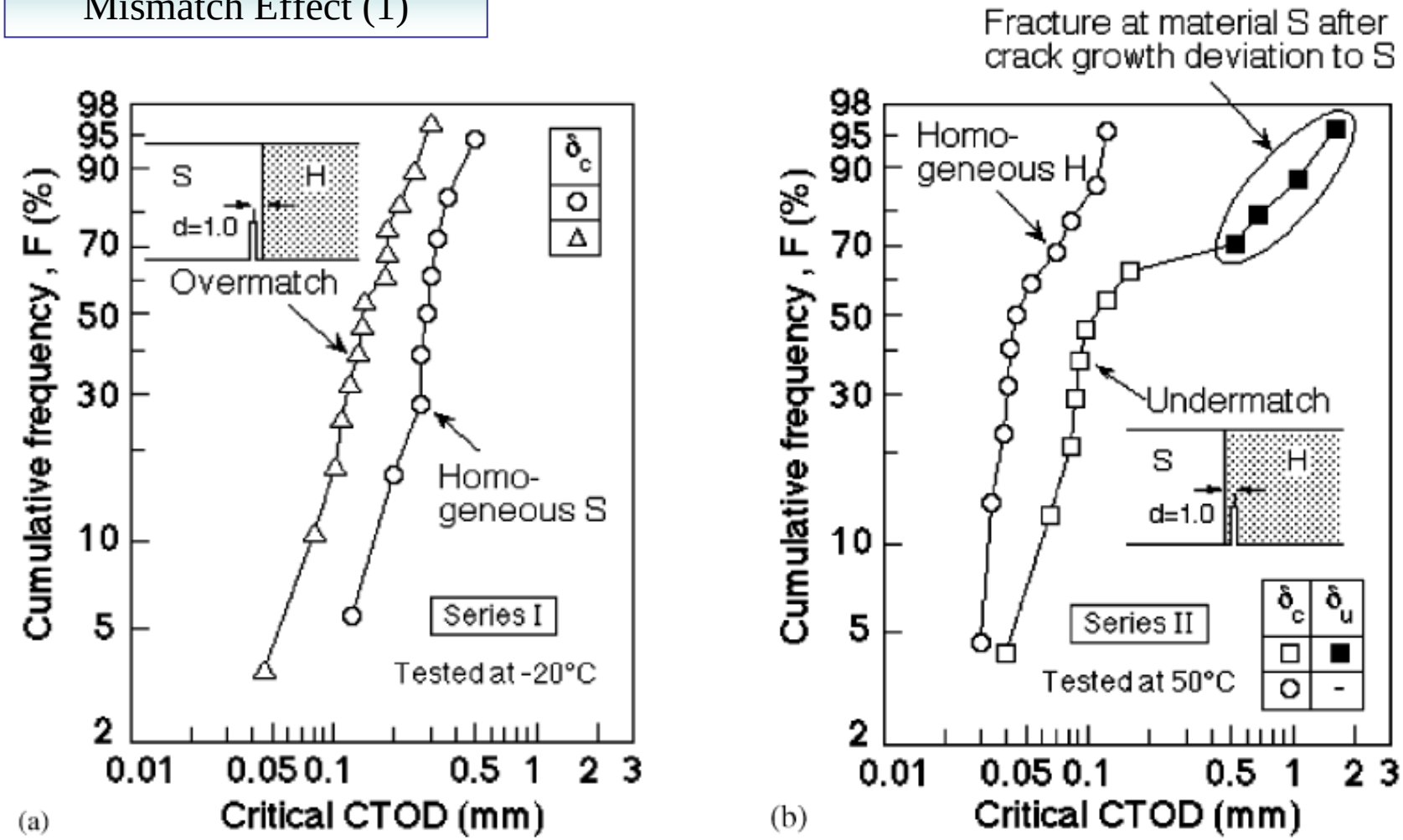


Fracture Toughness a) Overmatch Effect; b) Undermatch Effect

Material S $\sigma_Y$ = 283 MPa; Material H $\sigma_Y$ = 533 MPa - Assembled by Diffusion Bonding

# WELDS (3)

*M. Ohata et al., J. Phys., vol. 6, 1996, pp. C6-C6-269*

## Mismatch Effect (2)

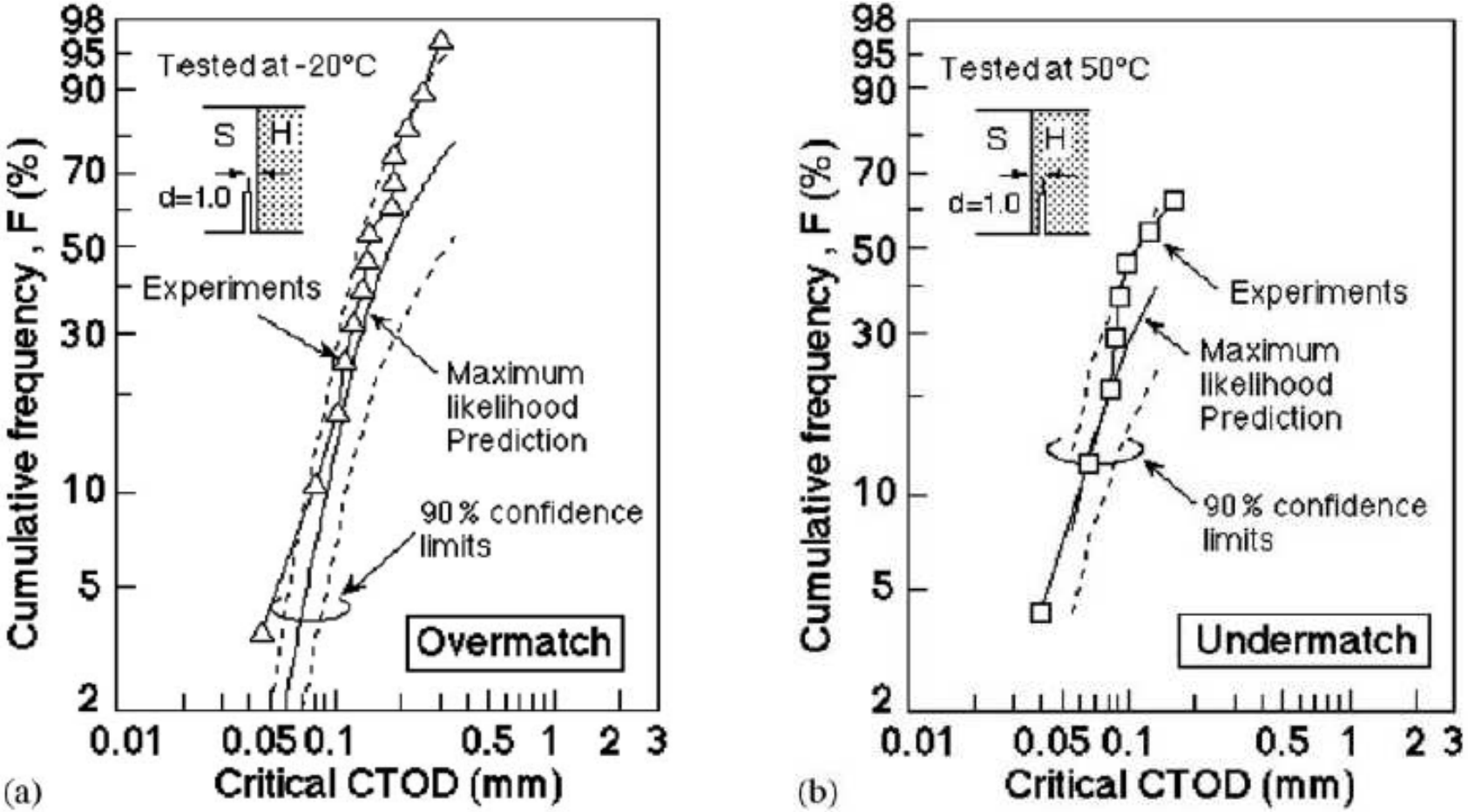


Comparison Theory & Experiments : a) Overmatch; b) Undermatch

# WELDS (4)

*M. Ohata et al., J. Phys., vol. 6, 1996, pp. C6-C6-269*

## Mismatch Effect (3)

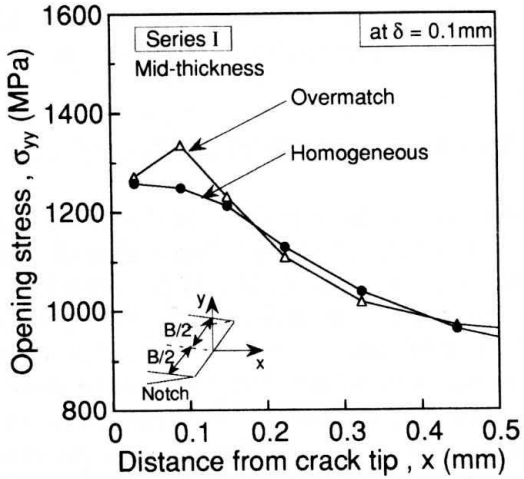


(a) Strength overmatch effect (Series I )

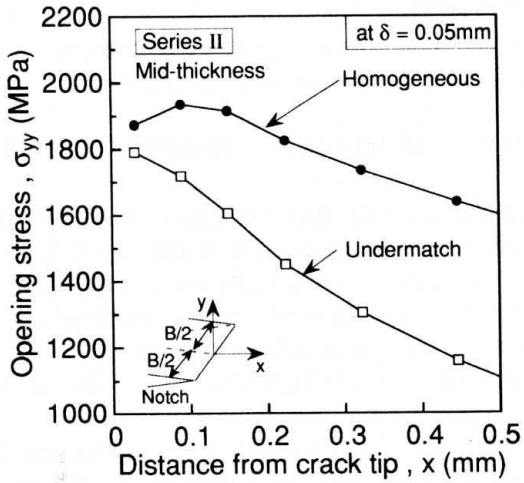


(b) Strength undermatch effect (Series II)

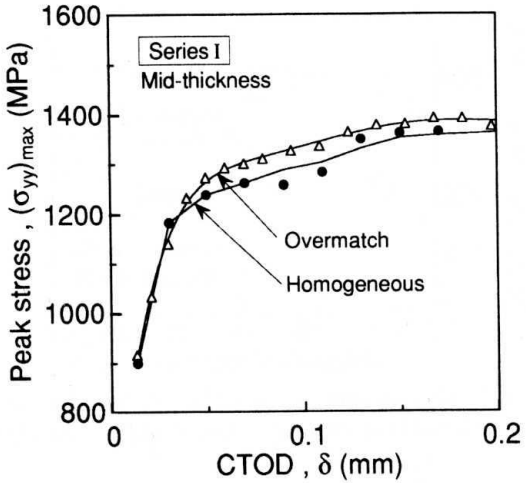


(a) Strength overmatch effect (Series I )

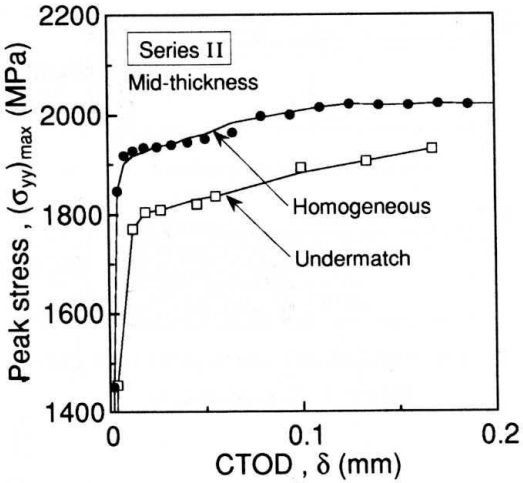


(b) Strength undermatch effect (Series II)

# WELDS (5)

*M. Ohata et al., J. Phys., vol. 6, 1996, pp. C6-C6-269*

## Mismatch Effect (4)

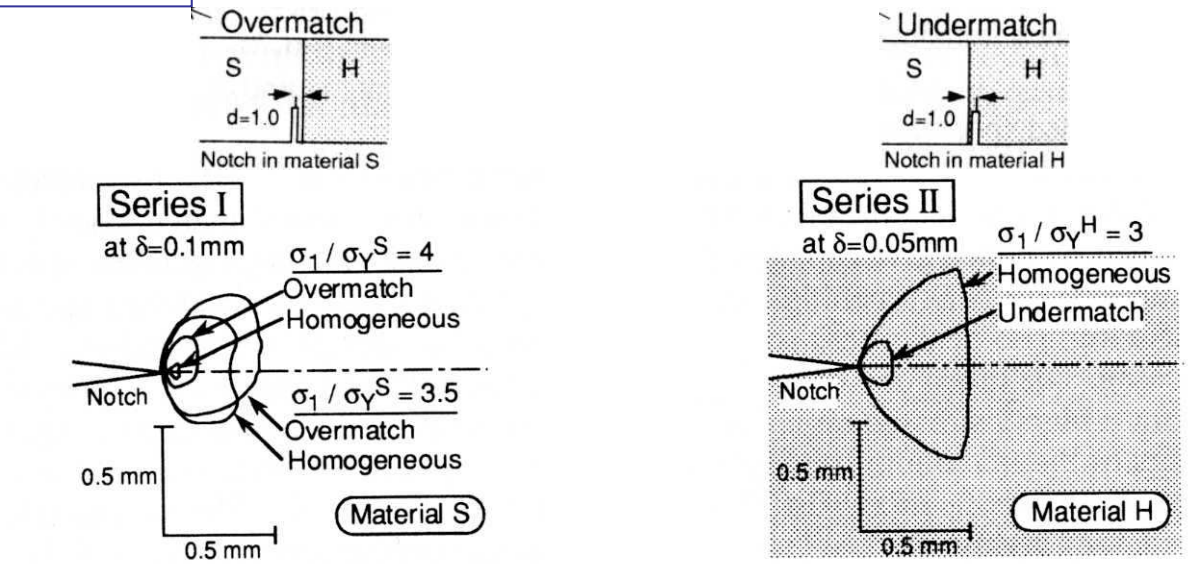


(a) Strength overmatch effect (Series I ) (b) Strength undermatch effect (Series II)

Contours of the Maximum Principal Stress around the Crack Tip at Mid-Thickness

| | | m | $\sigma_u$ (MPa) |
|---|---|---|---|
| **Series I (- 20°C)** | Homogeneous | 40 | 1246 |
| **Series I (- 20°C)** | Overmatch | 31 | 1197 |
| **Series II (50°C)** | Homogeneous | 43 | 1773 |
| **Series II (50°C)** | Undermatch | 43 | 1739 |

$V_0 = 1\ mm^3$

# BRITTLE FRACTURE & BRITTLE to DUCTILE TRANSITION APPLICATIONS TO COMPONENTS

André PINEAU
Centre des Matériaux - Ecole des Mines de Paris. ParisTech
UMR CNRS 7633
andre.pineau@ensmp.fr

# 3D CRACKS (1)

*T. Yuritzinn et al.,EFM, vol.77,2010,pp.71-83*

**Beremin Theory**


$$K_{IC} = 1/l^{1/4} \times \left(\int K_I^4(s)ds\right)^{1/4}$$

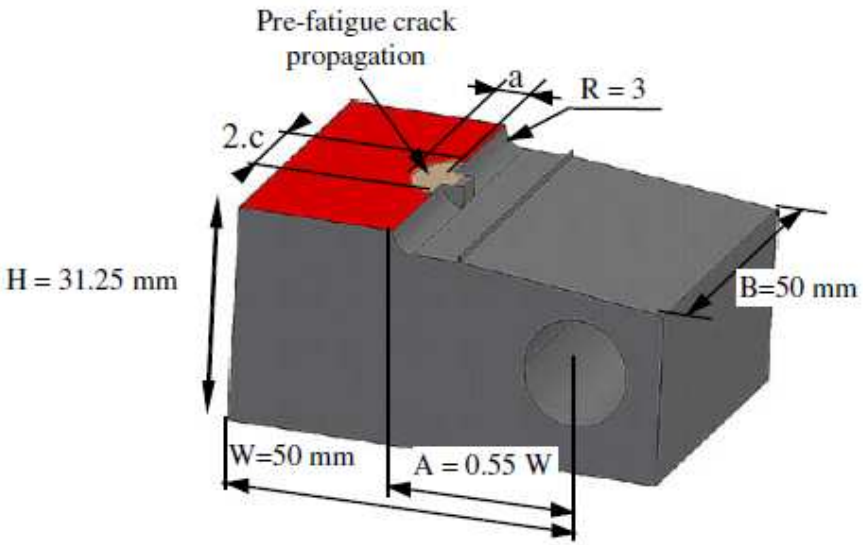


**Fig. 2.** Half of a $CT_{por}$ specimen before and after fatigue pre-cracking.

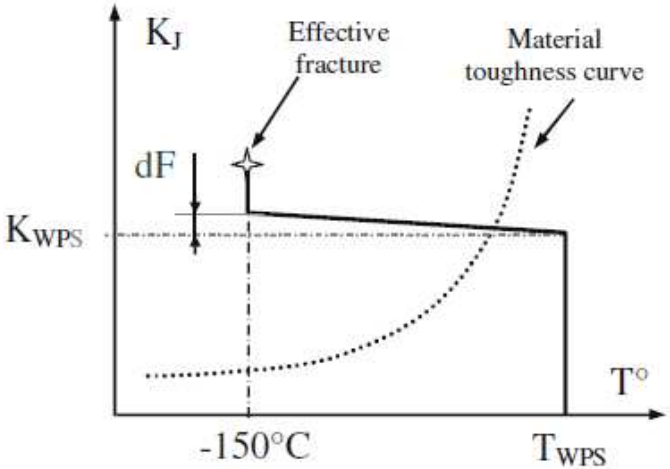


**Fig. 3.** Schematic representation of thermo-mechanical transients.

« por » = Probe Oberflache Riss (Specimen with Surface Defect)

# 3D CRACKS (2)

*T. Yuritzinn et al.,EFM, vol.77,2010,pp.71-83*

Summary of the WPS tests.

| Specimen | Type | $T_{WPS}$ (°C) | $F_{WPS}$ (kN) | $K_{WPS}$ (MPa $\sqrt{m}$) | dF/F | $F_{frac}$ (kN) | $a$ (mm) | $2c$ (mm) |
|---|---|---|---|---|---|---|---|---|
| 137C | LCF | 20 | 70 | 66 | 0 | 87.3 | 5.7 | 21 |
| 137E | LCF | 20 | 70 | 66 | 0 | 90.7 | 5.7 | 20.9 |
| 137O | LCF | 20 | 36 | 30 | 0 | 52.7 | 5.9 | 21.7 |
| 137I | LCF | 20 | 36 | 30 | 0 | 55.9 | 5.8 | 21.1 |
| 137B | LCF | −90 | 36 | 30 | 0 | 49.3 | 5.8 | 21.3 |
| 137K | LCF | −90 | 36 | 30 | 0 | 55 | 6 | 22 |
| 137A | LCIKF | 20 | 70 | 66 | 10% | 81.4 | 6.1 | 24 |
| 137M | LCIKF | 20 | 70 | 66 | 10% | 84.2 | 5.9 | 21.9 |

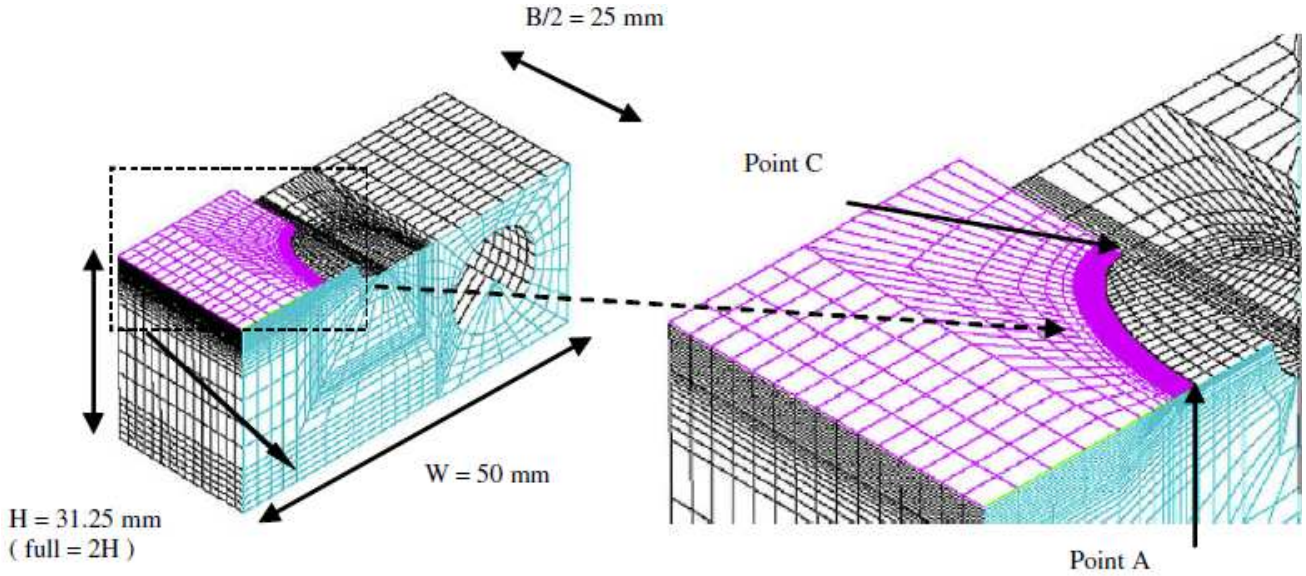


**Fig. 4.** 3D mesh for application of the Beremin model.

# 3D CRACKS (3)

*T. Yuritzinn et al.,EFM, vol.77,2010,pp.71-83*

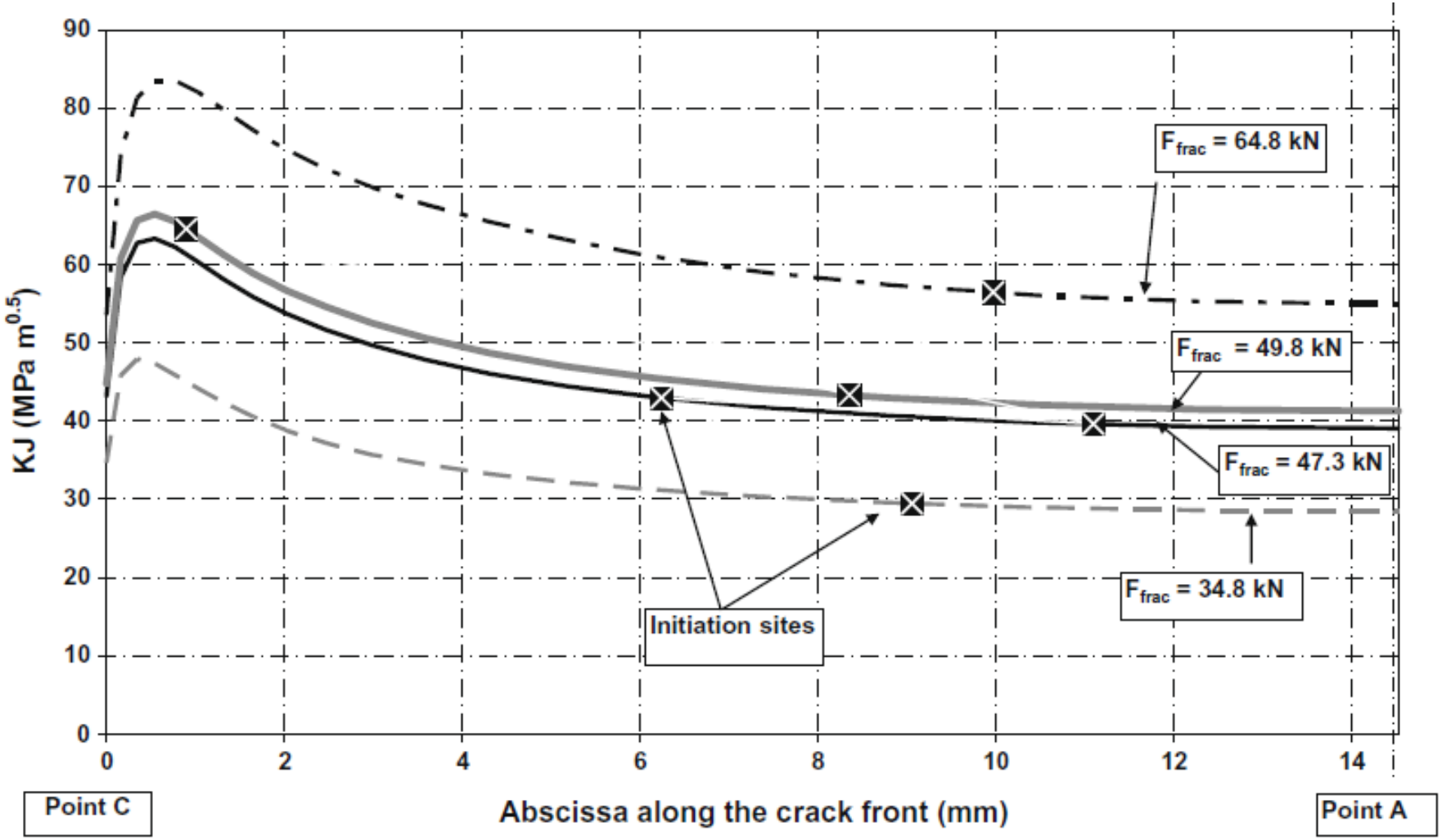


**Fig. 5.** Location of initiation sites and corresponding $K_J$ values.

# 3D CRACKS (4)

*T. Yuritzinn et al.,EFM, vol.77,2010,pp.71-83*

$$K_{J\,average} = \left( \int_0^L \left(K_J(s)\right)^4 \frac{ds}{L} \right)^{1/4}$$

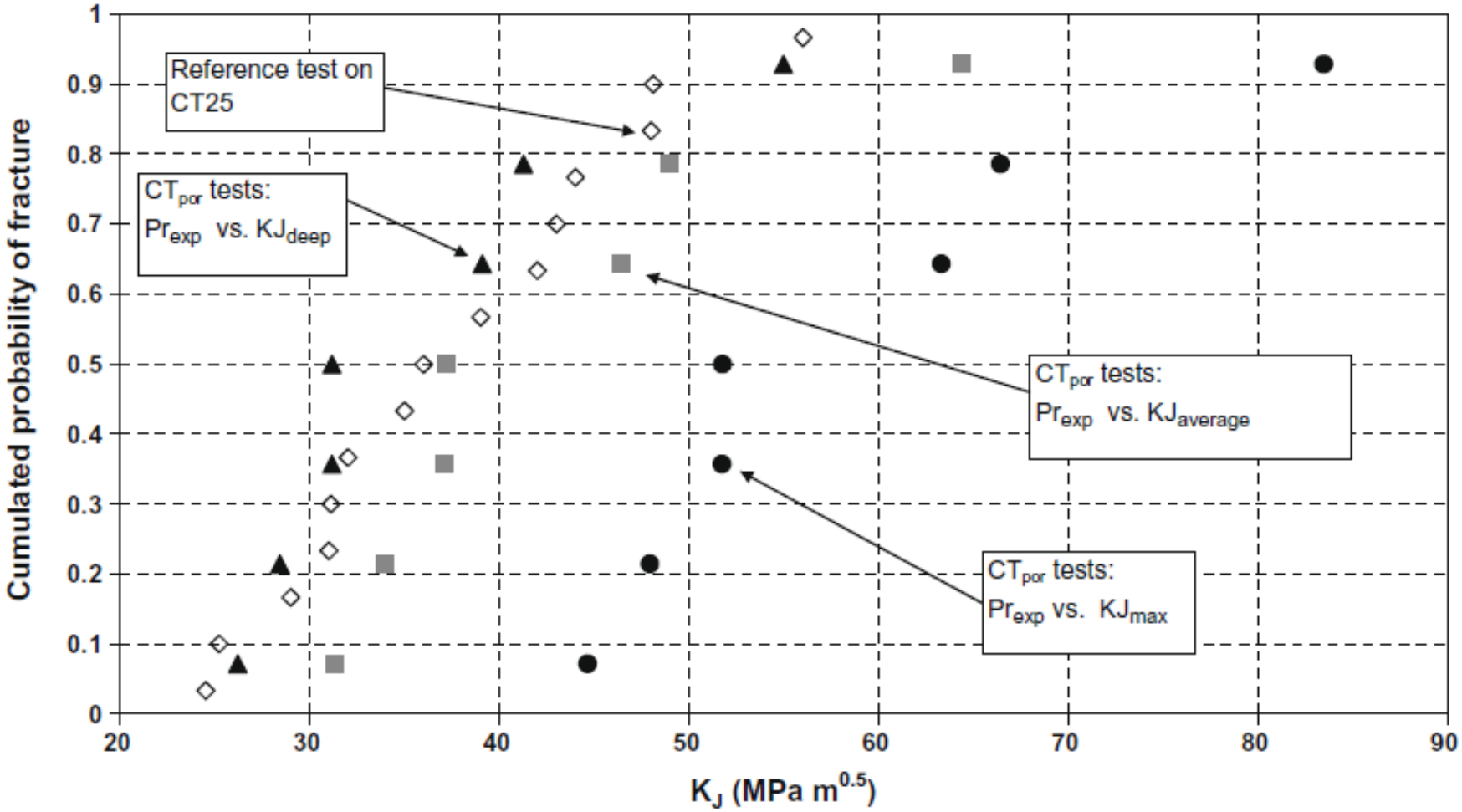


**Fig. 7.** Fracture probabilities as a function of isothermal $K_J$ values.

# 3D CRACKS (5)

*T. Yuritzinn et al.,EFM, vol.77,2010,pp.71-83*

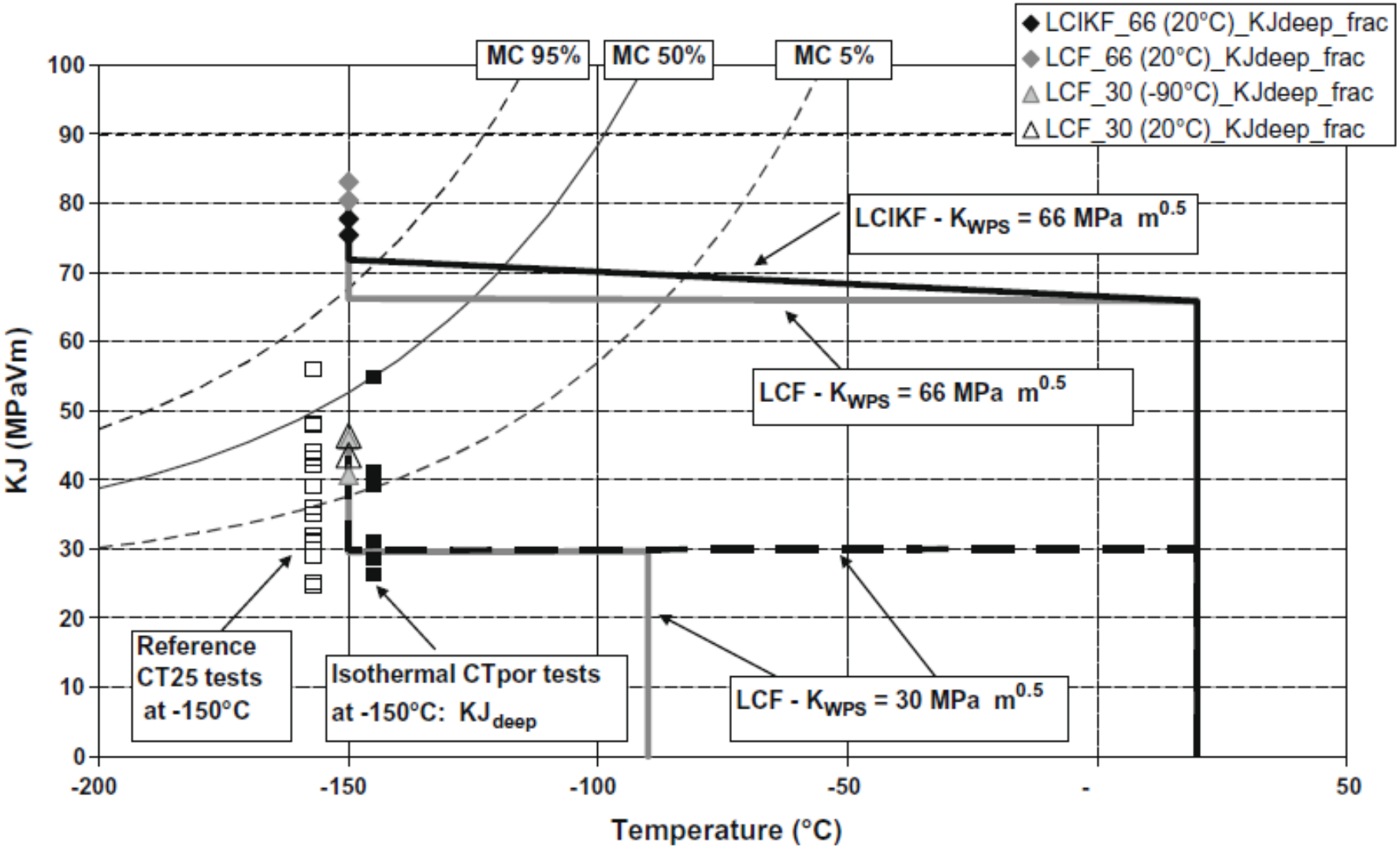


**Fig. 8.** WPS test loading paths and comparison with the master curves.

# 3D CRACKS (6)

*T. Yuritzinn et al.,EFM, vol.77,2010,pp.71-83*

**Table 4**
Beremin parameters identified for 18MND5 steel.

| | | | | | |
|---|---|---|---|---|---|
| $m$ | 23.43 | | | | |
| Temperature (°C) | −150 | −100 | −50 | −20 | 20[a] |
| $\sigma_u$ (MPa) | 2736 | 2907 | 3161 | 3421 | 4200 |

[a] At 20 °C, the fracture is ductile.

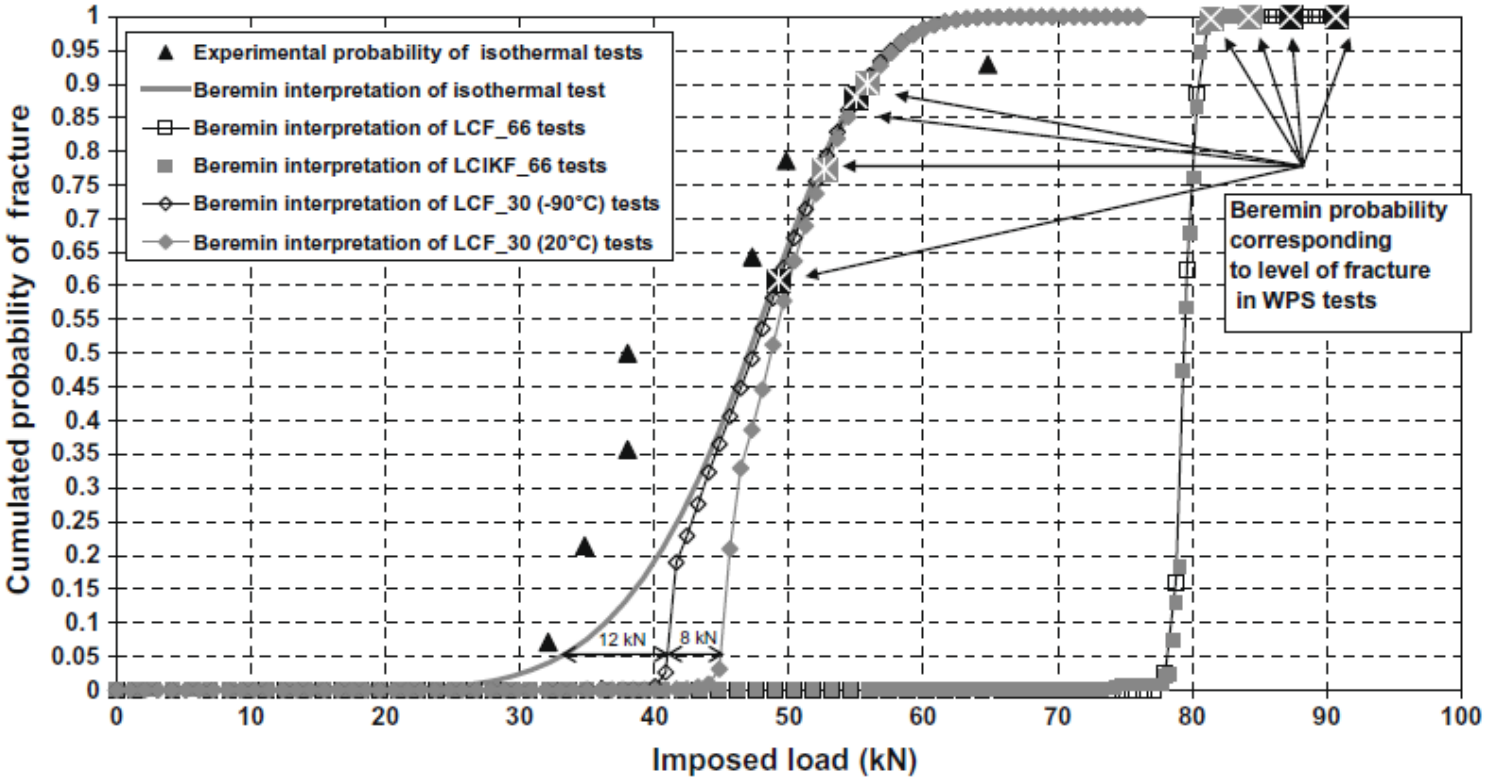


**Fig. 9.** Cumulated fracture probabilities as estimated with the Beremin model.

# 3D CRACKS (7)

*T. Yuritzinn et al., EFM, vol.77,2010, pp.71-83*

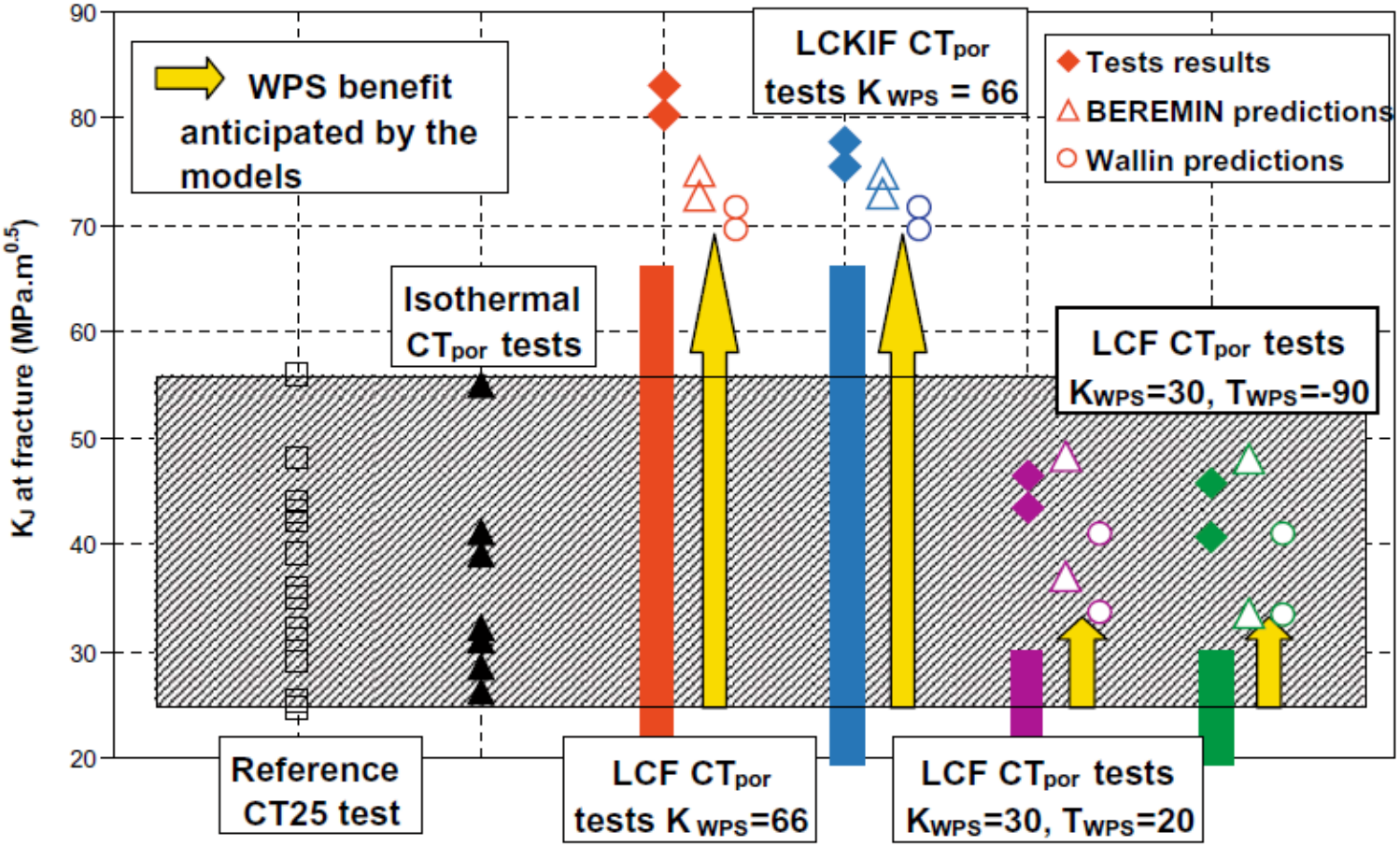


Vertical shaded bars indicate level of preload ; Shaded area = $K_{J\ Fracture}$ on isothermal $CP_{por}$ specimens ; Arrows = Beneficial effect of WPS effect

# CONCLUSIONS

- LAF - Practical Applications – Standards
- LAF will remain a tool for the analysis of complex situations – Safety Margins

- Many research areas remain to be explored :
  - Limitations to size effect
  - Macroscopically inhomogeneous materials
  - Dynamic crack propagation and crack arrest
  - Identification of model parameters